REPUBLIC OF IRAQ
MINISTRY OF HIGHER EDUCATION AND SCIENTIFIC RESEARCH
AL-FURAT AL-AWSAT TECHNICAL UNIVERSITY
ENGINEERING TECHNICAL COLLEGE- NAJAF

An Experimental Study To Enhance The Cooling Performance Of Power Distribution Transformer

A THESIS

SUBMITTED TO THE POWER TECHNICAL ENGINEERING DEPARTMENT IN PARTIAL FULFILMENT OF THE REQUIREMENTS FOR THE DEGREE OF TECHNICAL MASTER IN MECHANICAL ENGINEERING –THERMAL

BY

AYMEN ABDUL KAREEM ABBAS

(B.SC AUTOMOBILE ENGINEERING 2010)

Supervisor by

Asst. prof. Dr. ZAID M. Al DULAIMI

Asst. prof. Dr. HASSANAIN G. HAMEED

June 2021

﴿رَبِّ أَوْزِعْنِي أَنْ أَشْكُرَ نِعْمَتَكَ الَّتِي أَنْعَمْتَ عَلَيَّ وَعَلَى وَالِدَيَّ وَأَنْ أَعْمَلَ صَالِحًا تَرْضَاهُ وَأَصْلِحْ لِي فِي ذُرِّيَّتِي إِنِّي تُبْتُ إِلَيْكَ وَإِنِّي مِنَ الْمُسْلِمِينَ ﴾

سورة الأحقاف: آية ١٥

الإهداء

الى الحبيب المصطفى... وأئمة الاطهار اعلام الهدى... ومصابيح الدجى

الى من علمني النجاح والصبر... الى رفيقي في مواجهة الصعاب

الى من يرويني من حنانه ... أبي

والى من تسابق الكلمات لتخرج معبرة عن مكنون ذاتها

من علمتني وعانت الصعاب الى ما انا فيه

وعندما تكسوني الهموم اسبح في بحر حنانها ليخفف من الامي... امي

الى شريكة حياتي... الى من تقاسمت حملي في السراء والضراء... زوجتي

ال من هم سر سعادتي في الحياة بنتي وأولادي

الى أهلي وأخوتي الاعزاء

الى من علمني حرفا اصبح سنا برقه يضيء الطريق امامي

اساتذتي الاعزاء جزاهم الله عن احسانهم لي خير الجزاء

أهدي عملي المتواضع...

ACKNOWLEDGMENT

First of all, I thank Almighty God for all his boundless blessings. Thank you, Lord, for your success and access to this great matter in completing this research. I thank the Deanship of the Technical Engineering College / Najaf for all their assistance to me. I thank the Presidency of the Department of Power Mechanics represented by **Prof. Dr. Dhafer M. Hachim** for their efforts and continuous support for this work. My thanks and my great and sincere appreciation to the supervisors**, Asst. Prof. Dr. Zaid M. Al-Dulaimi**.

My thanks and my great and sincere appreciation to the supervisors**, Asst. Prof. Dr. Hassanain G. Hameed** for their supervision and eagerness to complete my research fully. I thank them for their humility in giving me their valuable time, indicating their parental supervision. My thanks and appreciation to the electric power transmission company in Najaf represented by Muhannad Shaker for his continuous support with equipment and devices to complete the research. Finally, I thank my brothers for standing by me until the end.

AYMEN ABDUL KAREEM ABBAS

(B.SC AUTOMOBILE ENGINEERING)

June 2021

SUPERVISOR CERTIFICATION

We certify that this thesis titled **" An Experimental Study To Enhance The Cooling Performance Of Power Distribution Transformer"** which is being submitted by **Aymen Abdul Kareem Abbas** was prepared under my/our supervision at the Power Techniques Engineering Department, Engineering Technical College-Najaf, AL-Furat Al-Awsat Technical University, as a partial fulfillment of the requirements for the degree of Master of Technical in Thermal Engineering.

Signature:
Name:**Asst. Prof. Dr. Zaid M. Al-Dulaimi**
(Supervisor)
Date: / / 2021

Signature:
Name:**Asst. Prof. Dr. Hassanain G. Hammed**
(Co-Supervisor)
Date: / / 2021

In view of the available recommendation, we forward this thesis for debate by the examining committee.

Signature:
Name: **Prof. Dr. Dhafer Manea Hachim**
Head mechanical Eng Tech of Power Dept.
Date: / / 2021

COMMITTEE REPORT

We certify that we have read this thesis titled **"An Experimental Study to Enhance the Cooling Performance of Power Distribution Transformer"** which is being submitted by **Aymen Abdul Kareem Abbas** and as Examining Committee, examined the student in its contents. In our opinion, the thesis is adequate for award of degree of Master of Technical in Thermal Engineering.

Signature:
Name: **Assist Prof. Dr. Zaid M. Al-Dulaimi**
Supervisor
Date: / / 2021

Signature:
Name: **Assist Prof. Dr. Hassanain G. Hammed**
(Co-Supervisor)
Date: / / 2021

Signature:
Name: **Assist. Prof. Dr. Tahsean A. Hussain**
(Member)
Date: / / 2021

Signature:
Name: **Dr. Hakim T. Khdhim**
(Member)
Date: / / 2021

Signature:
Name: **Prof. Dr. Hafidh H. Mohammed**
(Chairman)
Date: / / 2021

Approval of the Engineering Technical College- Najaf

Signature:
Name: **Ass. Prof. Dr. Hassanain G. Hammed**
Dean of Engineering Technical College- Najaf

Date: / / 2021

ABSTRACT

In the conversion process of an electrical transformer, some power is lost and converted into heat. These heat losses lead to temperature rises that have to be controlled with cooling solutions, since working with high temperatures lead to the deterioration of components and reduces the lifespan of the transformer. For this purpose, transformer's coils and core are generally immersed in an oil-filled corrugated tank. The oil is heated in this tank and then cooled in the external heat exchangers of electrical transformers. Standard radiators consist of thin vertical panels. Which transfers the heat of the oil to the air surrounding by the process of natural or forced convection.

Objective of this work is to find the maximum cooling capacity and temperature variations of vertical radiator panels experimentally. Three values of oil flow rates (1, 2, and 3 ℓ/min) and three variable values for temperature (50, 60, and 70 °C) were used. To cool the oil used in the transformer, two configurations are used namely oil-direct air natural (ODAN) and oil direct air force (ODAF). This work uses a new cooling method through a utilized Metal Foam Heat Exchanger (MFHE) by exploiting its porous medium and controlling its porosity value, which was (17% and 35%), respectively. The results showed a maximum cooling capacity for both models (ODAN) and (ODAF), compared when used the new cooling method (MFHA) with two different values of porosities (17% and 35%), where the results showed that the porosity with (35%) approved is active to develop heat exchanger of a transformer. Primarily results obtained when used (MFHE) cooled with (35%) of porosity when the case is (Fans Off); the maximum cooling capacities are (782, 1580.9, and 2278.9 W) at an oil flow rate 3 ℓ/min. Secondary results that showed when used (MFHE) cooled with (35%) of porosity, at case of (Fans ON), the maximum cooling capacities (1149.8, 2017.6, and 3000 W) at oil flow rate 3 ℓ/min.

The results of the experimental test showed an improvement in the oil heat transfer rate, especially after increasing the metallic foam sponges from 17%, to 35% for both transformer cooling methods.

CONTENTS

NOMENCLATURE

Symbol	Definition	Unite
I	The current through the conductor	A
R	The resistance of the conductor	Ω
V	The electrical voltage	V
N1	The turns number of primary coil	------
N2	The turns number of secondary coil	------
$\dot{Q}$	The volumetric of flow rate	m^3 /s
$\dot{m}$	Mass flow rate	Kg/s
R_{hpr}	Thermal resistance of the heat pipe radiator	m^2. $^oC/W$
T_{hb}	The maximum temperature of the heat source	^oC
T_a	The temperature of the inlet air	^oC
Q	The heat load of the heat source	W
T_{oil}	Temperature of oil	^oC
T_{wall}	Temperature of radiator wall	^oC
T_{air}	Temperature of surrounding air	^oC
K_{steel}	Thermal conductivity of radiator	W/m.K
K_{oil}	Thermal conductivity of mineral oil	W/m.K
$c_{p_{oil}}$	Specific heat of mineral oil	J/kg.K
T	The average temperature	^oC
Q.max	Max flow rate	l/min
Tin	Inlet temperature of oil	^oC
Tout	The outlet temperature of oil	^oC
d_p	The equivalent diameter of one of the dodecahedron unit's faces	m
PPI	The pore per linear inch	m
αsf	Specific surface area	m^2/m^3
S	total surface area inside the unit cell	m^2
V	Unit cell volume	m^3
$P_{radiator}$	The cooling capacity of radiator	W
Greek Symbols		
ρ_{oil}	Density of oil	Kg/m^3
μ_{oil}	Dynamic viscosity of oil	Kg/m.s
ε	The porosity ratio of metal	%
ΔT	Temperature difference	◦C

ABBREVIATIONS

Symbol	Description
MFHE	Metal-Foam Heat Exchanger
ONAN	Oil-direct air natural
ONAF	Oli-natural air forced
OFAF	Oil-force air forced
ODAN	Oil-direct air natural
ODAF	Oil-direct air force
NDOF	Non-directed oil-forced
EAHE	Earth air heat exchanger
l/min	Liter per minute
r.p.m	Revolution per minute
SEM	Scanning electron microscope
HST	Hot-spot temperature
OIP	Oil-immersed paper
FEM	Finite element method
AC	Alternate current
DC	Direct current
HP	Heat pipe radiators
G10	Group of ten
TFHPR	Traditional fin heat pipe radiator
MFHPR	Metal-foam heat pipe radiator
IEC 60076-7	The applicable for mineral oil immersed transformer
IEEE C57.19.100	The standard of bushing for high level-voltage circuit breakers and gas insulated for Switchgear
IEC 60296 Edition 5.0	The standard of classification of mineral insulating oil on it performances

CHAPTER ONE

INTRODUCTION

CHAPTER ONE

INTRODUCTION

1.1 Background

Electrical transformation stations are vital part of electrical grids as they usually used to reduce the voltage to meet the national consumer standard. High voltages are essential in transferring electrical current from remoted electrical generation plants to consumers. Such technique aims to reduce power loss in the form of heat dissipated during the transfer process. Transformers have the role of changing the voltage levels between two circuits, which results in the current values being changed as a result. Because power transformers run at high power levels, the heat losses will result in a temperature rise that will need to be regulated by means of cooling **[1].**

Too high temperatures can degrade the winding insulation and transformer oil, which are two factors that have a significant impact on the lifespan of a transformer **[2],** which are both important considerations. As a result, it is critical to have a reliable cooling system in place, especially in cases when high power is involved. When it comes to transformers, even though they have been optimized in terms of the electric conversion process, there is still a lot of work that can be done in terms of the cooling processes. The optimization of the transformer's cooling capacity allows for the use of more compact equipment and, as a result, a reduction in the amount of raw materials used in the manufacturing process **[2].**

As internal and external cooling mediums, transformers are typically cooled with oil and air, respectively. Oil is used to lubricate the coils and core, which are submerged in an oil-filled tank. In small transformers, the surface of the tank that is in touch with the outside air is sufficient to provide the heat dissipation required. Because of the increased heat created by larger transformers,

it is necessary for the oil to move from the transformer's tank to exterior heat exchangers. For these reasons, for oil-filled power transformers to operate well and minimize material degradation due to thermal damage, it is vital to design the cooling system optimally. Aside from that, thermal management for the purpose of maximizing power transformer utilization should be monitored on a continual basis, taking into account both technical and economic factors. The average winding temperature is mostly governed by the circulation of oil. It is possible to alter the oil circulation by selecting the appropriate power transformer cooling mode **[3].**

1.2 Power Transmission Network

In a power transmission network, energy flows from a generation source (thermal, turbine, hydroelectric, or renewable energy in limited places), through a step-up transformer (the transformer at this stage is usually a raised voltage), then through towers and transmission substations (the transformer at this stage is usually a voltage reducer), and ultimately distributed to consumers. Figure 1.1 displays the diagram of typical transmission grid **[4]**.

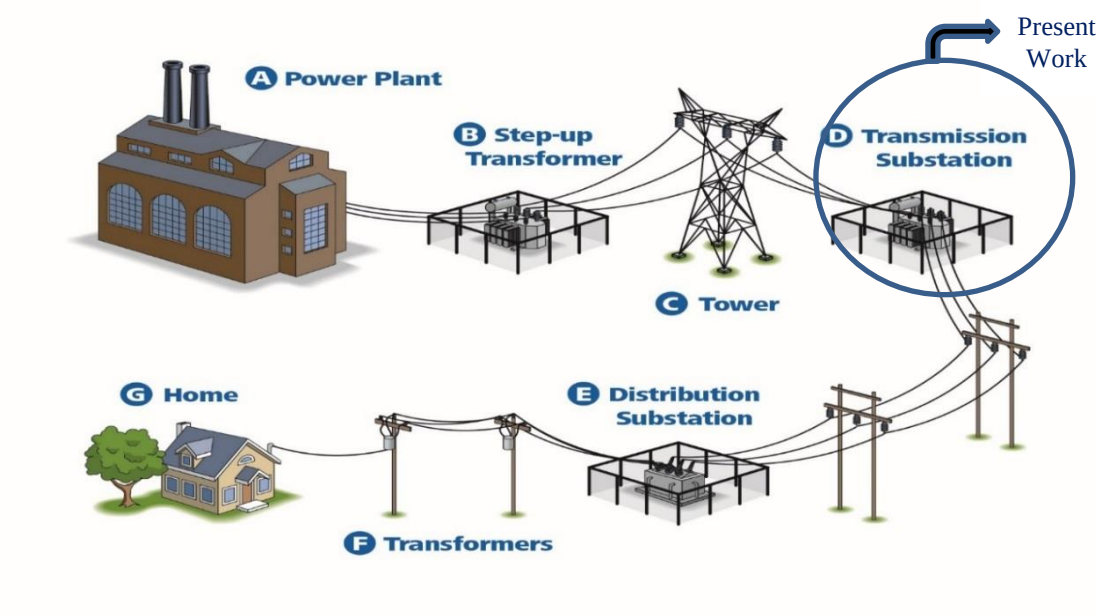

Fig 1.1: Power Transmission Grid [4]

1.3 Power Transformer

Transformers are electrical equipment that convert alternating current energy from one voltage to another voltage without altering the frequency of the current being transformed **[5]** and **[6].** Depending on their cooling mechanism, transformers can be divided into two categories. Dry type transformers as shown in Fig 1.2, and an oil-immersed transformers as shown in Fig 1.3. For this study, it is try explore heat transfer and fluid flow characteristics through two different of cooling types. Oil direct air natural (ODAN), and oil direct air forced (ODAF) of oil-immersed transformer radiator type.

*Fig. 1.2: dry transformer **[5]***

*Fig. 1.3: Oil-immersed transformer [**7**]*

1.4 Transformer Radiator

Typical heat exchangers used in power transformers are thin vertical panel radiators with a high heat transfer capacity. In Figure 1.4, an illustration of this type of heat exchanger in action. Because of the simplicity of their construction, which makes them more economically sustainable, there is a significant deal of interest in using these type of radiators **[8]**.

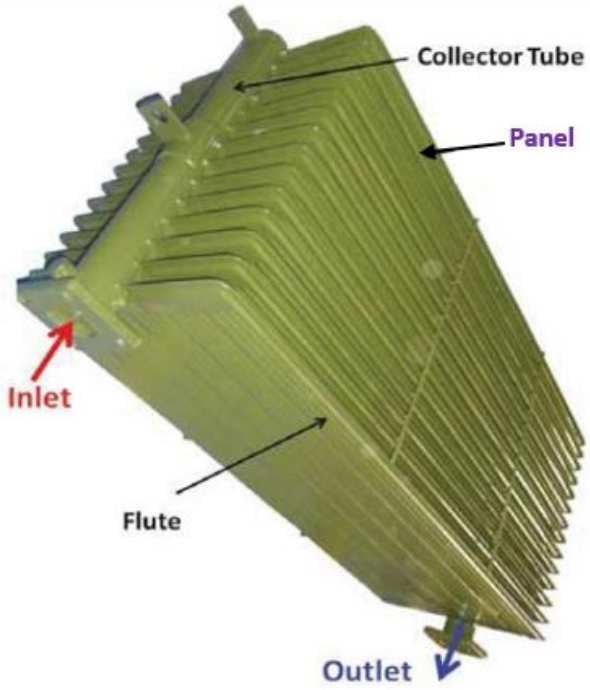

Fig 1.4: Transformer Radiator [8].

Figure 1.5 depicts a schematic representation of the oil circuit. The oil is drawn from the transformer's tank through the intake pipes and enters the radiator panels through the tops of the panels. After passing through the panels of the vertical plate radiators for the transformers, the oil returns to the tank through the outlet pipes, which are placed at the bottom of the radiators. An air circulation system, it is circulating at room temperature across the external surface of the plates by coupled fans are used [5].

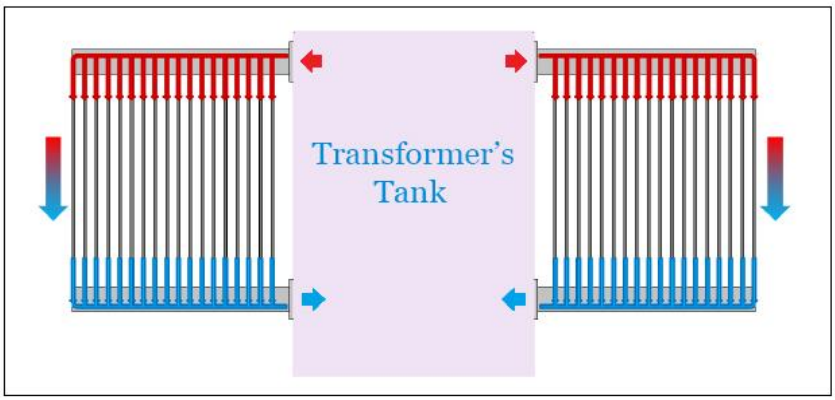

Fig. 1.5: Schematic representation of oil circulation [5]

The panels are evenly spaced apart and have the same width and length as one another. Each panel have seven oil channels to allow the oil flow from top oil header to down header. In order to accurately anticipate the cooling capacity provided by the radiators installed in a transformer, as well as the oil temperature at the radiators' outlet, it is important to take into account additional parameters in addition to the geometrical ones:

The parameters are the rate at which oil flows through the radiator; the temperature of the oil at the radiator's intake; the air temperature; the properties of the cooling mediums (oil and air); the properties of the radiators' material; a number of plates per radiator; and so forth the location and distribution of fans. There is a variety of layouts available for the placement of the fans. In general, fans can be found at the bottom or on the side of the radiators, depending on their design. In this studied, it is mounted on the side of the radiator.

1.5 Main Components of Power Transformer

The Transformers consist of main parts as arranged. Core, winding, and tank, see Fig. 1.6. In addition to auxiliary parts such as buchholz relay, low voltage bushings, and high voltage bushing [9].

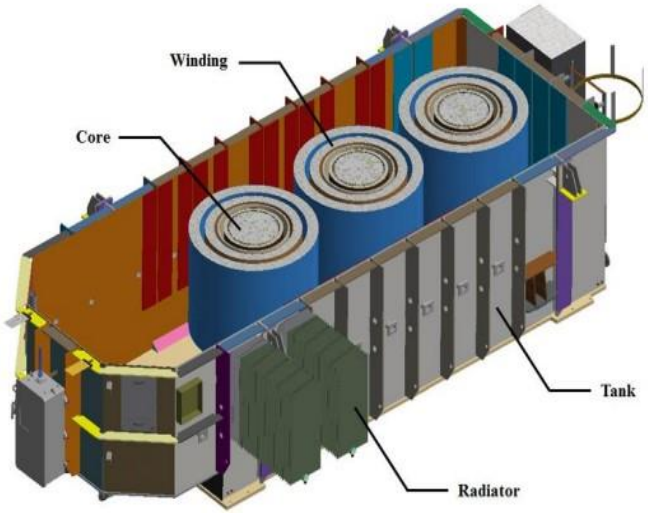

Fig. 1.6: Power Transformer components [9].

1.5.1 Core

The core of a laminated silicon steel core is made up of thin laminations that are individually insulated. Because of the low hysteresis loss and high permeability of the silicon steel core, it is an excellent choice. For the construction of the transformer core, the step-lap approach is used **[10].**

1.5.2 Coils (Windings)

It is constructed of the wire conductors, which are wound around the core and covered with a cellulose-based insulating material, as illustrated in Figure 1.8. Conductors are insulated in order to prevent electrical failure, creep age, and partial discharge from occurring. Insulation paper is a special type of paper that is used to insulate the windings of a machine **[11].** Transformers are separated into many small parts, and each piece is isolated from neighboring conductors using specific polymer-based epoxies in order to reduce the values of eddy currents in the transformers. This application aids in the reduction of eddy current and loss values in windings and capacitors. Every divided conductor, on the other hand, must be transposed for avoid the generation of circulating currents as a result of resistance differences **[12].**

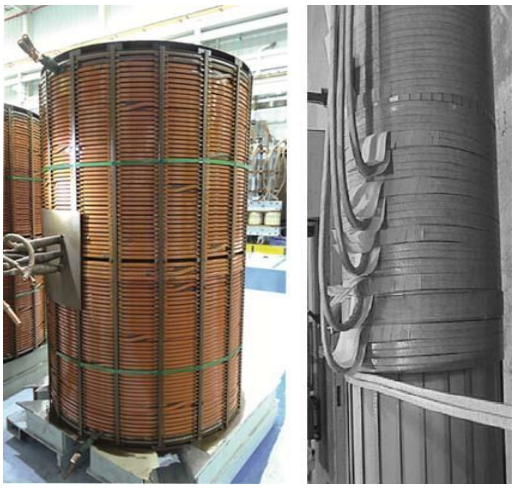

Fig. 1.8. Winding of Transformer [13].

1.5.3 Transformer Housing

The tank is an essential part of transformers. It houses the core, winding, and other vital components and insulating oil. Tank shapes are either cylindrical or cubical according to the transformers construction. A steel-made box as shown below in Fig. 1.9. Before installation, primer and paint are required to protect both the interior and exterior tank's walls against any corrosion or/and erosion (like rust) [14].

Fig. 1.9: The Transformer housing [14].

1.6 Power Transformer Cooling States

There are numerous cooling states that are employed for the cooling of power transformers. Depending on International Electro technical Commission (IEC) specifies [15], there are a four-letter code to indicate the state of cooling in that particular transformer. The first letter refers to the internal cooling media, and the second refers to the mechanism that circulates the cooling fluid. The third and fourth letters are related with the external cooling media and the mechanism that circulates the external cooling liquid. Table. 1.1, show a list of the letters that are used with their meanings.

Table 1.1: A four-letter identifier to identify the cooling state of a transformer [15]

Order	Letter	Meaning
First	O	Mineral oil or synthetic insulating liquid with fire point less or equal to 300°C.
	K	Insulating liquid with fire point over 300°C.
	L	Insulating liquid with no measurable fire point.
Second	N	Natural thermosiphon flow through cooling equipment and in windings.
	F	Forced circulation through cooling equipment, thermosiphon flow in windings.
	D	Forced circulation through cooling equipment, directed from the cooling equipment into at least the main windings.
Third	A	Air
	W	Water
Fourth	N	Natural convection.
	F	Forced circulation (fans or pumps).

A transformer can have multiple cooling states at the same time. For example, an ONAN/ONAF is equipped with a set of fans that can be activated when the system is under heavy load **[15]**.

There are two types of power transformer cooling which are classified as dry transformer and oil-immersed transformer types. These classifications can be expressed as follows **[6]:**

1.6.1 Dry transformer type: Cooling dry transformers exists in two types: natural air exposure (AN) and blower air blast (AB).

a) **Natural Type (AN):** The transformer's heat is cooled by natural air circulation shown in Fig. 1.10. When the temperature of the transformer is higher than the temperature of the surrounding air, the warm air replaces the cold air through the natural convection cycle. It's also referred to as a self-contained cooling system [11].

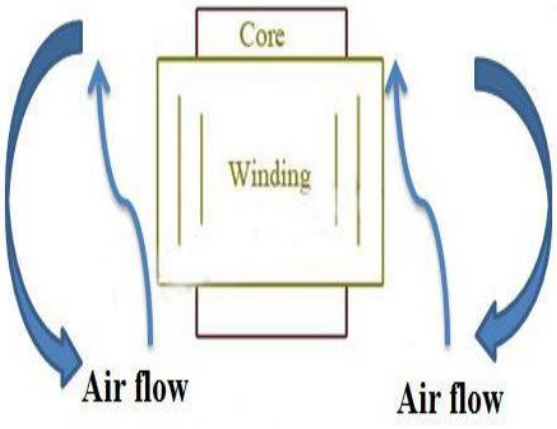

Fig. 1.10: Air Natural (AN) for dry transformer type [16].

b) **Air Blast Type (AB):** The heat produced in this process is cooled by forced air circulation. When the temperature inside the transformer rises above the acceptable standard point, an alarm is triggered, and the fans and blowers are automatically switched (on), the high air velocity is pushed onto the transformers using industrial fans (blowers), thus causing the transformer to cool, as show in Fig. 1.11.

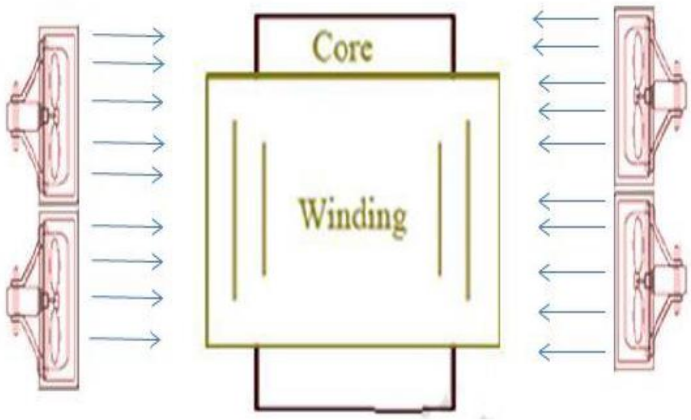

Fig. 1.11: Air blast (AB) for dry transformer type [16]

Air blast is used where fans blow air into the core. On the contrary, a natural way to cool power transformers is by direct exposure to the wind. This type of transformer has a power limit due to higher power losses.

1.6.2 Oil-immersed transformers types

Conductivity of the insulation materials, winding cooling duct dimensions, types of winding, disc width, the spacer thickness, distance between the discs, overall winding dimensions, thermal properties of the transformer oil type, and velocity of transformer oil are the parameters that influence heat transfer **[17]**.

Heat transferred from the transformer windings to the transformer oil is circulated through the transformer radiators to cool the transformer. Conduction, convection, and radiation are all responsible for the heat transmission in the radiators. When compared to convection-type heat transmission, conduction heat transfer type is exceedingly insignificant. Radiation heat transfer, on the other hand, is thought to be insignificant in transformers, according to the literature. If the heat created by the insulation material is not dispersed to the surrounding medium, the substance becomes brittle and eventually breaks down. This allows the conductor material to come into contact with one another, resulting in a short circuit between two adjacent conductors. This causes an excessive amount of electricity to travel between two conductors, resulting in the transformer exploding. This is a catastrophic failure that occurs in the presence of a fire **[17]**. This type of transformer is cooled using some different methods explained below.

a) Oil natural air natural (ONAN) type.
b) Oil natural air forced (ONAF) type.
c) Oil forced air forced (OFAF) type.
d) Oil Directed Air Forced (ODAF).
e) Oil natural air earth (ONAE).

a) Oil Natural Air Natural (ONAN) Type

When it comes to oil-immersed transformers, the ONAN cooling mode is the most basic cooling system. As shown in Fig. 1.12, the heated fluid rises and enters the radiator from the inlet, oil flows via the radiator ducts, and the cooled oil is introduced into the tank through the radiator outlet.

The oil is circulated through the area between windings and core. Natural convection causes air to move across the radiators' exterior surfaces, causing them to heat up. The oil is collected in the upper oil collector pipe and sent into the radiator. Then, through the bottom oil collector line, the cooled oil is transferred into the tank. In ONAN mode, the oil circulation between the transformer and radiator is extremely slow.

Essentially, thermosiphon effect is responsible for the circulation of transformer oil in both the transformer and the cooling radiator. The difference in temperature between transformer oil in tank and transformer oil in the radiator generates a pressure differential, and the pressure difference causes the transformer oil to be circulated [17].

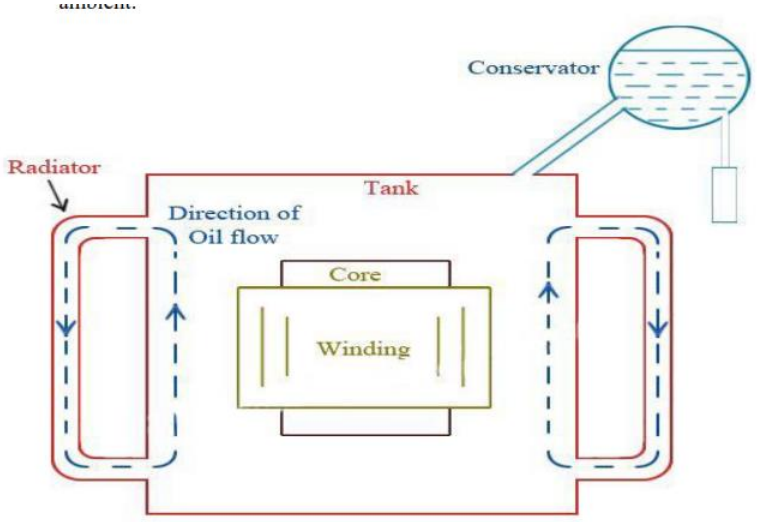

Fig. 1.12: Oil natural air natural (ONAN) cooling of transformer [17].

b) Oil Natural Air Forced (ONAF)

During operation in ONAF mode, fans are directed to the cooling surfaces, while the oil circulates spontaneously within the radiators themselves as shown in Fig. 1.13, air flow rate in this type is greater than that of the natural mode of air flow [18].

The ONAF mode is the most commonly encountered in power transformers. Transformers can be also benefit from the combination of ONAN and ONAF cooling modes. Natural cooling is used in this type of cooling mode until a particular load is reached. Automatic operation of the fans is triggered when the load surpasses a certain threshold. The rate of heat dissipation in ONAF mode is greater than that in ONAN mode [18].

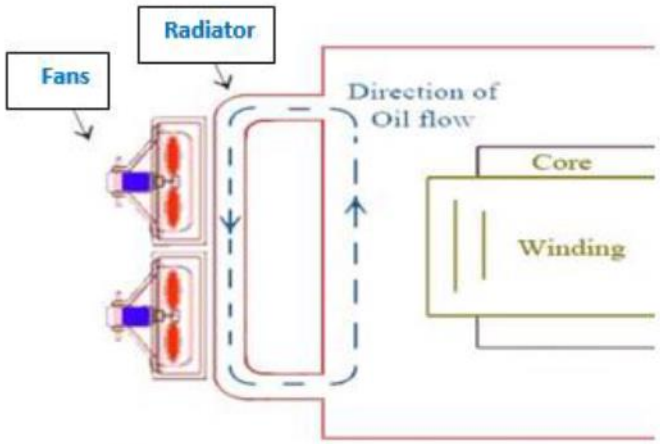

Fig. 1.13: Oil natural air forced cooling of the transformer [18]

c) Oil Forced Air Forced (OFAF) type

When operating in OFAF mode, coolant is moved by pumps and fans. The transformer is forced to circulate oil due to the high temperature. For the aim of cooling the circulated oil, fans are used to drive air into the system as shown in Fig. 1.14, [19].

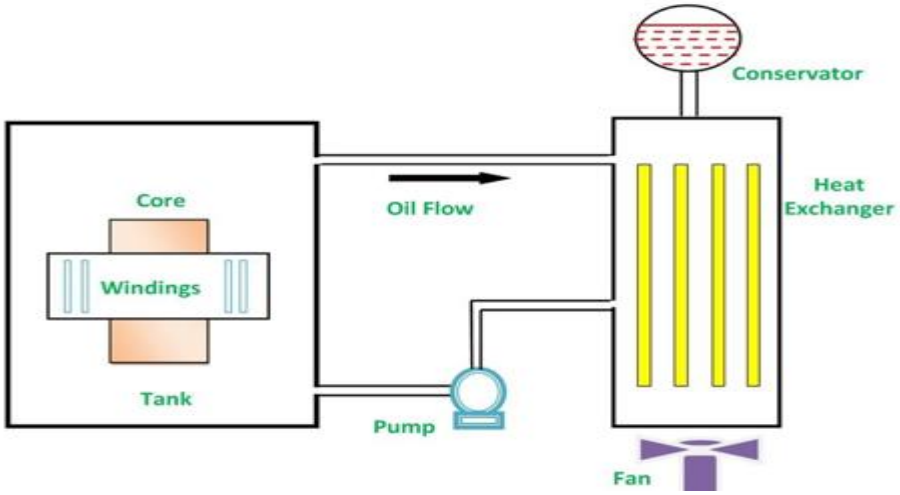

Fig 1.14: Oil Forced Air Forced Cooling of Transformer type [19]

d) Oil Directed Air Forced (ODAF)

In this unique type, oil is directed through the coil ducts, and fans are used in the ODAF mode. The oil is forced to pass through the ducts of large transformer windings. ODAF mode is commonly used in wide capacitance transformers; before the static electricity phenomenon failed with some power transformers, a higher heat transfer rate pattern was used as the pump capacity increased. Static electrification is influenced by transformer oil, temperature, flow rate, friction, surface conditions, pumps, nozzles, and AC / DC moisture content fields. As a result, the pump's choice in the OFAF and ODAF cooling modes is crucial in transformer design. On the other hand, a higher pump efficiency does not always imply a faster heat transfer rate. The two cooling methods OFAF and ODAF, are demonstrated in **[20]**. Oil pushed into the transformer tank in OFAF mode, whereas it is directed to the coil in the ODAF cooling mode, as shown in Fig.1.15. From previous studies (ODAF) is considered the best in cooling and therefore it's relied on this basis in this study.

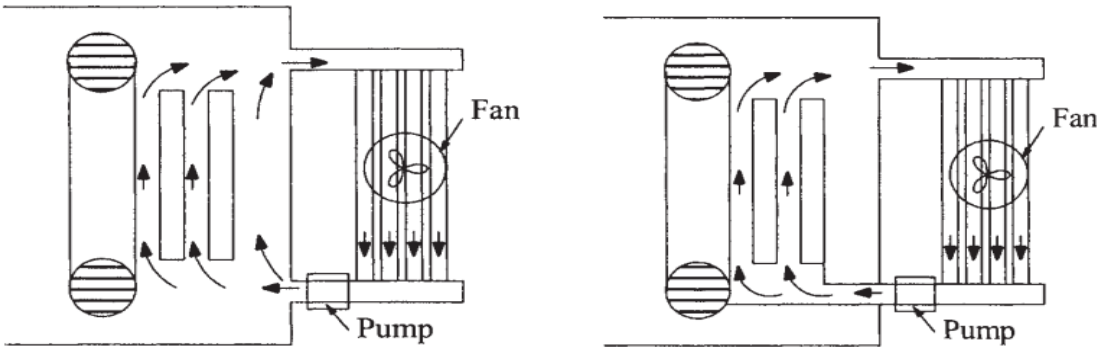

Fig 1.15: The image on the (left) OFAF type and ODAF type on the (right) of an image in cooling modes [20].

e) **Oil Natural Earth Air (ONEA)**

Using the (EAHE) earth air heat exchanger, as shown in Fig. 1.16, which is a tube buried inside the earth at a specific depth so that the earth's temperature is less than the temperature of the atmosphere (during the hot season), it is proposed to cool the power transformer, resulting in a thermal exchange between the tube's outer surface (which is preferred to be made of materials with high thermal conductivity) and the surrounding air. In addition, the location of an air intake fan at the entrance of the pipe allows this new kind to increase the velocity of air inside the tube; as the velocity of air inside the tube increases, the system efficiency (EAHE) and the temperature of the electric transformer both improve as well **[19].**

Several factors improve the efficiency of the system (EAHE), including increasing the pipe length, decreasing the diameter of the tube, increasing the velocity of air, and also decreasing the thickness of the tube, as well as the use of high thermal conductivity materials in the manufacturing pipe **[21]**. The new cooling system technique is comprised of two methods; one is natural air movement caused by natural heat convection, and the other is the use of an air intake fan caused by forced heat convection of air flow.

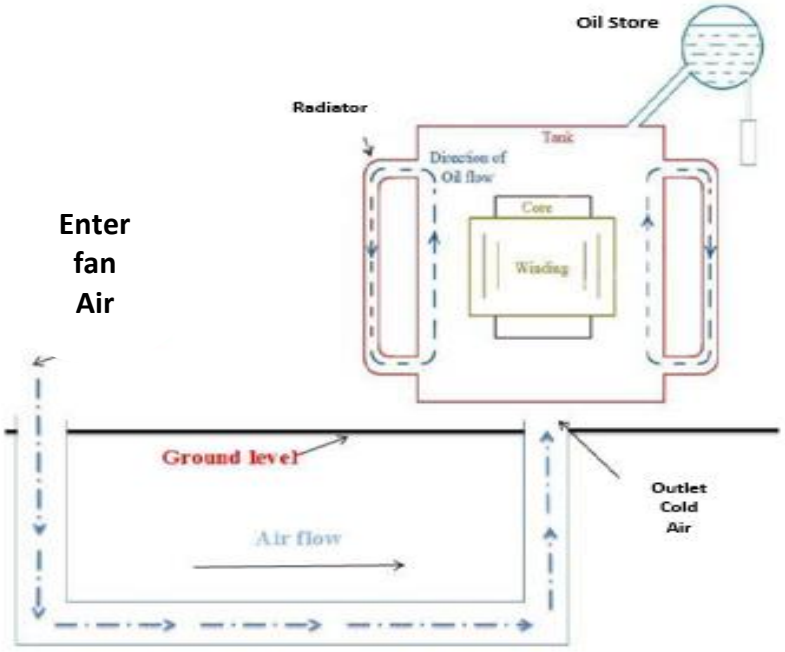

*Fig. 1.16: Type of cooling oil natural earth air (ONEA) for 25kV oil-filled transformers type **[19]***

1.7 Objectives and Overviews

In this respect, the goals of this study may be summarized below.

- Improving the radiator's performance through adding metal foam sponge between gaps of radiator panels.
- Comparing the cooling capacity of the radiator with and without the any of metal foam.
- Optimizing the cooling capacity of the new modified radiator over two different foams porosity (17% and 35%).
- Installing two fans on the radiator's right side and comparing between cooling by two methods (ODAN) and (ODAF) cooling for oil-immersed transformer type.

CHAPTER TWO

LITERATURE REVIEW

CHAPTER TWO
LITERATURE REVIEW

2.1 Introduction

For the purpose of understanding the significance of thermal and hydrodynamic research on transformers, the literature review in this chapter will be examined in depth. Each section will provide a concise summary of the major findings of the investigations. Transformer windings, many studies have been performed regarding the thermal behavior of transformer winding that has been presented in this chapter. Some of the studies on transformer winding hot spot temperature and cooling it were presented, further developments of new methods. Furthermore, a study with complete and slice models is reviewed in this chapter. Then, Studies about transformer oils and alternative cooling fluids are presented in this chapter. On the other hand, Studies on the effect of adding porous media to the outer surface of heat exchanger, such as metal foam sponge. Oil cooling studies in transformer radiator will be investigated experimentally in the light of this study. In this respect, this study plays an important role in characterization of thermal and hydrodynamic properties of transformer cooling systems. Studies about transformer oils and alternative cooling fluids are presented in this chapter.

2.2 Thermal Behavior of Transformer Windings

The higher the evolving temperature levels that are settling in oil-immersed transformer windings at a certain loading rate, the faster the insulation materials will age at that loading rate. Consequently, in order to make an accurate assessment of the component's power rating, it is necessary to have a thorough understanding of the temperature distribution inside the transformer. This knowledge also provides the possibility to reduce costs throughout the manufacturing process. Analytical and empirical methods have been used in the

past and continue to be used to some extent now to forecast the temperature distribution in transmission components and to determine the hot spot.

The aging rate of a transformer is defined as a function of temperature according to IEC Standards (International Electro technical Commission). The transformer's windings are the source of its heat, and the transformer's cooling equipment disperses the heat **[22].**

Rosas et al. (2005) [23] Heat pipes were used to improve the cooling process of electrical transformers immersed in oil. They discovered that if the coolant had a high Prandtl number fluid, the temperature distribution in the discs further downstream could manifest itself as hot streaks from the horizontal ducts outlets. However, fine discretization was required to capture this effect. The physical model was a transformer (75kVA). Thermal and fluid dynamic behaviors in two dimensions were included in the mathematical model. In the actual model, the simulation of the theoretical model is represented as heat generation loss. The experimental results were in excellent agreement with the hypothetical results, both with and without the heat pipes in the cooling process. Using the cooling process, the transformer's useful life was extended (heat pipes).

El-Wakil et al. (2006) [24] the heat transfer and fluid flow parameters of a three-phase step-down power transformer were investigated theoretically. Two windings around a transformer core were chosen to simplify their research. They used six different shapes with the same number of flow rates for oil cooling at the entrance, which was caused by the Joule effect and Foucault currents, which resulted in heat being generated within the transformer by a control volume method for solving the continuity, momentum, and energy equations in the case of steady-state to conclude the complex structure of flow and many rolls appeared at the bottom and top of the transformer. Because of the rolls, they discovered that a successful mixing of the oil resulted in a nearly uniform temperature.

Zhou et al. (2007) [25] Proposed a general model of calculating hot-spot temperature rise for the non-directed flow windings to understand the thermal overshoot phenomenon. The model employs heat transfer and hydrodynamics concepts, taking into account the velocity of the conduct oil flow. And is checked using experimental results obtained for step-changing load current in the cooling mode Oil Natural Air (ONAN), 40 MVA transformer. The study included two cooling modes, 40 MVA (ONAN) and 20 MVA (ONAN) oil natural-air natural. The result of analyses test by simulation on 40 and 20 MVA (ONAN). The researcher found that hot- spot temperature increases overflows due to the change in the velocity of the duct flow lags the difference in power dissipation after load change. He concluded that the overflow effect is greater with more significant disparity between the initialized and the steady velocity.

Torriano et al. (2010) [26] present a numerical study on the temperature distribution, mass flow rate, and condition of the inlet boundaries used in a disc-type transformer. Winding is studied using a commercial CFD code. They arrived at different results from those calculated using the full coupled heat transfer model. Data information from the CFD code used, the temperature profile (regular or irregular) at the input of the coil is a parameter that has a great influence on the prediction of the hot-spot temperature and the paper pressure required to capture this effect. The study results showed much cooling in the coil. The temperature distribution is primarily uniform, and the hot spot factor decreased.

Skillen et al. (2011) [27] The mixed-convection flow of coolant in a low-voltage transformer winding is predicted numerically through the use of an open-source CFD code, which is utilized for studying local hot-spot phenomena in transformer windings. The dielectric coolant fluid has a high Prandtl number, which is a significant characteristic of these flow patterns. In this study, it is discovered that the CFD model predicts the occurrence of hot plumes in certain of the horizontal cooling ducts under examination given the geometry under evaluation. Due to the highly non-uniform mass flow distribution around the

winding, it appears that this is the case. In addition, it is discovered that there is a substantial coupling between the flows in different passages.

Djamali and Tenbohlen (2017) [28] proposed a calculation for recognition of washout (by thermal model) in the fan's one-time step power transformers after the washout event comparing to one hour for each wind current cooling system. They depended on 600 MVA (OFAF) genuine values and 333 MVA (ODAF) energy transformers. By utilizing the algorithm can foresee the washout in the fan of the power transformer.

Radakovic et al. (2017) [29] A dynamic thermal model with low voltage and high voltage compartments mounted in a kiosk with outlet and inlet ventilation openings was proposed for an indoor oil-immersed transformer. The impact of solar radiation and wind speed on the transformer walls is considered. The case study involved a (500kVA) power transformer, and the results showed that the kiosk improved the power transformer's thermal performance.

2.3 Cooling of Power Transformer Windings

After reviewing the transformer coils and the thermal behavior of the transformer coils through previous studies, it should cool the heat generated in windings through maintained the fluid of power transformer under control because excessive heat in the windings directly contributes to the accelerated aging of insulation material **[30].**

2.3.1 Transformer Fluid Performance

Swift et al. (2001) [31] Started that the effect of oil or air cooling convection currents was represented by a nonlinear resistor analogy. The equations of thermal flow for power transformers were presented using an easy equivalent circuit. However, heat input due to losses was demonstrated using a current source analogy. Simultaneously, the heat input due to losses was presented

using a current source analogy. Variable ambient temperature represents an ideal voltage source; the physical experimental model had a capacity of 250 MVA, and the temperature of the hot-spot as measured under real-world conditions

Dejan (2005) [32] Presented new and legitimate strategies for evaluating a transformer's oil temperature, using the heat stir hypothesis and the combined capacitance technique. They found similarities between electrical and thermal resistance in a few regions within the transformer. Likewise, they considered changing the effect of oil consistency, temperature loss, and steady time on an electrical effect transformer's thermal conductivity. Through his investigation, they provided a logical illustration of the warming of hot spots with a numerical correlation with time. Its investigation relied on the ambient temperature, angle, and temperature of the tank's hot-spot temperature to assess the overall hot-spot temperature. The temperature of the oil tubes and the hot spot temperature of the windings were informed using optical fiber tests of (400 MVA ONAF, 80 MVA ONAN, 605 MVA OFAF, and 650 MVA ONAF) while thermocouples were used for (2500 kVA ONAN) and (40 MVA) OFAF) control transformer. The hot-spot temperature expands above the higher oil temperature caused by the heap in the time-dependent control transformers. For ONAN and ONAF cooling techniques, the stable time for upper oil temperature is shorter than the constant time suggested by the examination.

Meshkatoddini et al. (2008) [33] conducted an experimental correlation to predict oil operational life and the remaining lifetime of a power transformer to connect the relationship between the actual age of oil and its multiple specifications specify the appropriate features that can specify aging. Their research was based on the Arrhenius law, which predicted the oil's lifetime. Oil operational life and the remaining lifetime of a power transformer can be calculated utilizing their experimental relationship.

Gastelurrutia et al. (2009) [34] theoretically studied using the ANSYS program on corrugated wall transformers for ONAN cooling (with natural oil and natural air). Three geometries of the ONAN Distribution Transformer Cooling System have been introduced. The original model (Transformer-01) 630 kVA processor. The second model (Transformer-02) was smaller than the first and had more external fins in the corrugated wall. On the other hand, Transformer-03 was larger and had elongated fins. Different flow domains and porosity areas were used. For each model, the temperature was calculated with varying power losses when used. The hottest region of the panel (T9) was found on the inner upper surface. By comparison, the coldest point was measured at the base of a transformer. Moreover, temperature changes were measured according to experimental measurements. The vertical temperature difference was measured on fins at 14 K and 2.5 K laterally to influence the modelling perturbation results. They found that the heat transfer coefficient varies in the vertical direction.

Gholami and Taghikhani (2009) [35] tested a numerical simulation of a 32 MVA power transformer with mode cooling non-directed oil-force (NDOF) and directed oil-force (DOF) by utilizing the limited component technique. Their investigation acquainted new techniques with increment exactness to estimate most hot spot (HST) temperature and position. The results were indistinguishable contrasted, and virtual information tests. The proposed scientific expectation techniques fathomed numerically by utilizing a partial differential equation (PDE). A numerical model relied upon a hypothesis of thermal move and condition of thermal conduction by utilizing the finite element method (FEM) for three measurements to ascertain the temperature at any area in the power transformer.

Diaconu et al. (2010) [36] presented a nearly phase change material (PCM) to analyze natural convection heat transfer in a vertical spirally twisted tube, and

the results were published in the Journal of Heat Transfer. During the investigation, they used a novel type of microencapsulated PCM solution and used a concentration of up to 100 mg/mL. (45 percent). Their research includes the computation of natural thermal convection of water in the presence and absence of microencapsulated phase transition materials in the water (MEPCM). These investigators' findings suggested that during the phase shift period, the PCM's heat transfer coefficient was significantly higher than that of pure water. Additionally, their findings revealed that when (PCM) is used in water, the natural heat transfer coefficient is larger than when (PCM) is not used in water.

Fonte et al. (2011) [37] studied numerical CFD simulation to remove base-type heat in transformers and analyze flow rate distribution. This study, presenting ODAF and ONAF transformer cooling engineering. This investigation was taken into account the properties of oil physics, disc thermal conductivity, boundary state of ODAF type cooling, and boundary state of ONAF cooling. For conduction conditions and limits, include 2D simulation and 3D CFD simulation. They found digital simulations results: Under service conditions, CFD simulations can provide a non-intrusive method for evaluating transformers' thermal efficiency. A detailed distribution of temperature and flux along the windings and the hot spots' position and size can be obtained.

Krishnan and Srinivasan (2012) [38] recommended new estimates of hot-spot temperature and loss-of-life protection in electrical power transformers using a semi-physical model containing environmental variables. Several parameters can be affected by defining the winding hot pot temperature. Ambient temperature, air velocity, higher oil temperature, and the sun's directed heat radiation. They compared their business model to actual data of 100MVA, and the results indicated an important relationship with previous research.

Wittmaack (2014) [39] documented chemical corrosion in electrical insulation to influence transformers' life. Load losses were measured with

Maxwell EMF simulation software. The study aims to predict the temperature distribution using CFDs on cellulose-based insulators. The stable CFD model used in the study contains orthogonal and curved mesh elements organized on the surface. Temperature-based material properties were used—the equations for stability, energy. The study did not present any firm conclusions regarding insulation materials. However, it stated that a reduction in pressure and temperature distribution could be achieved. The heat was obtained from the manufactured simulation, and the input was 398 K at the top of the coil to the output of 379 K.

Shukla et al.(2015) [40] investigated the possibility of increasing the thermal conductivity of power transformer mineral oil by altering the molecular structure of the substance composed of nanodiamonds while maintaining the electrical dielectric and viscosity properties of the oil as a whole. The shelf life of a power transformer was extended by incorporating functionalized nanodiamonds into the mineral oil. As a result, when the volumetric ratio was 0.12 percent, the thermal conductivity improved by 14.5 percent at 40 degrees Celsius. The researchers have reached a 5 percent increase in their findings.

Fernndez et al. (2016) [41] Presented experimental testing for the dielectric paper (Kraft paper) by utilizing two sorts of protecting oil. Vegetable oil and mineral oil, by recreating it in specialized research facilities to record the problem area of oil temperature in control transformer. They found the variety of hot spot temperatures of mineral oil diminished around 20 °C than those registered with vegetable oils. It expands the thermal pressure suffered by Kraft (dielectric paper) inside power transformers when using vegetable oil.

Hasan (2017)[42] increased the cooling performance of a (250kVA) power transformer by employing an oil-based microencapsulated phase change materials (MEPCM) suspension to cool the internal sections of the transformer instead of

pure oil to cool the internal portions of the transformer. Because of its propensity to absorb heat, Paraffin wax is employed as a phase change material in this application. The results revealed that by utilizing (MEPCM), the temperature of the oil was decreased, hence preventing the transformer from failing. The finite volume method (FVM) is used to examine the theoretical model, and the segregated solver is used to solve the equations in algebraic form using the finite volume method.

The effective ambient temperature was taken into consideration when developing the theoretical transformer model. Using (MEPCM) with volume fraction (5–25) percent, the performance of the power transformer and breakdown voltage were improved, according to his research. The melting temperature of phase change material (PCM) should be adjusted to ensure that it is compatible with the operation of an oil power transformer and the surrounding environment.

2.3.2 Radiators Performance and Blowing Direction of Fans

Radiators and fans make up a significant component of the transformer's thermal system, and as a result, they contribute significantly to the weight of the thermal system. It is preferable to have a radiator fan system that is both efficient and lightweight. It is important for transformer manufacturers to lower the number of radiator fans in their systems in order to reduce the weight of the system, without compromising the thermal performance. Nowadays, modern technologies, such as computational fluid dynamics (CFD), make it feasible to practically view the air flow and temperature distribution over the radiators, which is a significant improvement over costly trials. Furthermore, the distribution of airflow provides additional knowledge into how to improve the thermal performance of the system **[43].**

A different investigation, carried out by **Fdhila et al. (2011) [44]** on the cooling capability of radiators in the ONAF state. They carried out CFD

simulations in which they used a porous medium technique to describe the mixed convection between oil and air flows in the radiators and a typical turbulent heat transfer model to model the heat transfer to the air surrounding the radiators. This examination will be carried out using a specific transformer that has been selected. This transformer, as well as the geometry of its CFD model, may be seen on the left and right sides of Fig. 2.1, respectively.

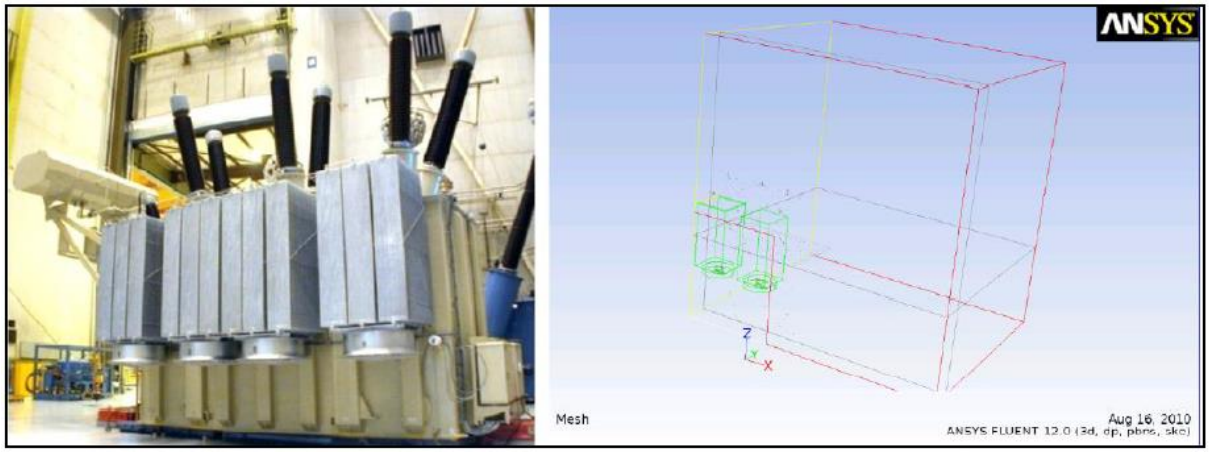

Fig. 2.1: the reference transformer (on the left) with the equivalent CFD model geometry (on the right) [44]

Because smaller fans provide better coverage of the radiator inlet area, the cooling capacity impact of using a greater number of smaller fans while retaining the total air flow was explored. The diameter of the fans was modified from 0.8 to 1.5m, and arrangements of two, three, and four fans were simulated using different fan diameters. There were two possible configurations taken into consideration in the case of the three-fan setup. Figure. 2.2 depicts the outcome of the experiment.

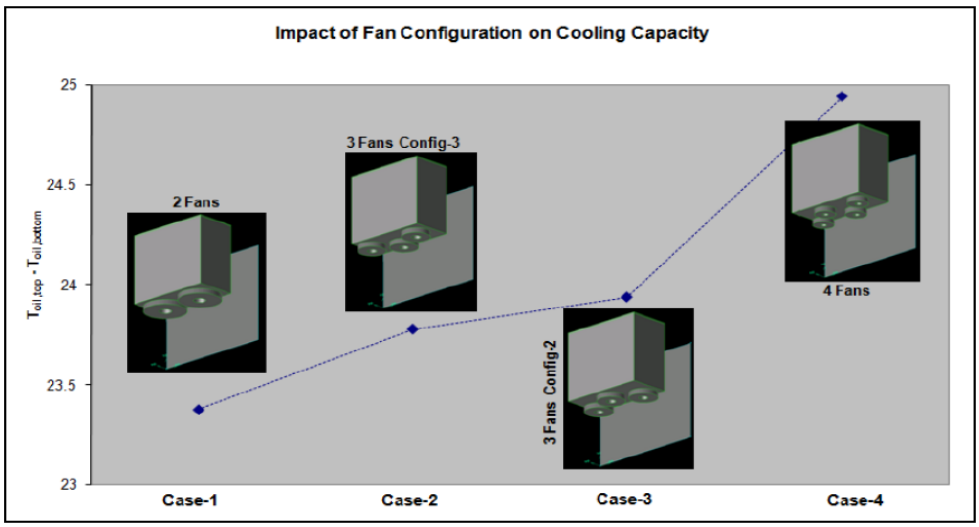

Fig. 2.2: For four different fan designs, the top-to-bottom oil temperature differential was measured [44]

The scientists stated that when the same volume of air is spread by smaller fans, the cooling capacity improves. They also determined that the wall of the transformer tank has some influence on the cooling capacity because the different configurations with three fans produce the same result.

Using funding from the Hyosung Corporation, **Min-gu Kim et al. (2013) [45]** carried out a study on the cooling performance of transformer radiators in the ONAN and ODAN states in order to determine how well they work. Using four radiators with 40 plates spaced 45mm apart and a total length of 3300mm, it was possible to evaluate a layout. In order to predict the cooling capacity of the arrangement, theoretical calculations and CFD simulations were carried out. The results obtained through these two methodologies were compared to those obtained from experimental data. Figure. 2.3, illustrates the experimental setup that was employed.

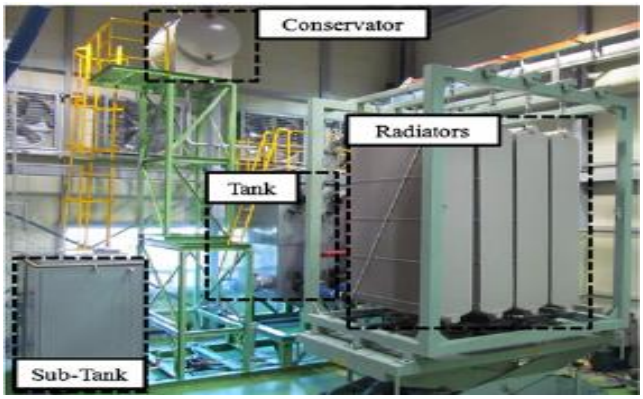

Fig. 2.3: Experimental setup used on [45]

Three experiments were carried out, one of which used thermally driven oil flow (ON – Oil Natural), and the other two of which used oil pumped at varying flow rates (OD – Oil Directed). Because there were no fans utilized (AN - Air Natural), the studies were carried out in ONAN and ODAN, respectively.

During the CFD simulations, a single radiator was designed to reflect the actual geometry of its surfaces while also taking into account the internal oil flow as well as external convection with the surrounding ambient air, among other things. On the Fig. 2.4, below is a representation of one of the temperature distributions that was produced.

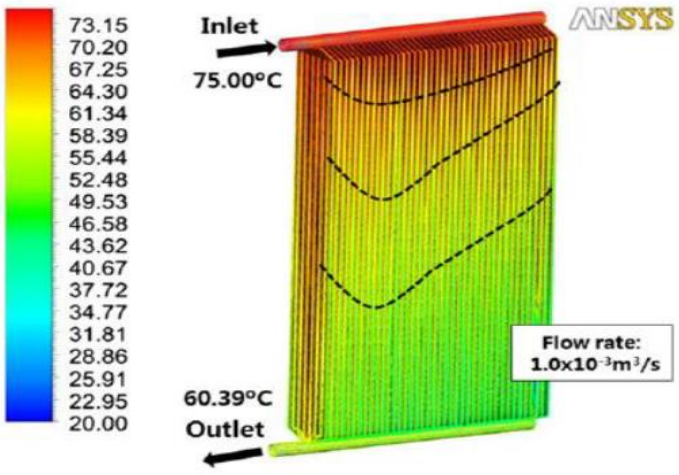

Fig. 2.4: The temperature distribution of the radiator as determined by CFD simulation [45]

Comparing the cooling capacity obtained from testing data, CFD simulation, and theoretical calculations is depicted in Fig. 2.5.

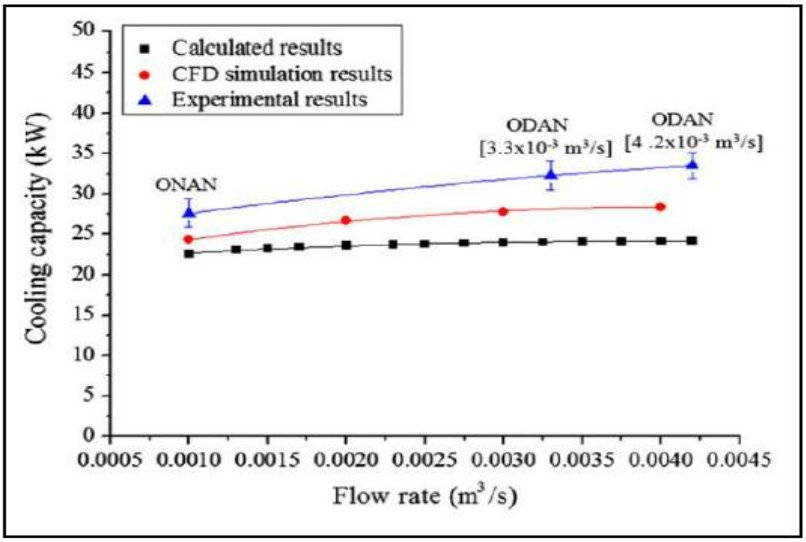

Fig. 2.5: Variations in cooling capability at various oil flow rates [45].

The average differences between estimated findings and CFD simulations and experiments are found to be 13.47 % and 31.6 %, respectively, according to the literature. The authors came to the conclusion that the primary source of their discrepancy was the usage of vertical flat plates with constant temperature in their calculations. It has been found that the cooling capacity obtained from CFD simulations differs by an average of 15.8 % from the cooling capacity obtained from experimental results. The radiation impact was not taken into account in these calculations, and the scientists believe that this is what caused the discrepancy between the simulations and the experimental data.

Paramane et al. (2014) [43] Numerical performance of the radiator mounting in the horizontal and vertical blowing direction of two separate fans at two speeds was investigated. In comparison with horizontal blowing, they determined that the dissipation of heat from the radiator mount discussed here is less efficient, since more air is wasted from the side. Although the vertical blowing setting is theoretically anticipated to have the best efficiency, these CFD studies reveal that horizontal blowing in this particular shape is more effective. This is because to reduced air leaking sideways. Two distinct types of fans have corroborated this (Fan A and Fan B). For horizontal blowing, the heat transfer rate

is up 7.2% and 6.7% compared with vertical blowing for fan A and fan B accordingly.

Paramane et al. (2016) [46] started that the results of experimental and numerical studies on radiator–fan assemblies for ONAN (Oil Natural and Air Natural) and ONAF (Oil Natural and Air Forced) cooling configurations are presented. In the ONAF configuration, air flow over the radiators is studied in two directions (horizontal and vertical) in the ONAF configuration. For the experiments, a custom radiator test facility is being built in-house, and commercial software is being used for the simulations. The experiment is carried out on a group of 5 radiators (each with 27 fins and 2.5 m in height) and 2 fans (of 1 m diameter). In order to investigate the influence of vertical air flow on thermal performance when compared to horizontal air flow, a numerical analysis is carried out. However, they came at the following conclusion based on the work:

1. Heat dissipation estimated from the present numerical model is shown to be reduced when compared to the experimental results, by 17.9 percent for ONAN configurations and 16.8 percent for ONAF (vertical air flow) configurations.
2. The direction of air movement (horizontal or vertical) has a major effect on the temperature field of the oil contained within the radiators.
3. As predicted by theory, the variation in oil temperature with height of the radiator is not linear (as is commonly supposed), but rather exhibits an exponential decline for both vertical and horizontal flow configurations of the ONAN and ONAF (vertical and horizontal flow) configurations.
4. In the current radiator–fan combination, horizontal air flow dissipates heat at a rate that is 6.1 percent greater than vertical air flow.

Garelli et al. (2017) [47] introduced thermos fluid dynamic simulation and analysis for an electric power transformer in an oil natural air force (ONAF) cooling mode. The heat was transferred by two methods in this study: one by the power transformer's radiator, which removed the heat by forced convection. On the other hand, the oil inside the power transformer's tank removed the heat by natural convection. The value of the most important design variables, such as oil velocity, oil temperature, and air temperature, may estimate with reasonable accuracy using the miniature model. Because about half of the transformer radiator is not blown, the air velocity along the body of the transformer by using a fan is not active, according to the theoretical and experimental study. If vertical blowing is expected, the use of a diffuser in conjunction with a superior design of the blades, as well as the use of smaller and more equally dispersed fans, may increase the efficacy of the cooling. On the other hand, the horizontal blowing that has already been investigated in **[43]** and which takes into account an offset of the fans is also worth investigating further.

Chereches et al. (2017) [48] numerically investigated the heat transfer by convection and fluid flow in a thermo-convective circuit with different inlet fluid velocities and some cooling channels to enhance the cooling. They concluded that placing an obstacle near the entrance leads to better cool with lower costs and does not affect the transformer performance with an optimal oil velocity of 1.2 m/s at entry, reducing the heat transfer by convection and fluid flow in a thermo-convective circuit with different inlet fluid velocities and some cooling channels. The study looked at how to cool a three-phase power transformer that was submerged in mineral oil. The volume flow rate in channels, the bulk temperature, the Richardson number, and the Reynold number are all factors that influence oil flow rate and heat transfer.

Radakovic et al. (2017) [49] proposed a dynamic thermal model for an indoor oil-immersed transformer with low voltage and high voltage compartments

located in a kiosk with outlet and inlet ventilation openings. An effect of both solar radiation and wind speed on the transformer walls is considered. The case study involved a (500kVA) power transformer, and the results showed that the kiosk improved the power transformer's thermal performance.

2.3.3 Influence of Fins

At this point, the research focused on the use of passive heat transfer to extend the lifespan of electrical transformers while also reducing their maintenance requirements. The effect of the various forms of the transformer along with different forms and arrangements of the fins on the cooling performing of the electrical transformer has been investigated. Proposed **Nawras et al. (2020) [50]** A 3D numerical simulation to test the cooling performance effects of geometrical and operational parameters of a three-phase electrical distribution transformer (250 kVA of natural air oil (ONAN)) as in Fig. 2.6.

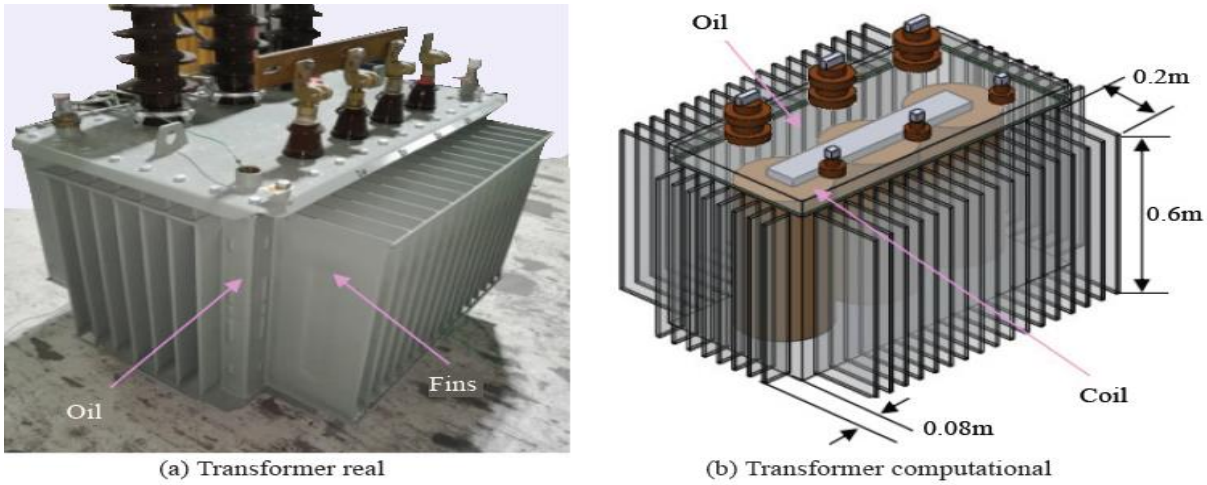

Fig. 2.6: ONAN conventional electrical power transformer with a capacity of 250 kVA [50]

The transformer shapes (rectangular, circular, and hexagonal) as in Fig. 2.7, fin shapes (rectangular, semicircular, and trapezoidal), and the arrangement of the transformer's fins are all examples of geometric parameters that can be measured (asymmetric fin heights and perforated fins).

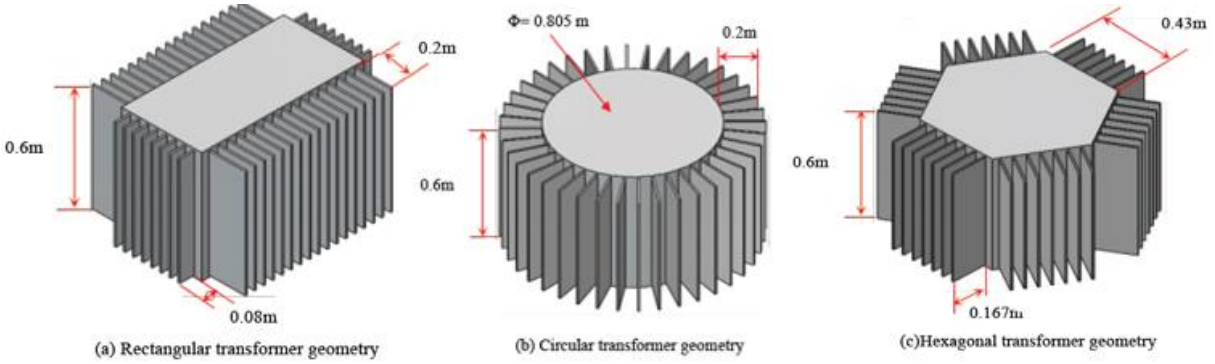

Fig. 2.7: Transformer geometries; traditional rectangular and proposed [50]

The results showed as in Fig. 2.8, that the circular and hexagonal shapes reduced the average oil temperature by 3.4 percent and 4.7 percent, respectively, when compared to the traditional transformer shape (rectangular). In addition, the best thermal performance was achieved with the perforated trapezoidal fin in comparison to other fins. Finally, by using hexagonal transformers with a perforated trapezoidal fin about 12% in comparison with the traditional rectangular transformer, the highest decline in oil was achieved. The shape of the transformer and fins can therefore be concluded as playing an important role in the thermal performance of these systems.

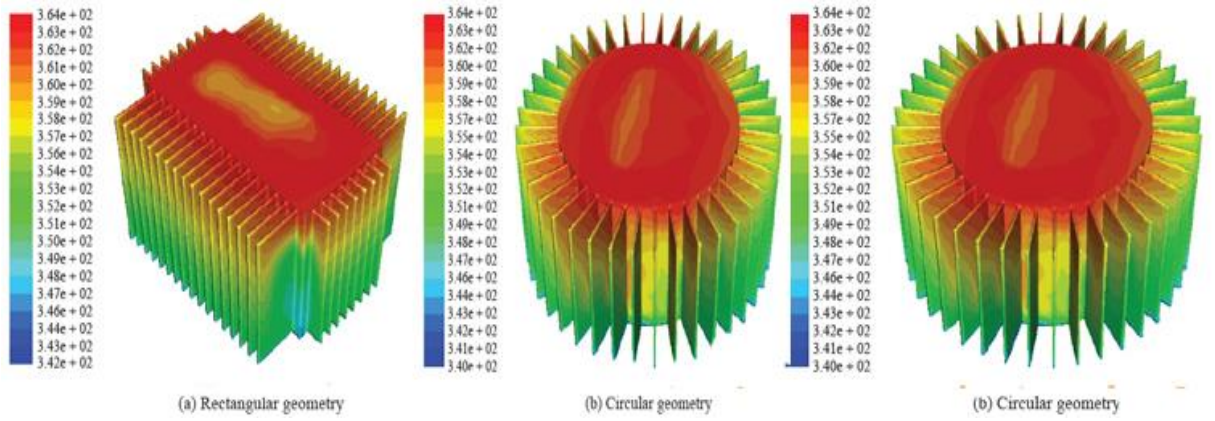

Fig. 2.8: Temperature oil contours for various transformer geometries [50]

2.3.4 Metal Foam Sponge Heat Exchanger (MFHE)

New Methods are being developed in greater depth at thermal design in the literature is accomplished by the use of metal foam sponge in heat exchangers.

Kim, Pike, et al. (2000) [51] experimented on finned heat exchangers using a porous finned aluminum alloy foaming material. The researcher observed a thermal performance similar to the conventional cleft fin's porous fin to measure the heat transfer and pressure drop. The experimental results showed that the porous fins' friction factor with low permeability is much less due to the relatively larger surface area. However, the results indicated that the coated fin had better efficiency at pressure drop. The correlations between friction and heat transfer for the porous fins were obtained using a Darcy number. It was found that the porous fins with low permeability and low porosity were often better than the porous pressure fins with heat exchanger.

Mohammed and Pavel (2004) [52] presented an experimental study on the effect of a porous metal matrix inserted in a tube upon the heat transfer rate. The tube is subjected to a constant flow of heat. This examines the porous matrix's porosity and thickness on the heat transfer rate and pressure drop. They obtained the largest increase of 5.28 times in Nsllet number achieved by total tube filling, at the cost of the maximum pressure drop of (64.8 Pa), and full tube filling where the partial filling has the advantage less rise in pressure drop.

Ken and Anthony (2007) [53] conducted an experimental study using convection heat transfer in aluminum foam sandwich panels. They used the finite element method to validate the numerical model. The effects of the metallic foam core's size are tested experimentally. The effects of the foam thickness on the convective transmission are calculated with four types of metallic foam. They found an improvement in the heat transfer coefficient. They considered the increase in the foam thickness to produce improved heat transfer efficiency, as

evidenced by a more significant load coefficient and the larger temperature difference between the foam surfaces .

Nawaz et al. (2012) [54] used highly porous mineral foams with novel thermal, mechanical, electrical, and acoustic properties in various industrial applications. They indicated the results as follows:

1. Metal-foam heat exchangers (MFHE) can be considerably smaller in volume and lighter in weight over many design spaces with the same fan power and heat transfer capacity.
2. Air and water inlet temperatures and the water mass flow rate do not affect the cost of a metal-foam heat exchanger that matches the heat exchanger output of louvre-fin.
3. Flat tube metal foam heat exchanger costs are sensitive to metal foam's load heat transfer coefficient.

Further experimental research is needed before more accurate estimates of costs can be made available.

Nawaz and Jacobi (2017) [55] focused in this study on aluminum metal foam open cell, which is considered a highly compact replacement for traditional fins in aluminum heat exchangers with braces. This investigation took SEM (scanning electron microscope) techniques to describe the foam and pore diameter properties. Experiments are performed through a wind tunnel with a closed-loop to calculate the pressure drop and heat transfer rate. The different effects of various porosity, fineness, bonding system, base metal, condensation, and frost are considered. From experimental results can be observed. Compared to porous metal foam, the pressure drop was minimal. The rate of heat transfer depends on the metal foam surface area. A more extensive transfer of heat is possible when the surface area is large per unit volume.

Nawaf et al. (2018) [56] studied six different types of heat sinks in aluminum foam attached to a horizontal heated surface. They investigated

numerically under the slot jets cooling impingement. The mathematical synthesis of the current problem is based on the assumptions as follows:

- Flow is laminar, 2D, and incompressible.
- Temperature and velocity profiles around the jet range are uniform.
- Thermophysical properties of the liquid are stable and are obtained at a medium temperature other than density.
- The Boussinesq approximation was used for the relationship between fluid density and temperature.
- In new laminar airflow, the effects of viscous dissipation in the energy equation are neglected.

The flow is designed as a homogeneous porous medium through the mineral foam. The results indicate that metallic foams sticking to the top of the hot surface increase the jet collision cooling compared to the base case (without metallic foam). Due to the relatively high permeability, heat dissipation enhancement is more successful by adding G10 foams than G20 foams.

Shenming et al. (2019) [57] propose a used metal foam heat pipe radiator to improve heat transfer between heat pipe condensed section air. Proto-types of traditional fins and metal foam heat pipe radiators were created to validate the heat transfer enhancement. The effect of pore density in metal foam on heat dissipation capability was discussed. Fig. 2.10, illustrates the structure of a traditional fin and metal foam heat pipe radiator. Traditional fins heat pipe radiators (TFHPR) are made up of three parts: an aluminum substrate, HPs, and flat fins, as shown in Figure. 2.6 (a). HPs have an evaporated section embedded in the aluminum substrate, and HPs have a diameter of 9 mm. Deionized distilled water is used as the working fluid. There are 45 aluminum fins with a total length of 90*300*0.48 mm^3 in terms of the proposed MFHPR, which appear in Fig. 2.9 (b). Fins are replaced with metal foam, which allows for a larger heat exchange area and longer ligaments.

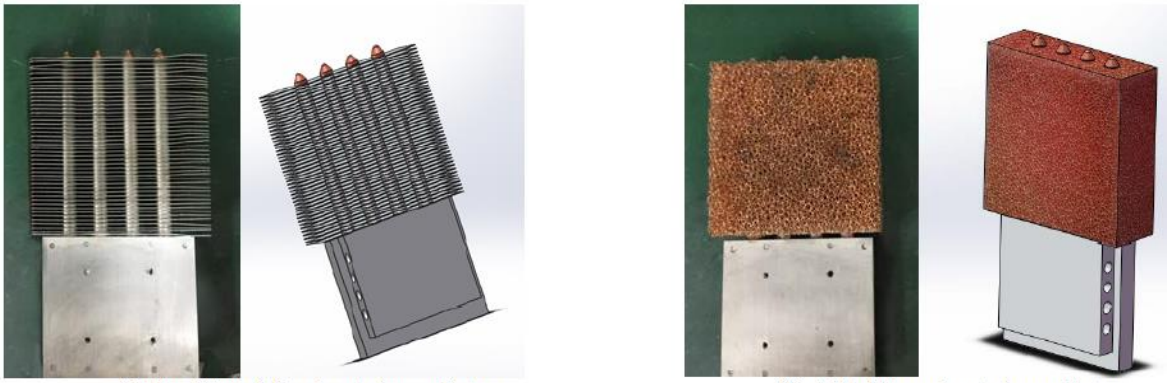

(a) Traditional fins heat pipe radiator (b) Metal foam heat pipe radiator

Fig. 2.9: Sketch of metal foam and traditional fins of heat pipe radiator [57]

Besides, to evaluate the thermal dissipation performance, the thermal resistance of the heat pipe radiator (R_{hpr}) was introduced, which is defined as the heat load of the heat source divided by the temperature difference between the maximum temperature of the heat source and the temperature of the inlet air, as given by

$$R_{hpr} = (T_{hb} - T_a)/Q \quad (2.1)$$

The experiment results showed that the metal foam heat pipe radiator could improve start-up and part-load times compared to the traditional fins heat pipe radiator. When the copper foam's pore density is 5 PPI (pore per line inch), the proposed radiators' thermal resistance could be reduced by 10% when a load of heating is 25W. On the other hand, they found that MFHPR has more excellent dissipation of heat performance than TFHPR. The MFHPR could also quickly achieve a new steady state.

Silva et al. (2019) [58] the transient 3D natural convection problem in horizontally placed rectangular finned heat dispersants was studied using OpenFOAM software. The domain was a closed system, and the investigation was digital using OpenFOAM simulation. The numerical work has been compared to experimental and analytical work in the literature review. Results from using a closed field are as follows:

1. It had little effect on numerical temperature values. It was well compatible with experimental temperature values below 0.7% in the study of convection in heat sinks.

OpenFOAM has proven to be a reliable tool and stands out as an important research tool because it is freely available and open source. OpenFOAM tools may be a good tool for searching inclined heat sinks with fins and fine heat dispersants.

2.4 Summary

Overviewing at the state of the art, it is clear that there have been some intriguing research on the performance of vertical plate radiators; however, a large number of parameters must be investigated in order to completely understand the effect of radiator layouts on cooling capacity. The thermal resistance of the oil was not taken into account in the calculations, despite the fact that it might be significant in the overall heat transmission process. The disparity between the calculated and experimental results is significant, and it is possible that a closer examination of the air convection phenomena will lead to the development of a new correlation that is more appropriate for the radiator instance. Also limited experimental and numerical work has been reported on the cooling performance of power transformer radiators. In past studies, the focus was on thermal design and techniques for preventing hot spot and high oil temperatures. In the current work, a new technique is proposed to enhance the cooling performance of power distribution transformers. This technique involve inserting metallic foam between the vertical radiator panels of the transformer. Table 2.1 shows the tabulated of the literature review.

Table. 2.1: Tabulated of literature review

Reference Name	Reference	Type of Study	Cooling Type	Method of Heat Transfer	Findings
Rosas et al.(2005)	[23]	Experimental	ONAF	Forced	Excellent results, for both with and without the heat pipes in the cooling process. Using the cooling process, the transformer's useful life was extended (heat pipes)
El-Wakil et al. (2006)	[24]	Numerical	ODAN	Forced	Simulated on six different flow rates of the cooling oil with inlet oil value was 338 k.
Zhou et al. (2007)	[25]	Experimental & Numerical	ONAN & NDOF	Natural	Concluded that the overflow effect is greater with more significant disparity between the initialized and the steady velocity.
Torriano et al.(2010)	[26]	Numerical	ONAF	Natural	The results were showed much cooling in winding and the distribution of temperature is uniform and fot spot decreases.
Skillen et al. (2011)	[27]	Numerical	ODAN	Forced	Used inlet mass flow rate to found hot spot.
Djamali and Tenbohlen (2017)	[28]	Numerical	ODAF	forced	By utilizing the algorithm can foresee the failure in the fan of the power transformer. They depended on 600 MVA (OFAF) genuine values and 333 MVA (ODAF) energy transformers.
Radakovic et al. (2017)	[29]	Experimental & Numerical	ONAN & ODAF	Natural & Forced	Investigating thermal design and enhancement in thermal performance and reducing cost.

Swift et al.(2001)	[30]	Numerical	ONAF	Natural & Forced	Utilizing a simple equal circuit on 250 MVA.
Dejan (2005)	[31]	Numerical	ONAN & ONAF & OFAF	Natural & Forced	Presented new and legitimate strategies to assess the oil temperature of a power transformer.
Meshkatoddini et al.(2008)	[32]	Experimental	OFAF	Forced	Determine the appropriate highlights that can indicate maturing in oil.
Gastelurrutia et al (2009)	[33]	Numerical	ODAN	Forced	Temperature Vertical fins = 14 k Temperature Horizontal fins = 2.5 k
Gholami and Taghikhani (2009)	[34]	Numerical	NDOF	Forced	Using (PDE) and (FEM) for three measurements of temperature.
Diaconu et al (2010)	[35]	Numerical &Theortical	ODAF	Forced	When (PCM) is used in water, the natural heat transfer coefficient is larger than when (PCM) is not used in water.
Fonte et al (2011)	[36]	Numerical	ODAF & ONAF	Forced	Through CFD used, enable to evaluate the thermal efficiency without intrusive way.
Krishnan and Srinivasan (2012)	[37]	Theoretical	ONAF	Natural and Forced	Focus on measuring some parameters (surrounding temperature, airspeed, top oil, etc.)
Wittmaack (2014)	[38]	Numerical	ONAF	Natural Convection	Monitor this study to pressure drop and Temperature distribution by used CFD.

Shukla et al. (2015)	[39]	Numerical & Theoretical	ODAN	Forced	The thermal conductivity improved by 14.5 percent at 40 degrees Celsius.
Fernndez et al. (2016)	[40]	Experiment	OFAF	Forced	. They found the variety of hot spot temperatures of mineral oil diminished around 20 °C than those registered with vegetable oils
Hasan et al. (2017)	[41]	Theoretical	ONAF	Forced	Using (MEPCM) with volume fraction (5–25) percent, the performance of the power transformer and breakdown voltage were improved.
Paramane et al (2014)	[42]	Experimental &Numerical	ODAF & ONAF	Forced	The heat transfer rate is up 7.2% and 6.7% compared with vertical blowing for fan A and fan B accordingly.
Fadhil et al (2011)	[43]	Numerical	ONAF	Forced	Applied CFD on Radiator and tried with Four change fans.
Kim et al (2013)	[44]	Experimental & Numerical	ONAN & ODAN	Natural Conv & Forced	The cooling capacity for the ODAN method 20.1 % More than the ONAN cooling method.
Paramane et al. (2016)	[46]	Experimental & Numerical	ONAN & ONAF	Natural and Forced	Heat dissipation estimated from the present numerical model is shown to be reduced when compared to the experimental results, by 17.9 percent for ONAN configurations and 16.8 percent for ONAF (vertical air flow) configurations.

Garelli et al.(2017)	[47]	Theoretical	ONAF	Natural and Forced	The theoretical and test study, utilizing fan isn't dynamic since about portion of transformer radiator isn't blown.
Chereches et al. (2017)	[48]	Numerical & Theoretical	OFAF	Natural & Forced	With extreme temperatures under 98°C, and oil speed of 1.2 m/s,
Radakovic et al. (2017)	[49]	Theoretical	NDAF	Forced	Effect sun oriented radiation and wind speed on (500KVA) transformer.
Nawras et al. (2020)	[50]	Experimental & Numerical	ONAN	Natural	The shape of the transformer and fins can therefore be concluded as playing an important role in the thermal performance of these systems.
Kim and Paek (2000)	[51]	Experimental	Porous Metal	Natural	Porous fin foam: 1- little pressure drop; 2- sometimes used Louvered fin: 1- low-pressure drop; 2- often used
Mohamad and Pavel (2004)	[52]	Experimental	Metal Foam	Natural	The resulting heat transfer rate & pressure drop More efficiency.
Ken and Anthony (2007)	[53]	Experimental & Numerical	Metal Foam	Natural	An aim of this study is to found the amount of heat or thermal efficiency
Nawaz et al (2012)	[54]	Experimental	Metal Foam	Forced	• More heat transfer with effect fan power • The cost is less than louver-fin.
Nawaz and Jacobi (2017)	[55]	Experimental	Metal Foam	Natural	The effects were different (porosity, fineness, bonding system, base metal, condensation, and frost)—the goal to get a larger transfer of heat from the surface.

Nawaf et al (2018).	[56]	Numerically	Heat Sink By Metal	Forced	Enhancement in heat dissipation by adding G 10 foam than G20 foams.
Shenming et al. (2019)	[57]	Experimental	Used Metal Foam	Forced	The experiment results showed that the metal foam heat pipe radiator could improve start-up and part-load times compared to the traditional fins heat pipe radiator
Silva et al. (2019	[58]	Experimental & Numerical	Heat Sink By Metal	Natural Convection	In this case, it's using OpenFoam software and compared the value with empirical & analytical data.

CHAPTER THREE

EXPERIMENTAL WORK

CHAPTER THREE

EXPERIMENTAL WORK

3.1 Introduction

This chapter describes the components and functions of each part of the system used in experimental work. All parts are illustrated with the aim of sketches and images. Thereafter, the proposed modifications by using metal foam sponge are presented with different porosity ratios. Then the effect of using axial fans to achieve force convection are presented. The experimental procedure and preliminary calculations described at the end of this chapter.

3.2 Rig Layout

Hot oil flows vertically in radiator plate channels. The forced convection heat transfer of oil will be achieved by circulating oil utilizing a pump. Heat transfer in the plate wall by conduction to the metal foam sponge, and heat transfer to ambient air by either natural or forced convection. In case of forced convection, fans are positioned at the right side of the radiator panels.

In either kind of heat transfer for the present system, oil is directed using a pump to circulate it. Simultaneously, air works once as natural by allowing it to flow through panels without using any blowing, which is called oil direct-air natural (ODAN). While in the second case, air is forced to flow through radiator panels using one or two fans which is called oil-direct air forced (ODAF). Rig is built using many parts, as shown in Fig. 3.1. The main components are detailed below.

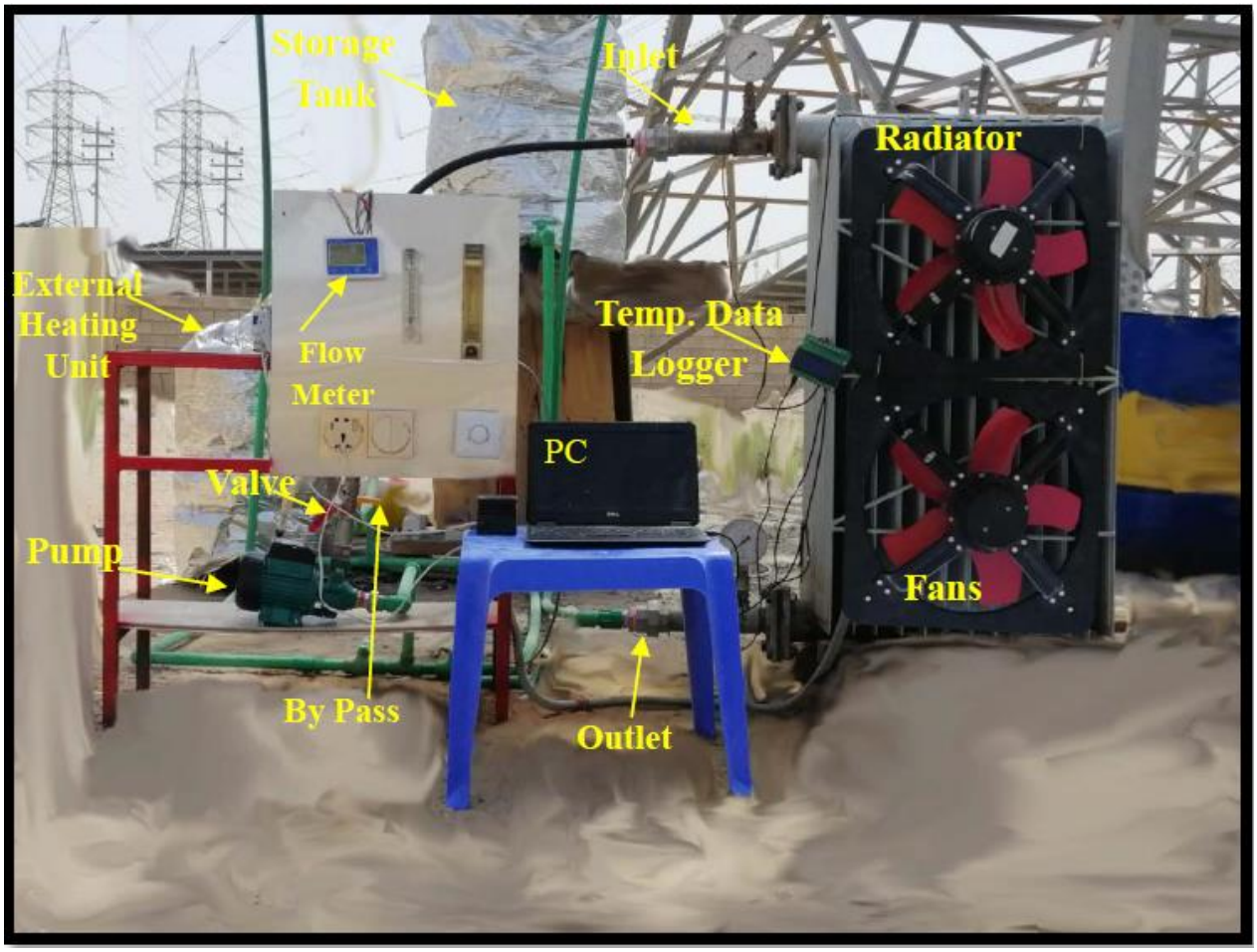

Fig. 3.1: Experimental rig.

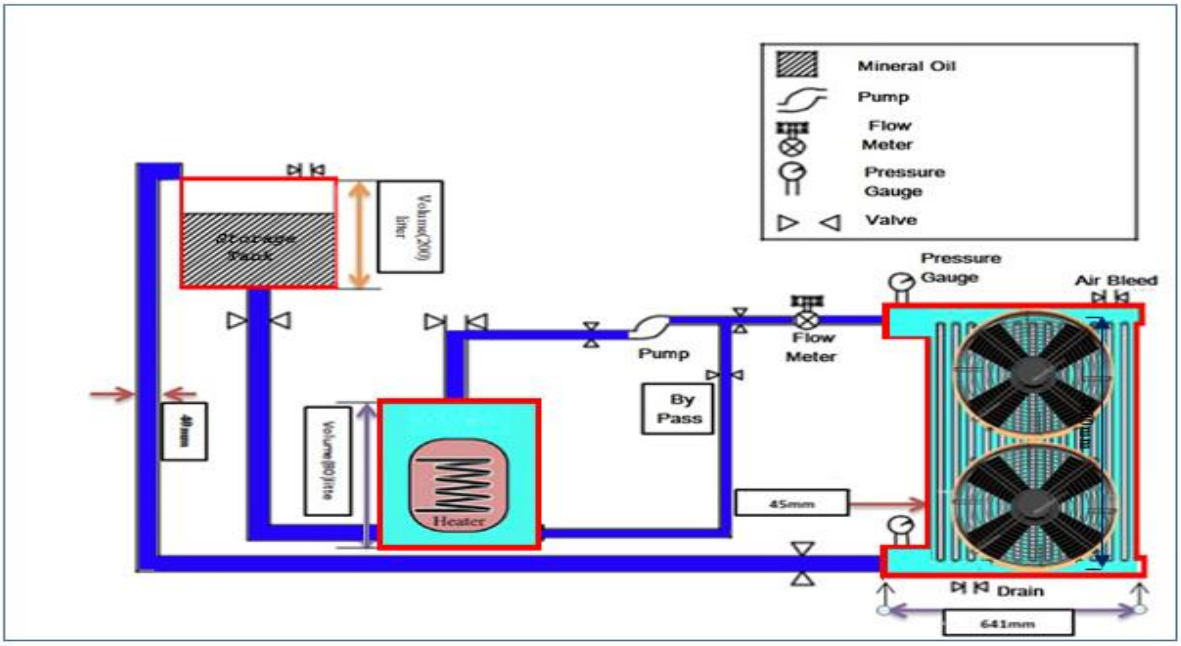

Fig. 3.2: Feeding system piping and instrumentation diagram

3.2.1 Transformer Radiator

The radiator installed in experimental rig is a part of "Oil-immersed transformer, made by Iran-Transfo Company, according to (TOZIE IRAN TRANSFO ZANGAN/ CO.(P.J.S)), Type - TSUE6346,

N0. S0680543, Year 2008, Standard IEC-60289, 60076" **[69].** The radiator consists of thirteen panels with a smooth inner surface. The outer surface is coated with protection paint film to protect services from corrosion and surrounding conditions.

The radiator used in the experimental rig consists of the details tabulated in Table. 3.1, the Radiator is utilized as a heat exchanger with air to cool the hot oil. Vertical radiator panels are made of carbon steel, with total thermal conductivity of 54 W/ m. K **[56].** The radiator has two header pipes with length (641 mm) and thirteen semi-circular sections of (12 mm) in width. At the center, which decreases to reach (3mm) by the edges, the first is positioned at the top of the radiator. The second is positioned at its bottom. Both header pipes are welded to the radiator panels. The diameter of the header pipes is 82.7 mm. The geometry of the radiator is shown in Fig. 3.3.

Table. 3.1, Transformer radiator specifications

Specification	Dimensions
Panel Length, mm	1000
Element space, mm	45
Panels thickness, mm	1.2
Thermal conductivity,(K_{steel})W/m. K [56]	54
Top & bottom header diameter, mm	80
Panels number, __	13
Channels number for each panel,__	7
Panel width, mm	520
Channel width, mm	60
Oil total volume, liter	70

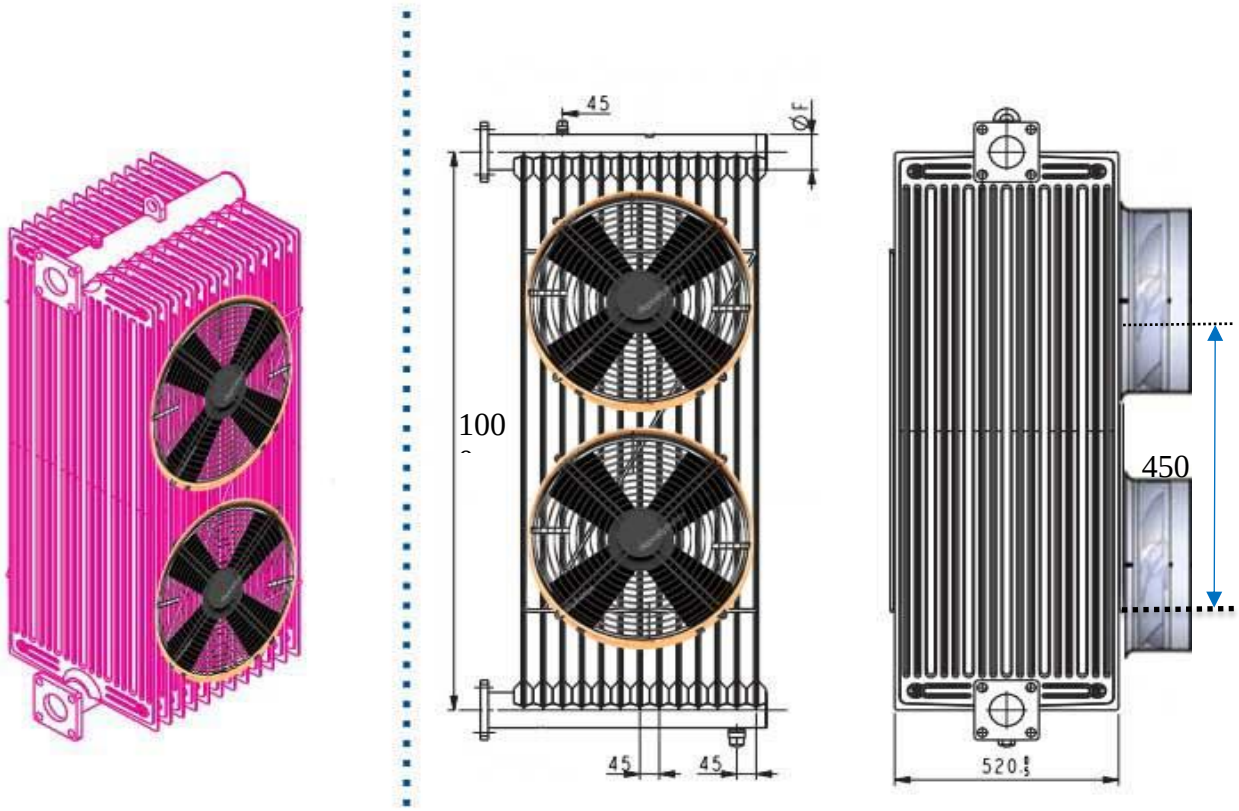

Figure: 3.3. Transformer radiator sketch with thirteen vertical panels and two fans (all dimensions in mm).

3.2.2 Mineral Oil

Oil used in the present experimental work is manufactured by Nyans oil Company **[70].** The oil is IEC 60296 Edition 5.0, including those for particular applications. Nynas Oil Company was developed and formulated to provide high resistance to degradation and excellent oxidation stability for a longer transformer life and less maintenance. The oil has been designed specifically for use in oil-filled electrical equipment, such as power and distribution transformers, rectifiers, circuit breakers, and switchgear. Heat transfer is exceptional. This high grade has excellent heat transfer characteristics due to its low viscosity and viscosity index, ensuring that heat is efficiently extracted from the core and windings. This grade was developed and formulated to provide exceptional resistance to oil degradation and excellent oxidation stability to increase transformer life and low maintenance.

Low-temperature properties are excellent. The transformer's naphthenic characteristics allow it to start at the lowest possible temperature without pour point depressants. Dielectric strength is extremely high. When stored and treated properly, this insulating oil meets and exceeds the most stringent dielectric strength requirements. The properties of the oil are calculated using Eq. 3.1 to 3.5. **[71]** As below.

$$\rho_{\text{oil}} = 868 \times [(1 - 0.00064) \times (T - 20)] \quad (3.2)$$

$$k_{\text{oil}} = -(0.000077 \times T) + 0.132949 \quad (3.3)$$

$$c_{p_{\text{oil}}} = (3.4566 \times T) + 1796.5 \quad (3.4)$$

$$\mu_{oil} = 1.433 \times 10^{-7} \times \exp\left({}^{3479.5}/_{(T + 273.15)}\right) \quad (3.5)$$

Where;

ρ_{oil} is density in (Kg/m^3).

k_{oil} is thermal conductivity in (W/m.K).

$c_{p_{\text{oil}}}$ is specific heat in (J/kg.k).

μ_{oil} is dynamic viscosity (Pa.s).

3.2.3 Feeding System

This current work tried to simulate the reality of the situation as if it were a real transformer. Therefore, an external heater is installed to heat the oil at different temperatures, pump to circulate the hot oil, fans, storage tank, pipes line connection, metal foam, and measurement instruments (flowmeter, anemometer, and temperature sensors).

3.2.3.1 External Heating unit

A galvanized tank, 60 liters, and insulated with a thick layer of fiberglass, is used to keep the working fluid at a constant temperature in experimental work. An electric heater was (Rico type, 3000W, 220V), fitted to the tank. The heating element with length and diameter of 300mm and 8mm, respectively. The heater

is provided with an automatic element (thermostat) that for limited the desired temperature.

3.2.3.2 Pump

The electrical Centrifugal Pump with specifications described in table 3.2 is used to circulate the oil through the experimental rig. This type of pump is used previously with such experimental test **[56]** and showed its adequacy. The pump is used to achieve oil-direct (OD) circulation through the testing rig and direct hot oil to the radiator top header.

Table. 3.2 Pump specifications

Model	QB60L1 CE
Voltage/Amber	220V /50H_z 2.7A 0.37KW 0.5HP
Q. max.	40 l/min
H max.	33 m
Model Number	19072220351
Max. Ambient Temperature	45 ^oC
Pump speed	2850 r.p.m
Continuous duty	Thermally protected

3.2.3.3 Fans

Two axial fans were installed on the transformer radiator. The specifications of fans are illustrated in table 3.3. The fans are attached on the right side of the transformer radiator to improve coverage. Thereby, cooling capacity increases if the same quality of air is spread more evenly with a more significant number of fans.

Table. 3.3 Fan specifications

Voltage/Amber	220V /50H_z 0.7A
Q. max.	2000 m^3/h
weight	6.4 Kg
Speed	1400 r.p.m
Diameter	400 mm

1.2.3.5 Storage Tank

In the present work, a cylindrical shaped storage tank of 200 liters volume is used to store the oil to ensure that the transformer radiator and feeding system is filled with working fluid (mineral oil) continually. The tank receives the cooled oil returned from the radiator and delivered to the external heating unit.

1.2.3.6 Pipelines

A 3/4 inch diameter polyvinyl chloride (PVC) pipes are used to connect the feeding system and deliver working fluid to and from the transformer radiator. This type of pipes is used for its high flexibility, resistance to corrosion and heat resistance. In addition, to its little interaction with external conditions for a good quality insulator with thickness reaches to 2 mm. Figure. 3.2 shows the piping and instrumentation diagram for the feeding system pipeline.

1.2.4 Measurement Instruments

In these experiments, four types of measurement equipment have been used. These equipment may be classified according to their respective functions as following:

3.2.4.1 Oil Flow Meter

A 13mm fuel oil flow counter diesel gasoline Gear flow sensor is used to measure the oil quantity that passing through as Fig. 3.4. The device is located between the pump and the inlet of the transformer radiator. The specifications of the flow meter are flow speed range and total setting (0.1-9999 liters. The power input is DC 12-24V. Accuracy is ±0.5%, and the operating voltage range is DC 24V ± 8V / 1A.

Fig. 3.4: An image of oil flowmeter [72]

3.2.4.2 Temperature Data Logger V2

An eight-channel temperature data logger V2, shown in Fig. 3.5, is used. Six calibrated temperature sensors were distributed on the surface of the radiator and at an inlet and outlet of the radiator. The specifications of the data logger are shown in Table. 3.4. The locations of sensors are sketched and depicted in Fig. 3.6 and 3.7, respectively.

Fig 3.5: Temperature Data Logger V2 and sensors [73]

Table. 3.4: Temperature Data Logger V2 specifications

Model	DS18B20
Power circuit	USB power supply
Temperature sensor material	stainless steel tube size: 6x50 mm
Temperature range	-55 ~ 125°C / -67 ~ 257°F.
Device dimensions	(98mm x 82mm x 30mm)
Accuracy	±0.5°C/ (-55 ~ 125°C / -67 ~ 257°F)
Resolution	0.1°C / 0.1°F

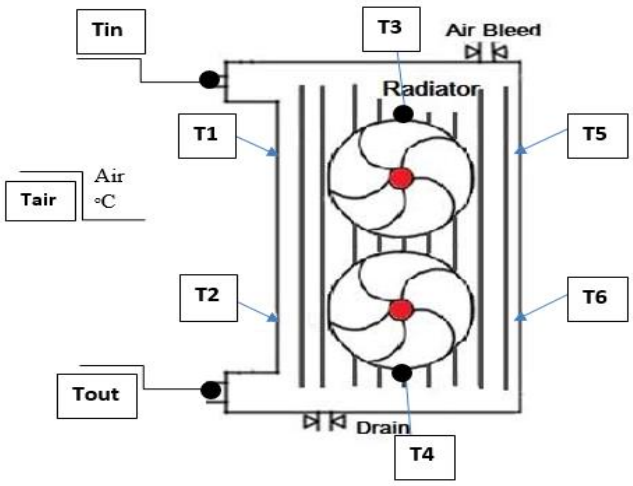

Fig. 3.6: A sketch of the radiator with temperature sensors location, specification, and position as flowing in Table. 3.7.

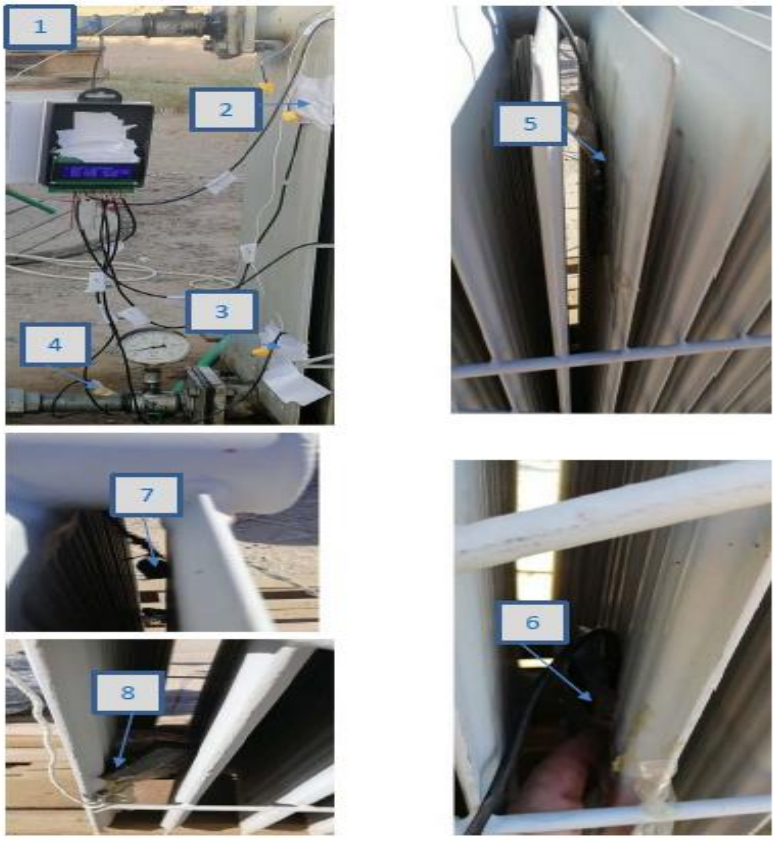

Fig. 3.7: Temperature sensors and thermocouples location on the cooling system

3.2.4.3 Thermometer data logger

This data logging thermometer used to measure the temperature of different points at the surfaces of the radiator utilizing calibrated thermocouples of type (K). Three thermocouples were used, two at the end panel on the radiator and the other to measure ambient air temperature. The device is shown in Fig. 3.8; all specifications are tabulated in Table. 3.5. Furthermore, the position and function of the temperature sensors utilized for both thermometers are tabulated in a Table. 3.6.

Fig. 3.8: Thermometer devises with thermocouple sensor [74]

Table 3.5: Thermometer device specification

'Display Type	LCD
Item Weight	0.280 kg
Measurement Accuracy	±0.4
Model Number	SD-947
Power Source Type	(1.5 V) X 6 Batteries
Temperature Range	-199.99-850.0 degrees_ Celsius
Height	45 mm
Length	177 mm
Width	68 mm

Table. 3.6: Temperature sensors position and function

Number of Location	Position of Sensor
Tin	Inlet oil temperature
T1	Upper of the first plate at (15 cm) from top of center oil collector
T2	Bottom of the first plate at(15cm) from down of center collector
Tout	Outlet oil temperature
T3	Upper of the sixth plate at (15 cm) from top of center oil collector
T4	Bottom of the sixth plate at(15cm) from down of center oil collector
T5	Upper of the thirteenth plate at (15 cm) from top of center oil collector
T6	Bottom of the thirteenth plate at (15 cm) from down of center oil collector
T air	Measuring the surrounding air

3.2.4.4 Anemometer

An AM-4206M anemometer, shown in Fig.3.9, is used to measure the wind speed to predict the average air speed with natural heat transfer convection. In the case of forced heat transfer convection, an anemometer is used to measure the air speed produced by using fans after passing through the radiator panels. The range of speed reading of the anemometer was 0.1 to 30 m/s, with an accuracy of (±1.8%); where its calibrated the anemometer in the present (rig) used is calibrated with (Davis weather station), based at "10 m" above the ground of Najaf- technical engineering college- Iraq

Fig. 3.9: Airflow meter device (anemometer)

3.3 Metal Foam Sponge

Metallic foams are structurally described by their cell topology, whether open or closed, relative density, cell size, form, and anisotropy. The microstructure of open-cell materials with a high porosity is often composed of small ligaments forming a network of interconnected dodecahedral-like cells. A shape and size for these open cells varies in the medium, creating a random and anisotropic structure as Fig. 3.10. Metal foam is described by the following geometrical and physical parameters [75]:

i. The pore density is defined which as the number of pores that can be measured in a linear inch, and its unit is PPI (pores per linear inch).

ii. The pore size, denoted by (d_p), is defined as the equivalent diameter of one of the dodecahedron unit's faces. As a result of the nominal pore density (PPI), the average pore diameter, (d_p), can be determined as follows [76]:

$$d_p = \frac{25.4}{PPI} \quad (3.6)$$

iii. Specific surface area (αsf), represents the surface area of the foam In contact with heat in a given volume of foam. A greater specific surface area leads to a great fluid/ metal contact area. Which in turn will increase turbulence created by foam passageways, thus increasing heat transfer. Finally, a more efficient heating exchange will be achieved in less volume.

$$\alpha sf = \frac{S}{V} \quad (3.7)$$

Where;

S is the total surface area m^2 inside the unit cell

V is unit cell volume m^3

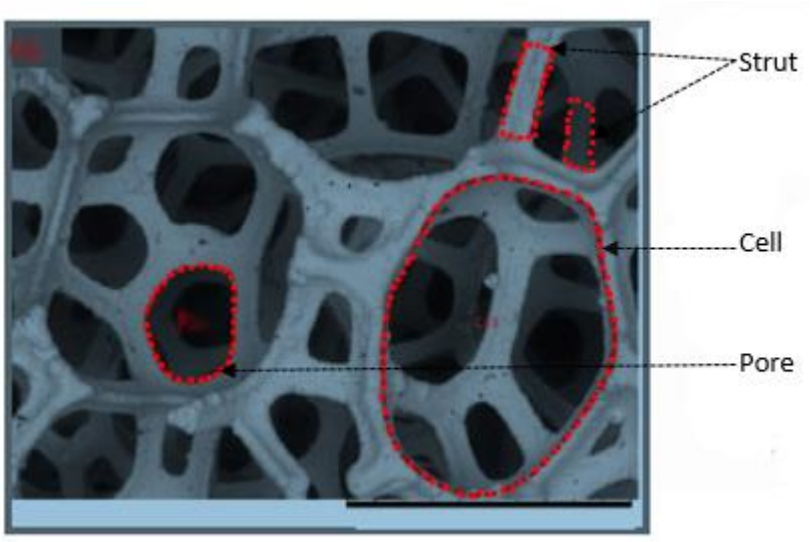

Fig. 3.10: A typical image of metal foam [76]

iv. porosity

Porosity plays a crucial role in heat transfer behavior. Porous media focused on many researchers over the past decades who are interesting in heat transfer enhancement. Metal foam has been recognized as a viable option in various thermal engineering applications due to its distinctive characteristics such as high

surface area density, low weight, and ability to mix fluids [77]. Porosity (void volume fraction, ε) is ratio of the void volume to total volume [76] and [78].

$$Porosity\ \varepsilon = \left(\frac{Vv}{Vt}\right) \times 100\% \qquad (3.8)$$

$$V_v = Vs - V \qquad (3.9)$$

Where;

ε is the porosity.

V_v *is* void volume.

V_t is total volume.

Vs is solid volume.

V is a volume of metal in laboratory pote

Transformer radiator used in our experimental work consists of thirteen panels, which means there are twelve gaps between panels. A Metal foams sponge is crammed in these gaps in two stages. First stages, where 240 pieces of metal foam sponge are distributed evenly all over the radiator, (20) pieces for each gap. In this case, the porosity calculated depending on the above equations is found to be 17%.

On the second stage, the metal foam sponge is doubled (40) pieces per gap with 480 pieces in total. The added pieces are crammed in spaces between the pieces crammed at the first stage. In this case, porosity reached 35%. Figure 3.11, shows a sketch of the transformer radiator with crammed metal foam sponge. All details of porosity calculations are in appendix B.

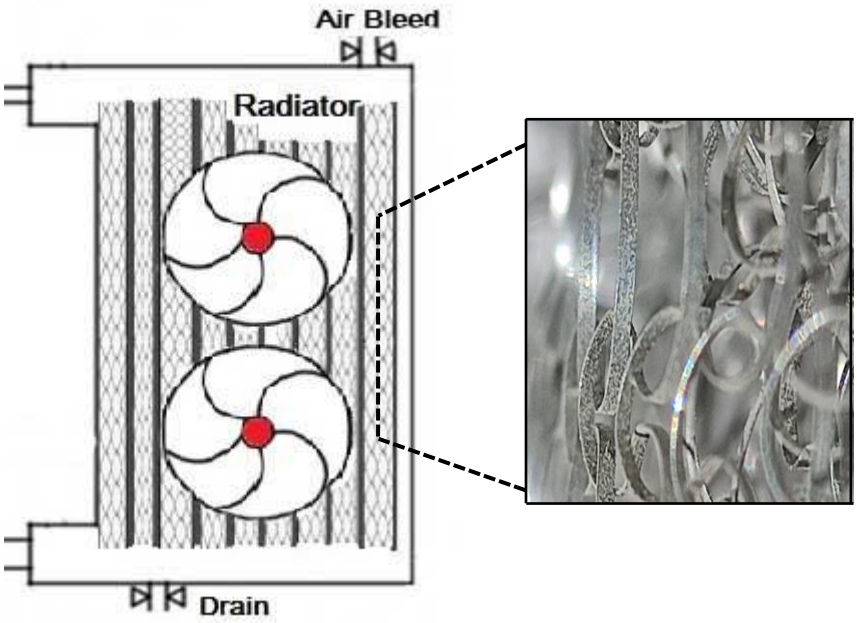

Fig. 3.11: Sketch for radiator crammed with metal foams sponge

3.4 Preliminary Calculations

The experiments results can be computed transformer radiator cooling for two different oil-direct air natural (ODAN) models and oil-direct air forced (ODAF).

Cooling capacity may computed from the following equation [55]:

$$P_{\text{radiator}} = \dot{m}_{\text{oil}} \cdot c_{p_{\text{oil}}} \cdot (T_{\text{in}} - T_{\text{out}})_{oil} \quad \ldots\ldots (3.6)$$

Where;

P_{radiator} is a cooling capacity in (W).

$T_{\text{oil; in}}$ and $T_{\text{oil; out}}$ are inlet and outlet temperature in (^{o}C).

$\dot{m}_{\text{oil}}$ oil mass flow rate in (Kg/s).

$c_{p_{\text{oil}}}$ oil specific heat in (J/kg.K)

On the other hand, mass flow rate used in experiments of (0.0167, 0.0333, and 0.05Kg/s), where equivalent to (1, 2, and 3l/min) as flowmeter scale used.

Therefore, from one preliminary case calculation for this study, it can be indicated the data as the below table.

Table. 3.7: Calculation of experimental results for one case of ODAF mode

Test specification	Symbol	used values	Calculated value
Time (min)	t	60	----
Average ambient temperature (°C)	$T_{ave, amb}$	40	----
Average fans speed (m/s)	V_{ave}	6.5	----
Average inlet oil temperature (°C)	T_{in}	70	----
Outlet oil temperature (°C)	T_{out}	41.5	----
Temperature difference (°C)	ΔT	28.5	----
Average oil temperature (°C)	$T_{oil, ave}$	55.75	----
Volumetric oil flow rate (LPM)	Q_{oil}	1	----
Mass flow rate (Kg/s)	$\dot{m}$	$1.67*10^{-2}$	----
oil specific heat (J/kg.K)	$c_{p_{oil}}$	----	1989.20545
Heat Transfer (W)	$P_{radiator}$	----	946.7623339

3.5 Operating Procedure:

In order to minify reused and take more accurate readings, the following procedures must be followed.

3.5.1 Checking Pipelines and Panels

Checking all pipelines, valves, and fittings must be done before each run for the rig. First of all, all pipes and fittings must be visually checked for any apparent defects or leakage. Furthermore, instruments must be checked to ensure that fully performers with all electrical connections are in place and secured. Finally, the storage tank must be checked for the oil level, and it is enough to fill all pipes and radiator panels with an additional quantity.

3.5.2 Experimental procedure

1. After completing the checking procedures, the experiment is now ready to be held. First of all, all the system must be filled with oil, and open each of (main oil tank, pump, bypass, air bleed, exit radiator, and outlet valve).
2. Put the oil pump on and ensure all the system is filled with oil without any visible air bubbles. Subsequently, check the flowmeter if it is run, go to adjust each one of (Adjust the bypass valve to make sure the flowmeter is on the correct reading progress, and adjust oil pump valve to control oil quantity passing through a radiator by a flow meter)

3. Check the heating unit and put the thermostat on the requested degree. Thereby, start the pump, make sure the oil is circulating, and check the temperature sensors and ensure that the oil inlet to the radiator is at the required oil temperature.

4. Recheck the rate of oil flow through the flow meter. After all, they are checked. Then we start taking readings every ten minutes and wait until the case becomes steady-state with continuous readings each one parameters of (an ambient temperature, wind speed, inlet and outlet temperature, and temperature on the panels of radiator)
5. Recheck the system to change the parameters and start taking a new reading. These parameters that are required to be changed which involves each of (volumetric flow rate, inlet oil temperature, fan speed, and metal foam).
6. Finally, after taking the readings for all cases, close the system, the valves, electrical, and finish the work for this day.

3.5.3 Operation Procedure Flow Chart

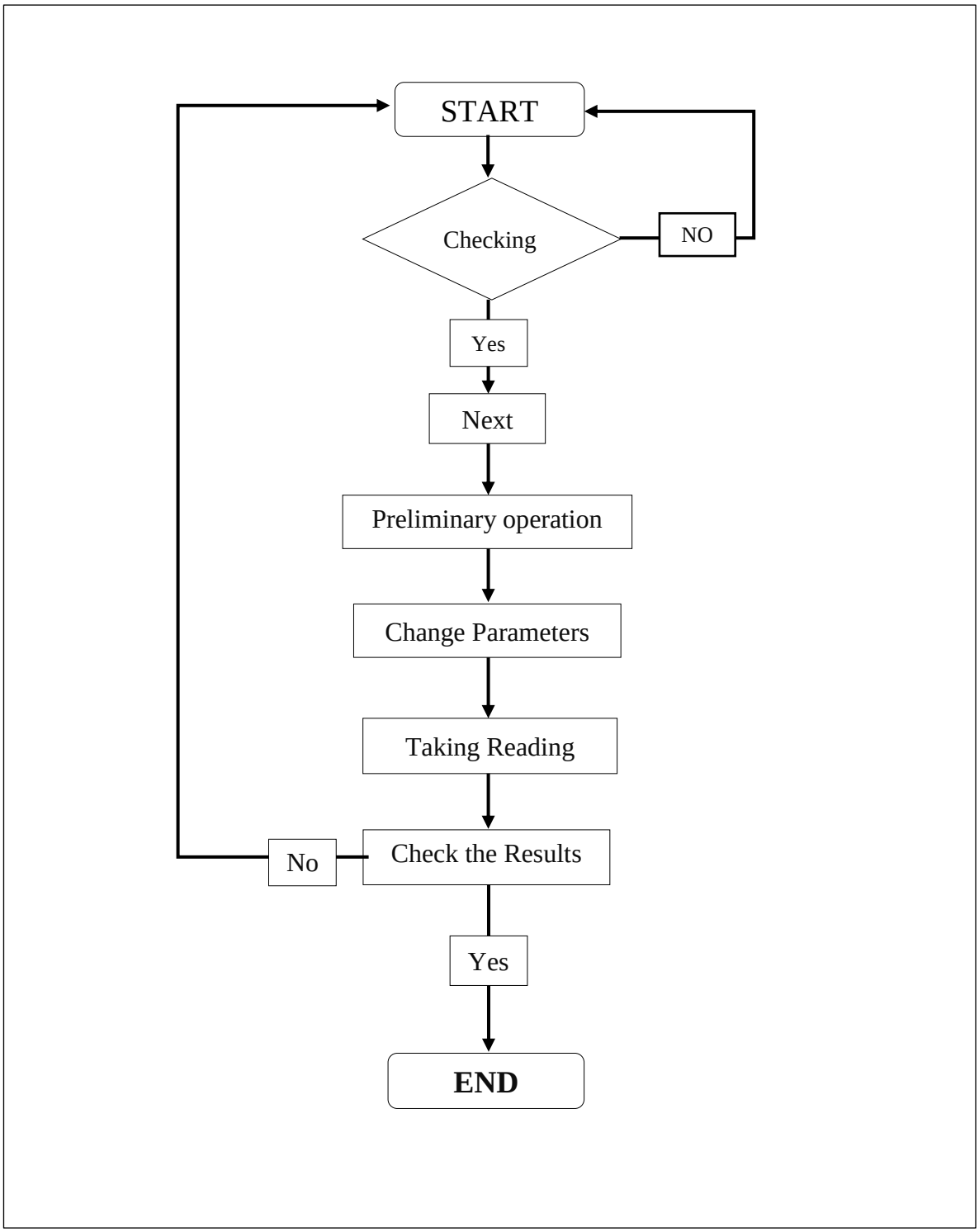

Fig. 3.12: Flow-chart of operation procedure

CHAPTER FOUR

RESULT AND DESCUSION

CHAPTER FOUR

RESULTS AND DISCUSSIONS

4.1 Introduction

This chapter reviews the results obtained from the experiments that were conducted using the transformer radiator system device. The study includes the experiments and results recorded, which were done using six models to investigate the cooling capacity and the temperature distribution of transformer radiator and the effect of using metal foam on the radiator cooling system. The models are oil-direct air natural (ODAN), oil-direct air forced (ODAF), oil-direct air natural (ODAN) with metal foam porosity of (17%), oil-direct air forced (ODAF) with metal foam porosity of (17%), oil-direct air natural (ODAN) with metal foam porosity of (35%), and oil-direct air forced (ODAF) with metal foam porosity of (35%). All tests were performed with different oil mass flow rates ($1.6*10^{-2}$, $3.333*10^{-2}$, and $5*10^{-2}$ Kg/s), corresponding to (1, 2, and 3 ℓ/min). All experiments were carried out at North Najaf electrical transmission station/Iraq, from 5:00 PM to 12:00 AM of 1 to 9 Sep. 2020. The details of experiments may illustrate as follow:

4.2 Oil-Direct Air Natural (ODAN) Model

The results were obtained under this model. Oil circulated by a pump and without fans are used for external air handling, considered three values of oil flow rates as mentioned above and three inlet oil temperatures 50, 60, and 70 °C. The average ambient temperature and average wind velocity through this interval time are 40 °C and 1.65 m/s, respectively. The variation of temperature with time at all specified points along with the radiator, for (3 ℓ/min) flow rate and the same above

inlet oil temperatures, is shown in Figures 4.1, 4.2, and 4.3. In general, the figures showed an increase in temperature at some points with time progress, by a value not exceeding 10 ^{o}C.

This is due to the transient behavior, which starts from the beginning of the experiment until the 50 minute. After that, the system reaches the steady state, and there is nearly, no variation in temperature with time. The same trends are occurred for the two other flow rates, 1 and 2 ℓ/min.

Figures. 4.4, 4.5, and 4.6 show the behavior of radiator cooling capacity along the operation time, nearly uniform, with inlet oil temperatures of (50, 60, and 70 ^{o}C) respectively, at all oil flow rates. When looking at the Figures, it is obvious to see the cooling capacity increases with the increase of flow rate due to the increase of heat exchange, to reach maximum values of (587.6, 1444.4, and 1816.5 W) respectively, at a flow rate of 3 ℓ/min.

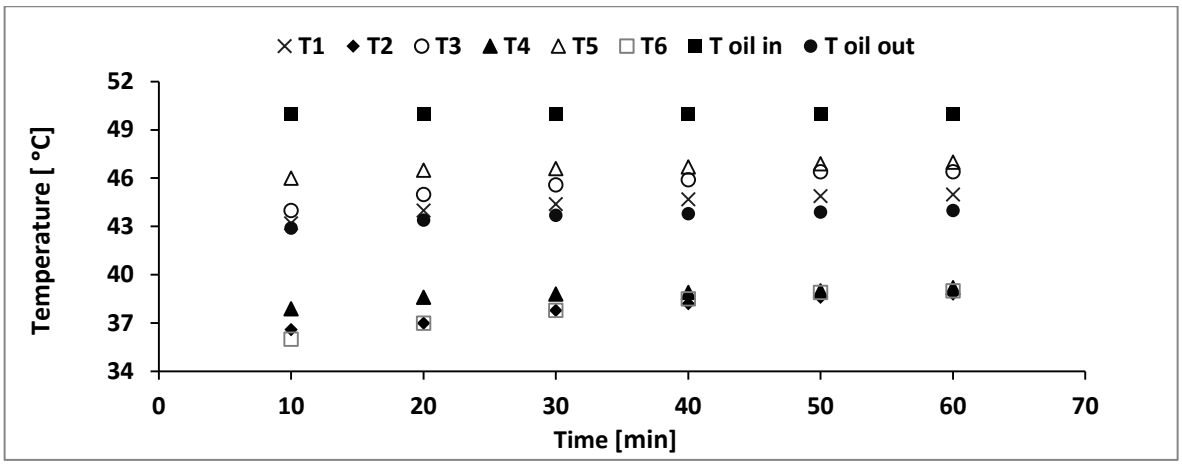

Fig. 4.1: Variation of radiator temperatures with time for oil flow rate (3 ℓ/min), inlet oil temperature (50 °C) and (ΔT = 6 °C)

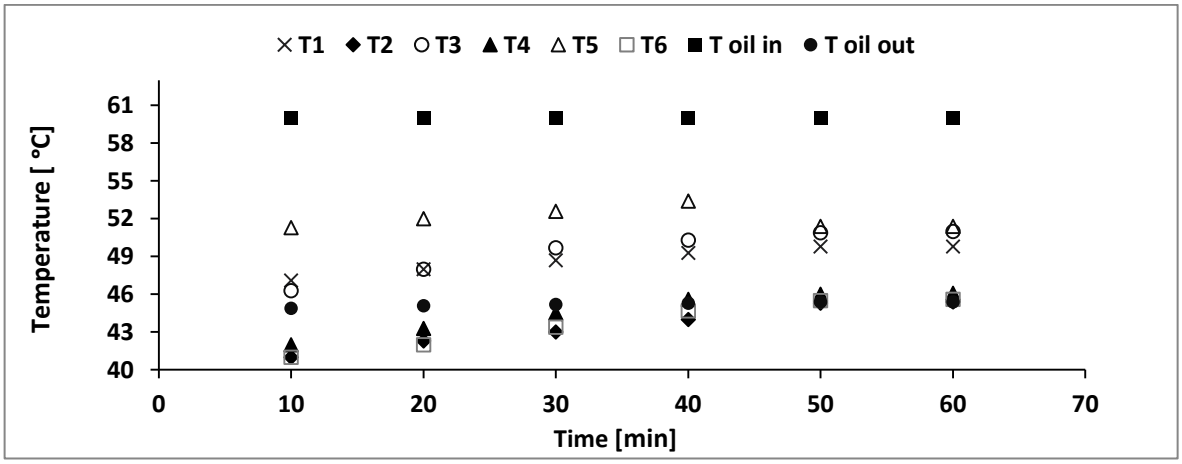

Fig. 4.2: Variation of radiator temperatures with time for oil flow rate (3 ℓ/min), inlet oil temperature (60 °C) and (ΔT = 14.6 °C)

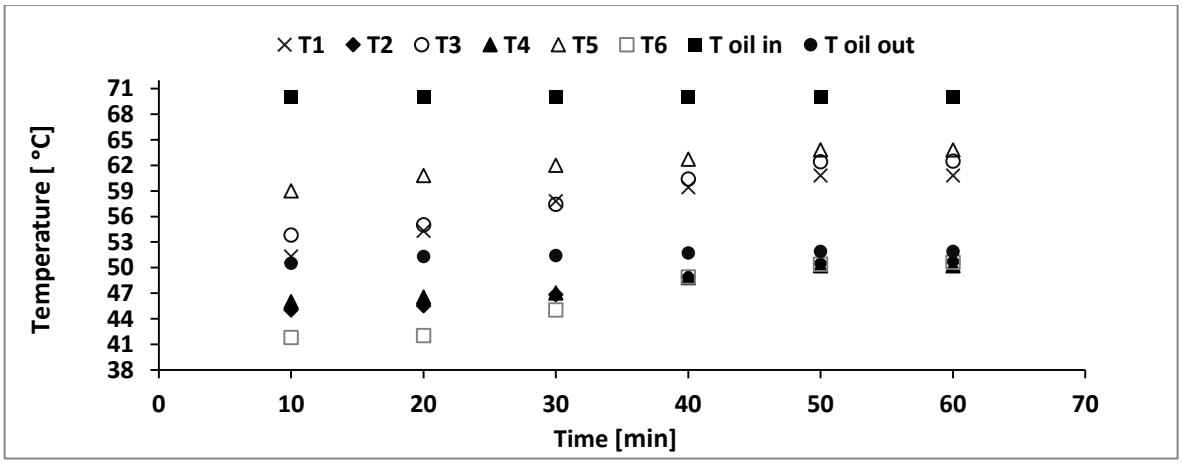

Fig. 4.3: Variation of radiator temperatures with time for oil flow rate (3 ℓ/min), inlet oil temperature (70 °C) and (ΔT = 18.1°C)

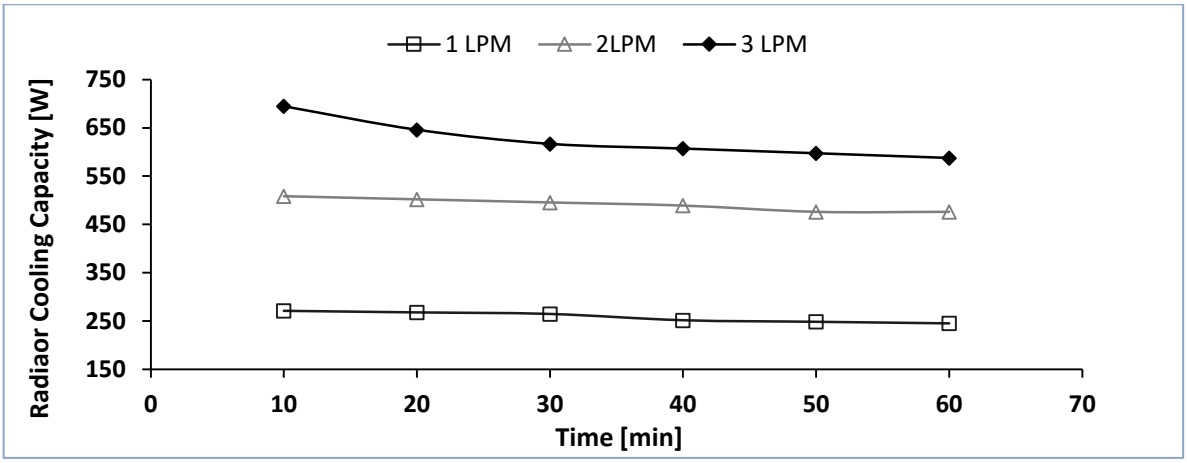

Fig. 4.4: Variation of cooling capacity with time for inlet oil temperature (50 ^{o}C).

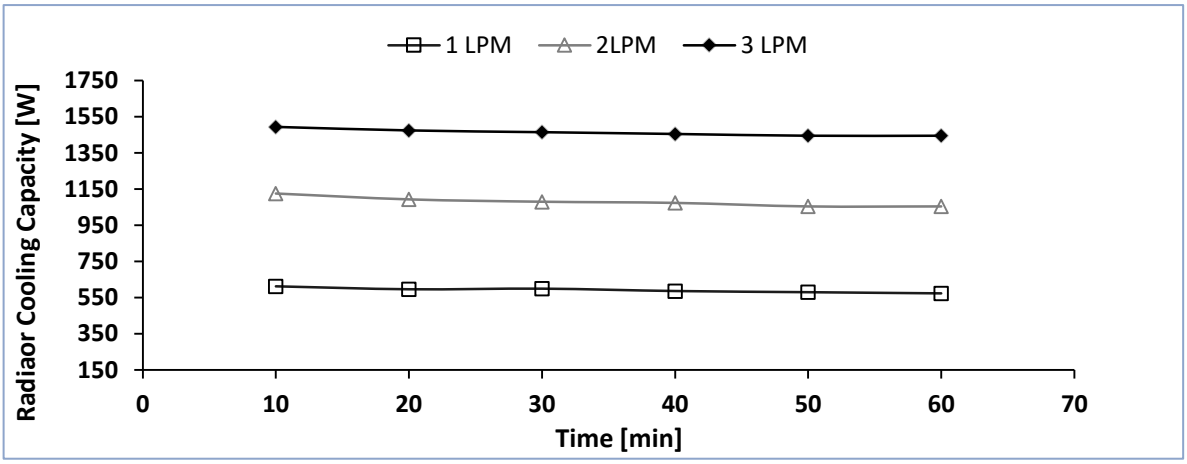

Fig. 4.5: Variation of cooling capacity with time for inlet oil temperature (60 ^{o}C).

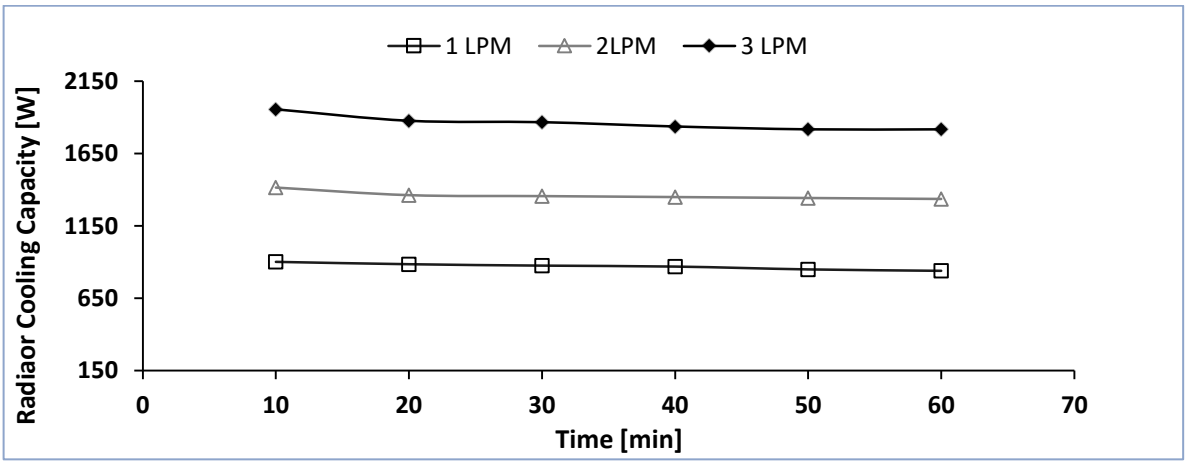

Fig. 4.6: Variation of cooling capacity with time for inlet oil temperature (70 ^{o}C).

4.3 Oil-Direct Air Forced (ODAF) Model

The results under this model add fans for exceeding external air handling, the average fans' speed (6.5 m/s). In contrast, the date and time of experiments and temperature degree of ambient are the same as the previous experiments.

The temperature variation over time, at all specified points along with the coolant, for the maximum flow rate (3 ℓ/min) and the same inlet oil temperature are shown in Figures 4.7, 4.8, and 4.9. In general, the numbers showed a decrease in temperature at some points over time, with a value of no more than 7.5 ° C; this is due to transient behavior that starts from the beginning of the experiment until the forty minute and the fan's performance, which improves the coverage to cool more radiator surface areas. After that, the system reaches a steady-state, and there is virtually no temperature difference over time. The same trends occurred for the other two flow rates, 1 and 2 ℓ/min.

Figures. 4.10, 4.11, and 4.12 show the radiator cooling capacity's behavior along the operation time, nearly stable, with inlet oil temperature of (50, 60, and 70 ^{o}C) respectively, at all oil flow rates. Also, after applied the results in cooling equation (3.6), it's indicate that as the flow rate increases, the cooling strength increases, to reaches its maximum value of (801.6, 1717.2, and 2591.6 W) respectively, at a flow rate of 3 ℓ/min.

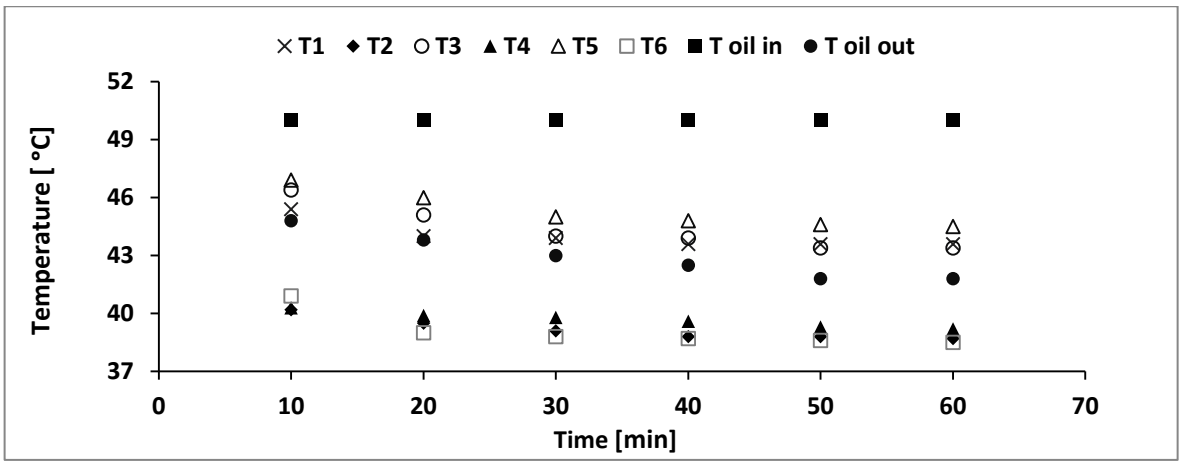

Fig. 4.7: Variation of radiator temperatures with time for oil flow rate (3 ℓ/min), inlet oil temperature (50 °C) and ($\Delta T = 8.2$ *°C)*

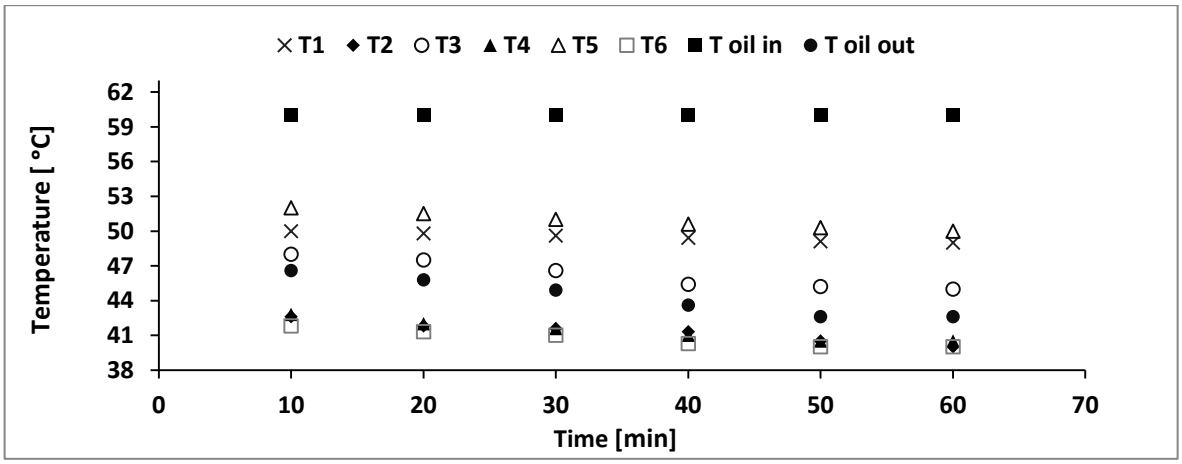

Fig. 4.8: Variation of radiator temperatures with time for oil flow rate (3 ℓ/min), inlet oil temperature (60 °C) and ($\Delta T = 17.4$ *°C)*

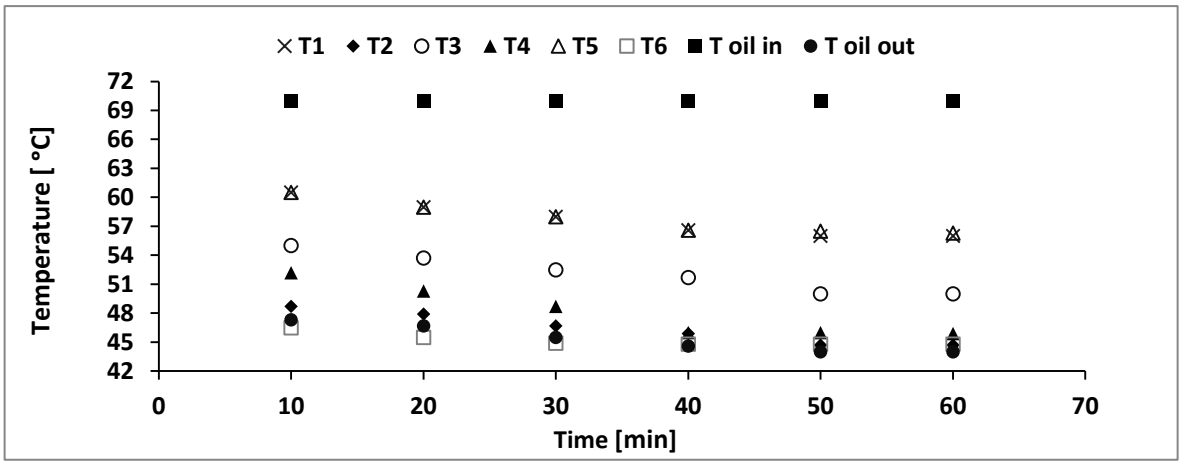

Fig. 4.9: Variation of radiator temperatures with time for oil flow rate (3 ℓ/min), inlet oil temperature (70 °C) and ($\Delta T = 26$ *°C)*

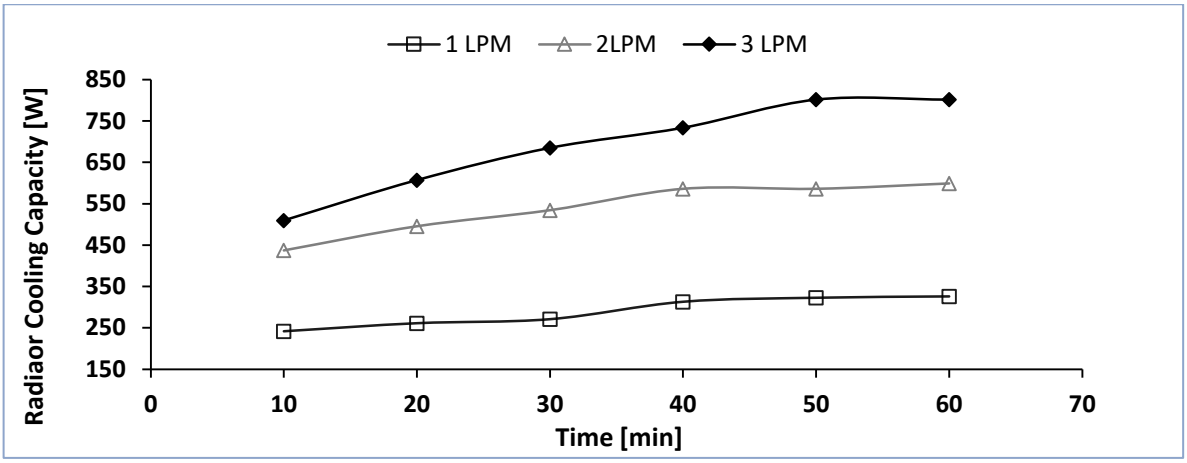

Fig. 4.10: Variation of cooling capacity with time for inlet oil temperature (50 ^{o}C).

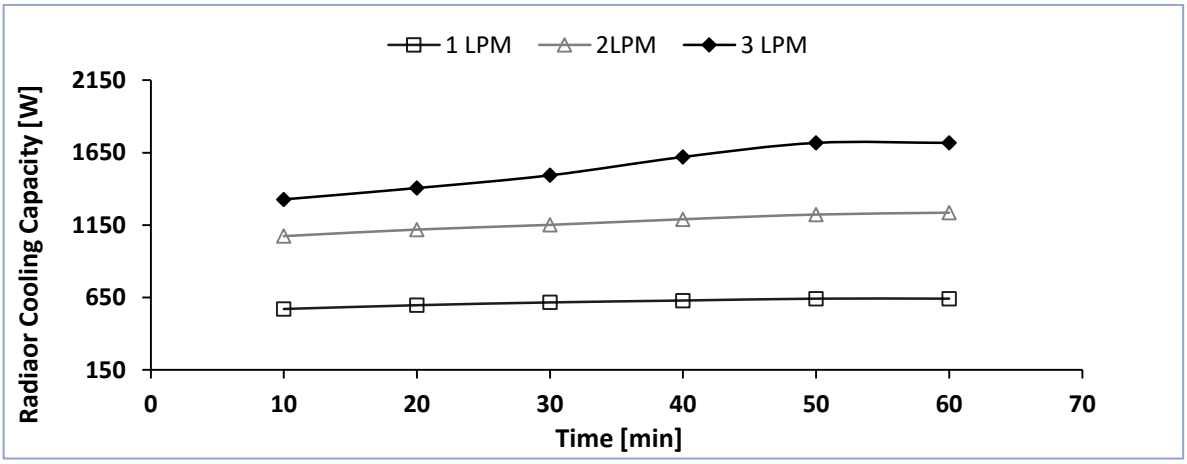

Fig. 4.11: Variation of cooling capacity with time for inlet oil temperature (60 ^{o}C).

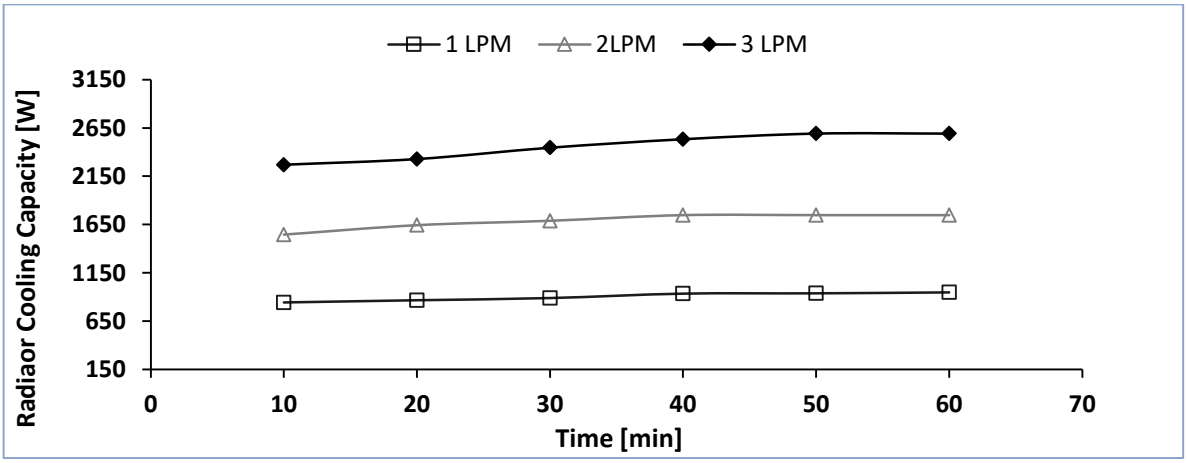

Fig. 4.12: Variation of cooling capacity with time for inlet oil temperature (70 ^{o}C).

4.4 Oil Direct Air Natural (ODAN) Model with Metal Foam Heat Exchanger (MFHE)

This section describes a cooling system with convection force through directing the oil and free convection of naturalizing air, with the considering effect of metal foam in a heat exchanger. This section was divided into two values of porosities of metal foam (17% and 35%) as follows.

4.4.1 (ODAN) Model with (17% MFHE)

The results were obtained by adding metal foam sponge of porosity 17% between radiator panels spaces, that is cooled by oil circulated and without fans, considered values of oil flow rates and inlet oil temperatures, through this model used are (1, 2, and 3 ℓ/min), and (50, 60, and 70^{o}C), respectively. The average ambient temperature and average wind velocity through this interval time, 40.5^{o}C and 1.62 m/s.

Figures from 4.13, 4.14, to 4.15 show the variety of the temperature with the time at all specified radiator points for a (3 ℓ/min) flow rate and the same above inlet oil temperature. As such, the figures showed that at certain times the temperature increases slowly by a value not exceeding 4°C. This is due to the transitory conduct, which starts from the start of the experiment to the 45 minutes and effect of metal foam used. After that, a state of stability has occurred, with almost no temperature variation with time. For the other two flow rates, 1 and 2 ℓ/min, the same trends are present. Also, the heat dispersed from the first and end of the radiator panel is more dispersed than the middle panels due to its close to the surrounding air.

It's clear from Figures 4.16, 4.17, and 4.18 the stability of radiator cooling capacity along the operation time with inlet oil temperatures at all oil flow rates. Also, it's evident from the Figures that the cooling capacity increases with an increase of flow rate to reach maximum values of (685, 1483.5, and 2003.9 W) respectively, as Figures showed at flow rate 3 ℓ/min.

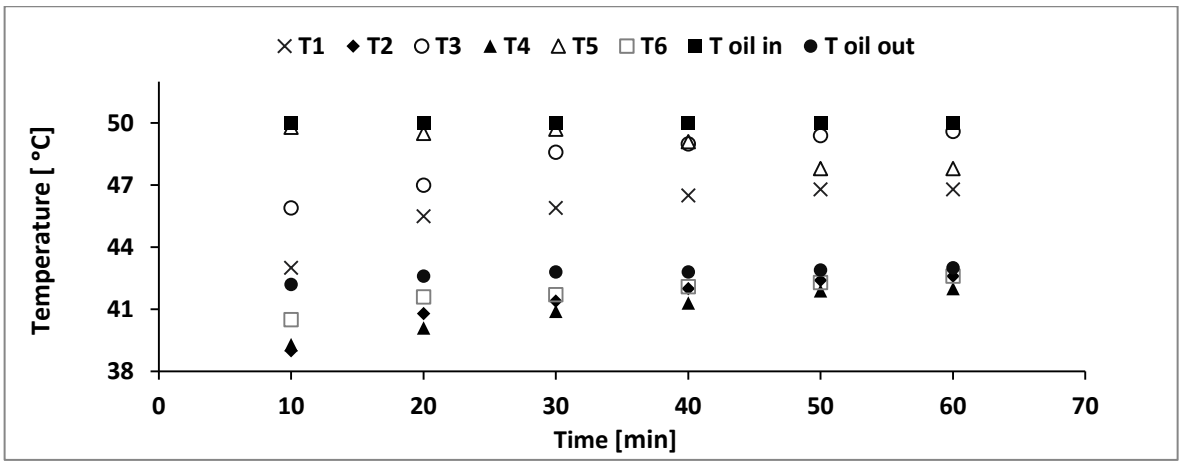

Fig. 4.13: Variation of radiator temperatures with time for oil flow rate (3 ℓ/min), inlet oil temperature (50 °C) and ($\Delta T = 7^{o}C$)

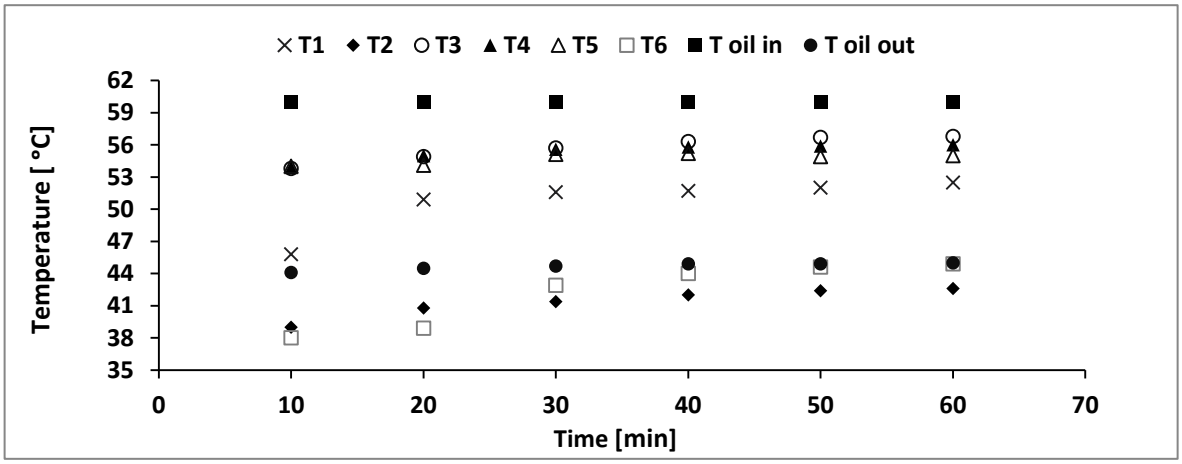

Fig. 4.14: Variation of radiator temperatures with time for oil flow rate (3 ℓ/min), inlet oil temperature (60 °C) and ($\Delta T = 15\ ^{o}C$)

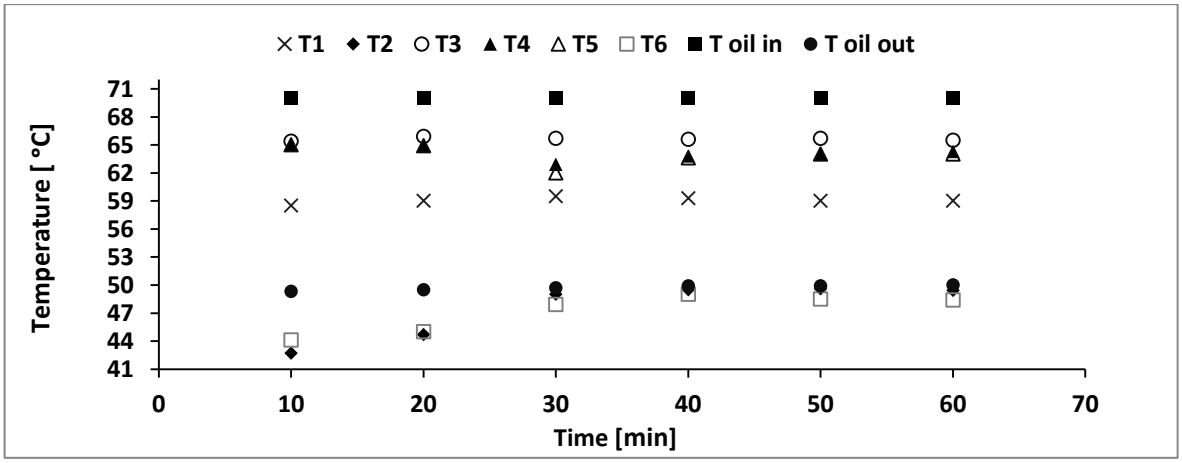

Fig. 4.15: Variation of radiator temperatures with time for oil flow rate (3 ℓ/min), inlet oil temperature (70 °C) and ($\Delta T = 20\ ^{o}C$)

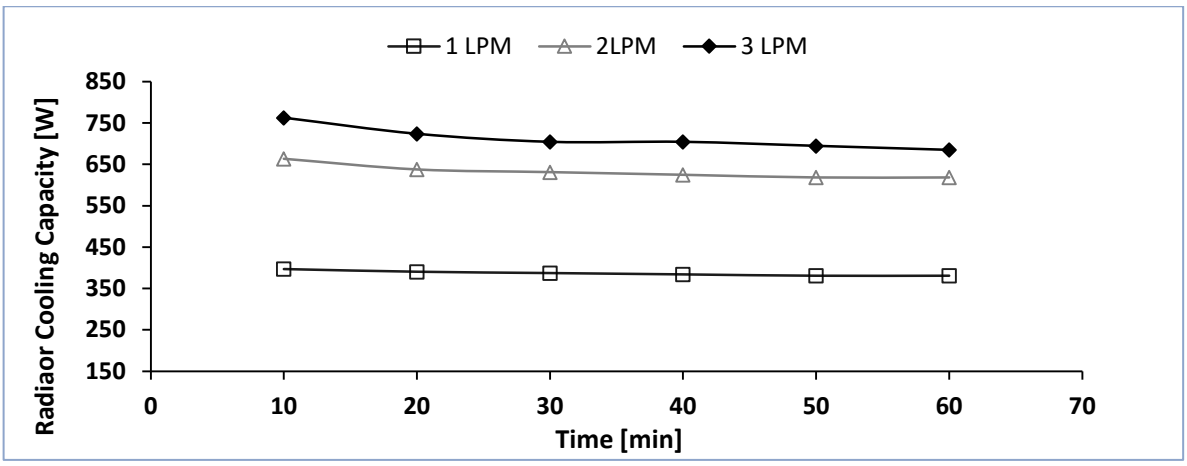

Fig. 4.16: Variation of cooling capacity with time for inlet oil temperature (50 ^{o}C).

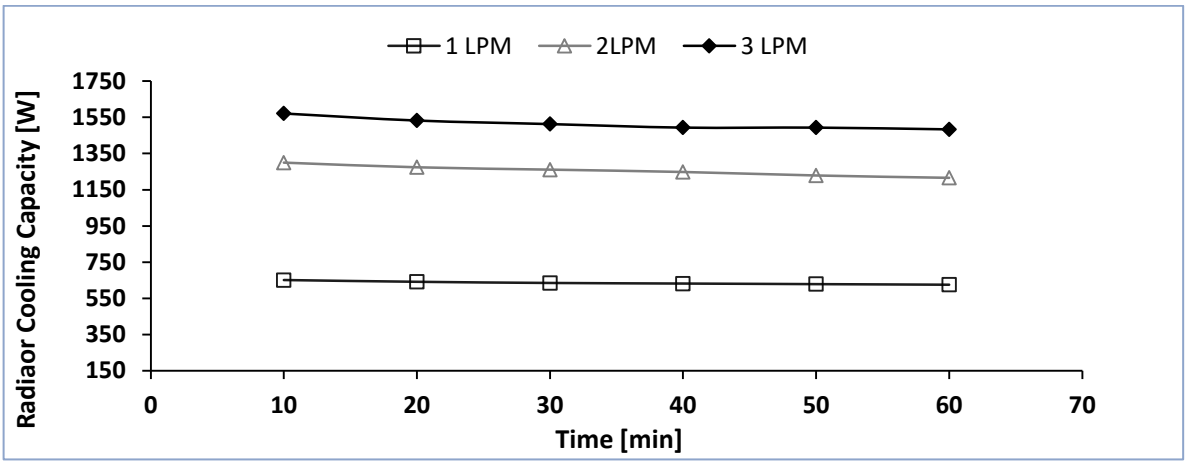

Fig. 4.17: Variation of cooling capacity with time for inlet oil temperature (60 ^{o}C).

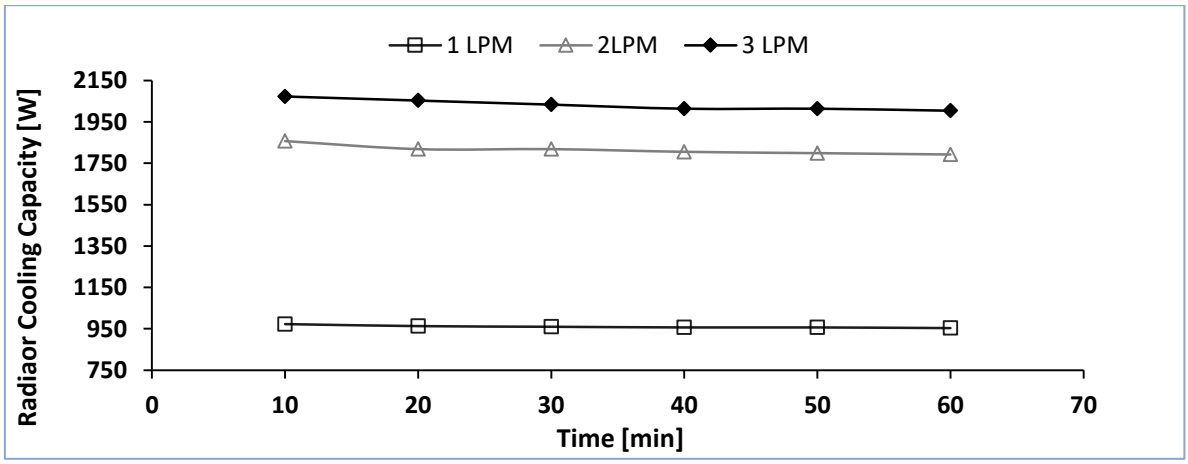

Fig. 4.18: Variation of cooling capacity with time for inlet oil temperature (70 ^{o}C).

4.4.2 (ODAN) Model with 35% Metal Foam.

In this model, experimental results were carried out by adding a Metal Foam of porosity 35% between radiator panels space. From figures (4.19) to (4.21) temperature stability performance has improved over time. This is due to the addition of more metallic foam between panels space. Also, it is visible from the figures that there is an increasing temperature at some points with time progress, by a value not exceeding 3.5 ^{o}C; this is due to the transient behavior, which starts from the beginning of the experiment till the 40 minute. After that, the system reaches the steady-state, and it is near, with no variation in temperatures with time. Simultaneously, the temperatures in points (T2 and T6) good agreement at cooling than (T4) due to direct exposure to the air surrounding and the positive effect of increasing the volume of metal foams between the voids of radiator panels, which leads to a significant increase in heat transfer.

Figures 4.22, 4.23, and 4.24 show the relationships between coolant cooling capacity and time using the same parameters entered for the previous experiments: oil temperature and flow rate. The result shows that the cooling capacity increased with the increase of the flow rate**,** where the maximum cooling capacity was (782, 1580.9, 2278.9 W) with a flow rate of (3 ℓ/min). As such, figures show regulation of radiator cooling capacity along the time of operation.

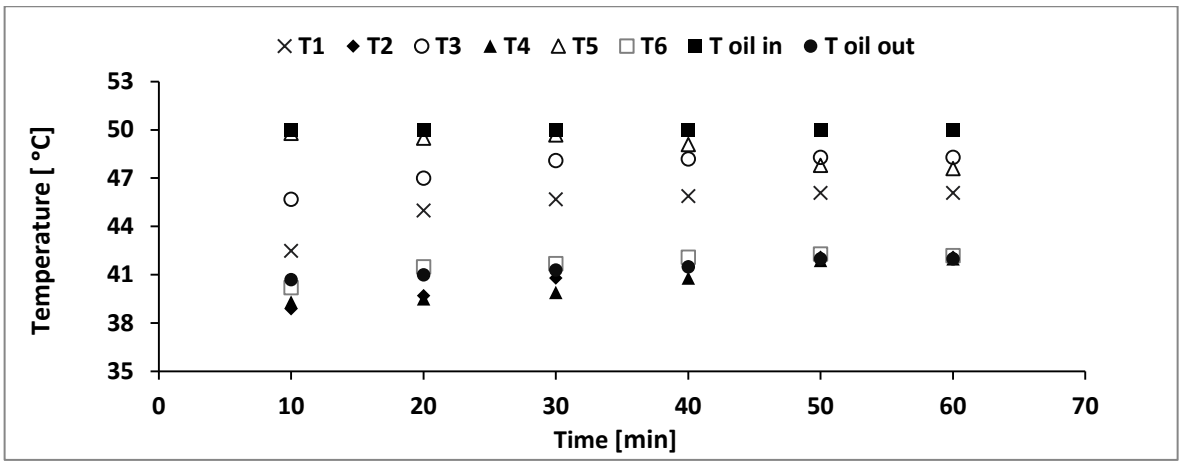

Fig. 4.19: Variation of radiator temperatures with time for oil flow rate (3 ℓ/min), inlet oil temperature (50 °C) and (ΔT = 8 °C)

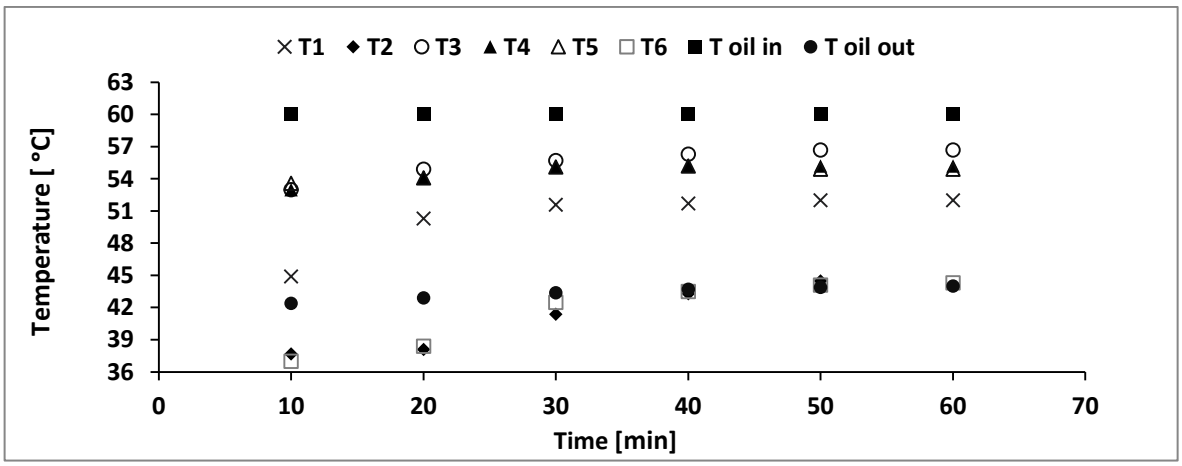

*Fig. 4.20: Variation of radiator temperatures with time for oil flow rate (*ℓ/min*), inlet oil temperature (60 °C)* and (ΔT = 16 °C)

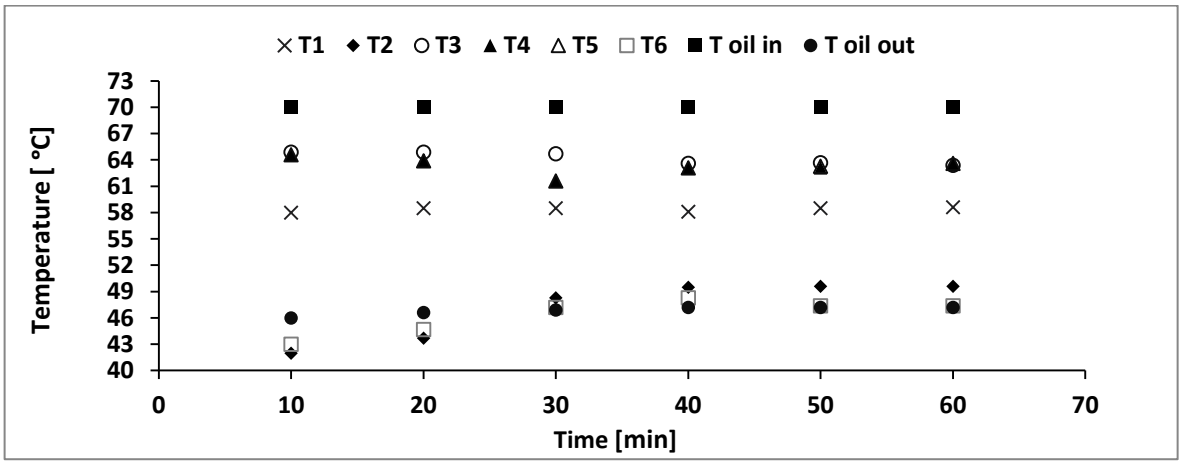

Fig. 4.21: Variation of radiator temperatures with time for oil flow rate (ℓ/min), inlet oil temperature (70 °C) and (ΔT = 22.8 °C).

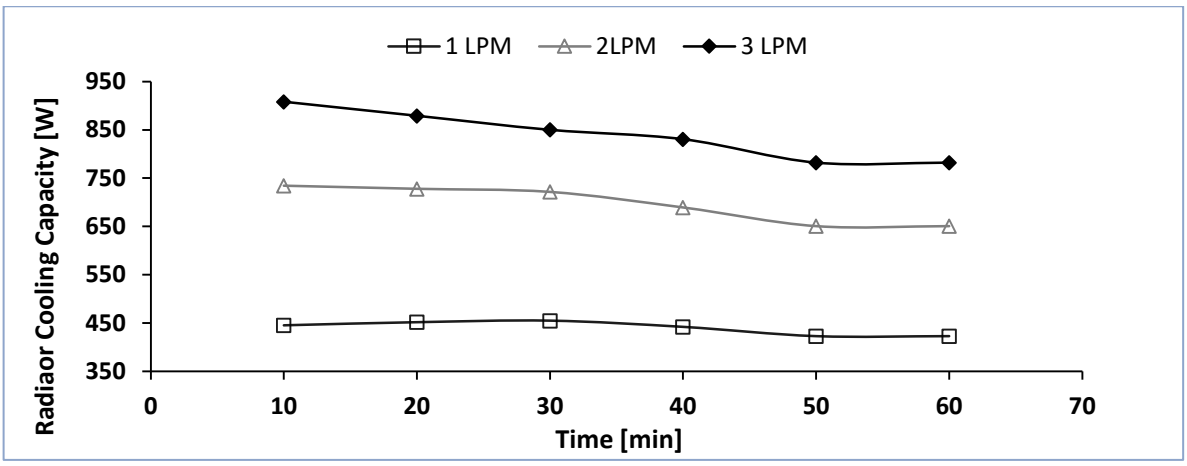

Fig. 4.22: Variation of cooling capacity with time for inlet oil temperature (50 °C).

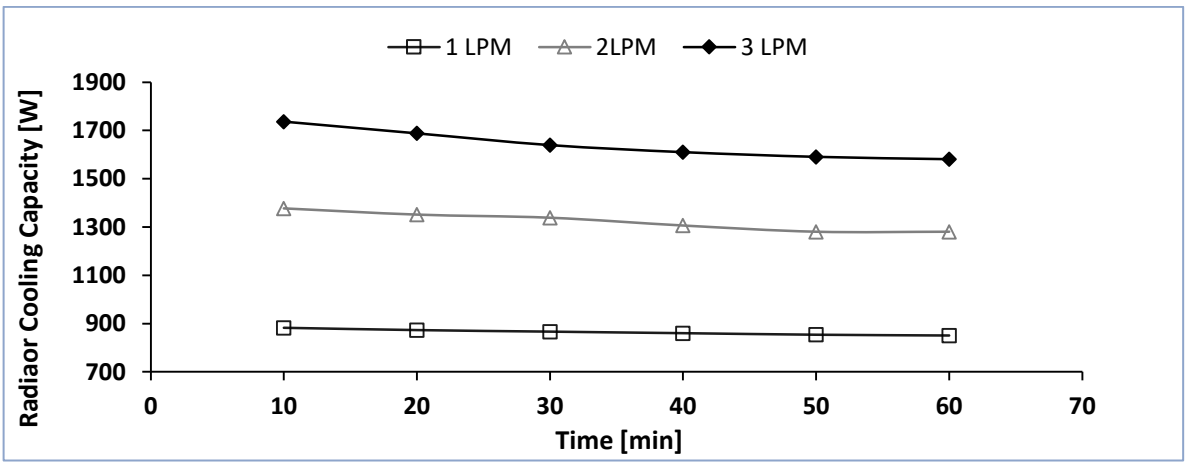

Fig. 4.23: Variation of cooling capacity with time for inlet oil temperature (60 °C).

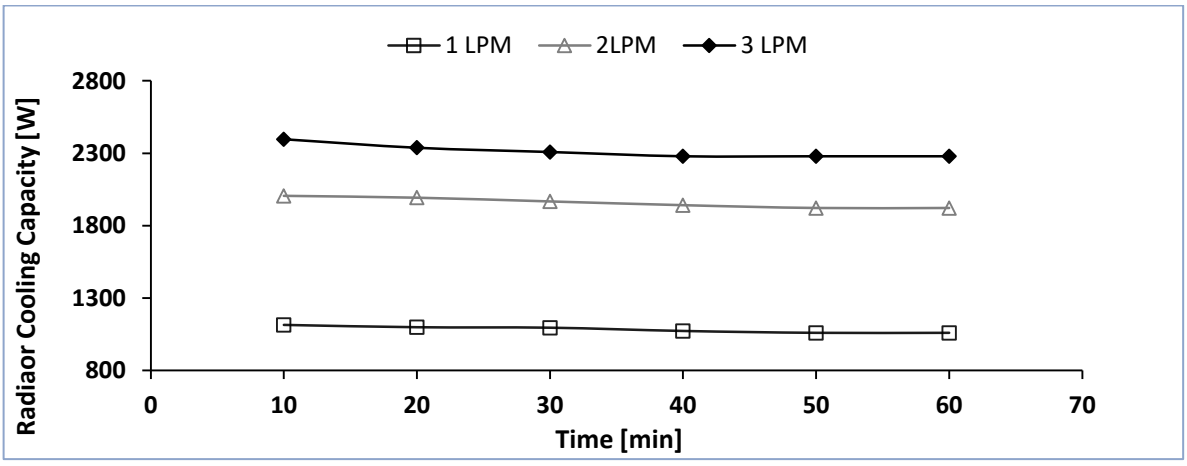

Fig. 4.24: Variation of cooling capacity with time for inlet oil temperature (70 °C).

4.5 Oil Direct Air Force (ODAF) Model with (MFHE)

This section illustrates a cooling system with convection force through directing the oil and free convection of naturalizing air, with the considering effect of metal foam in a heat exchanger. This section was divided into two values of porosities of metal foam (17% and 35%) as follows.

4.5.1 (ODAF) Model with (17% MFHE)

The results of this department were implemented by adding a porosity of 17% metallic foam between radiator panel voids. The average speed of the fans (6.5 m / s). In contrast, the date and time of the experiments and the ambient temperature are the same as before in the previous model.

Figures 4.25, 4.26, and 4.27 show the low-temperature increases at certain times by a value of no more than four °C, due to the transient comportment that starts from the beginning of the experiment until the thirty-five minutes. After that, a steady- state was occurred, with almost no temperature variation with time. For the other two flow rates, 1 and 2 ℓ/min, the same trends are present. Meanwhile, figures show that the temperature points in the center panels of the radiator are outperformed the other panels because they receive a large amount of air from the fans. On the other hand, the increases in low temperature can be attributed to significant conduction when the volume of metal foam porosity reaches 17%.

It is illustrated from Figures from 4.28 to 4.30 that radiator cooling capacity stabilizes over time with inlet oil temperatures (50, 60, and 70 °C) at all oil flow rates. Furthermore, the cooling power increases as the flow rate increases compared with propose validate of [45], reaching its maximum value of (917.9, 1940.3, and 2844.3W) at a flow rate of 3 ℓ/min.

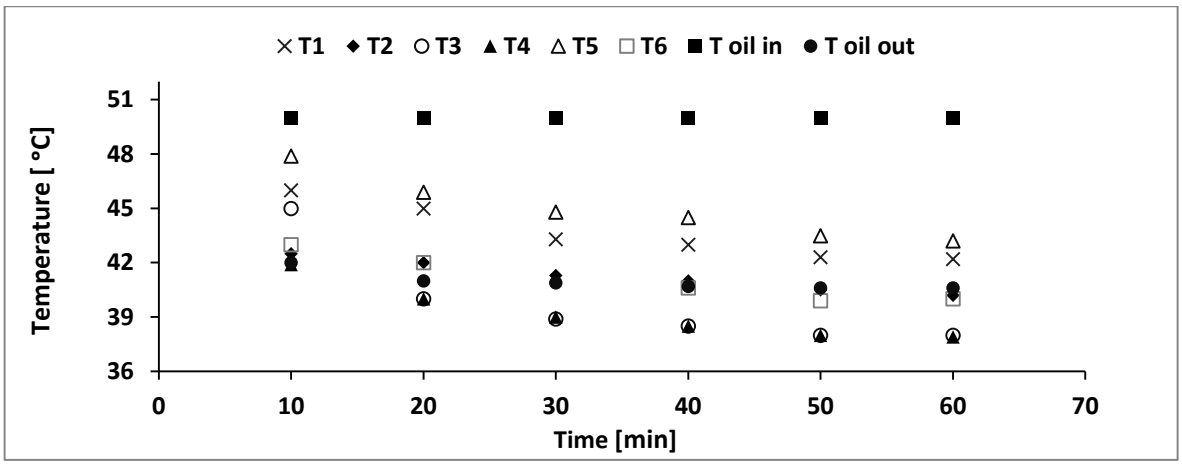

Fig. 4.25: Variation of radiator temperatures with time for oil flow rate (3 ℓ/min), inlet oil temperature (50 °C and (ΔT = 9.4°*C)).*

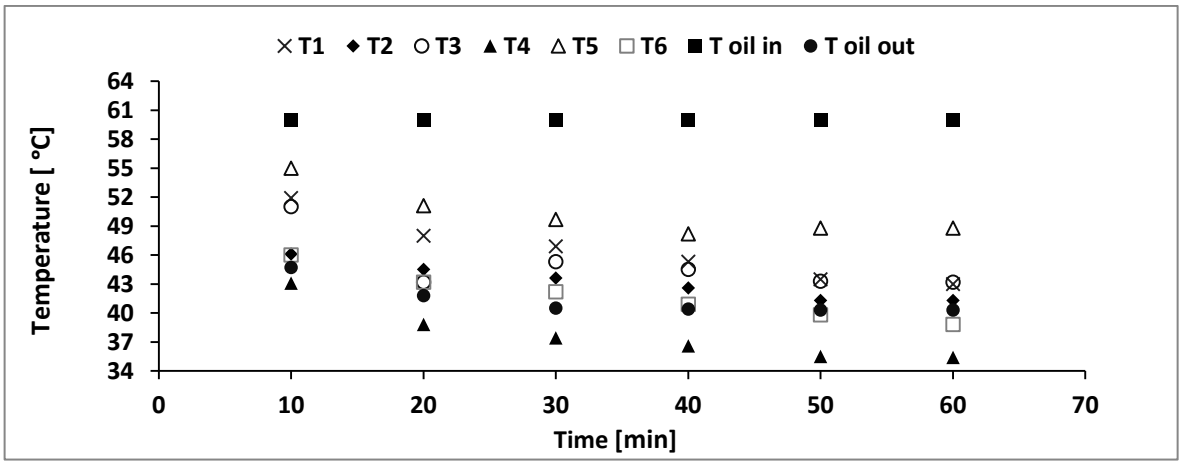

Fig. 4.26: Variation of radiator temperatures with time for oil flow rate (3 ℓ/min), inlet oil temperature (60 °C) and (ΔT = 19.7 °*C).*

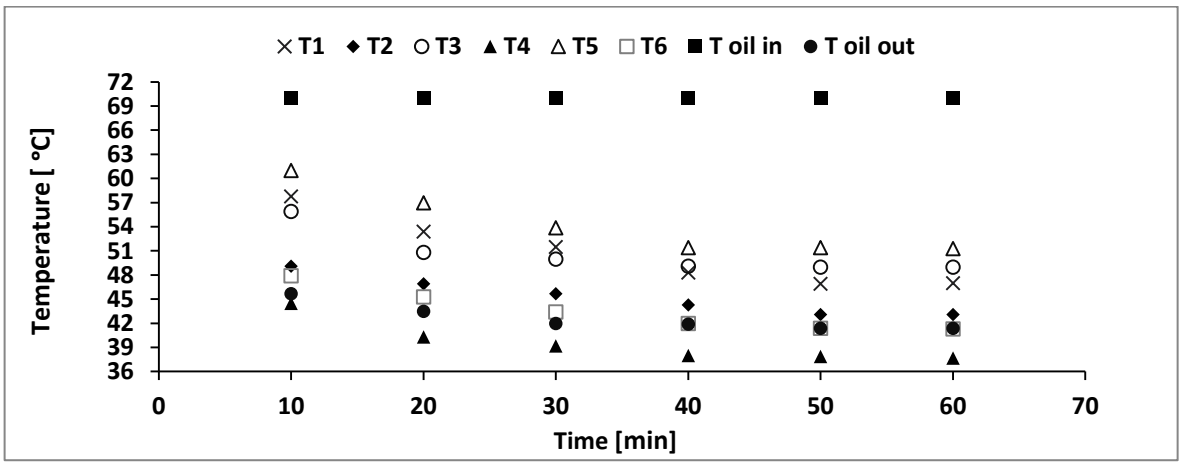

Fig. 4.27: Variation of radiator temperatures with time for oil flow rate (3 ℓ/min), inlet oil temperature (70 °C) and (ΔT = 28.6 °*C).*

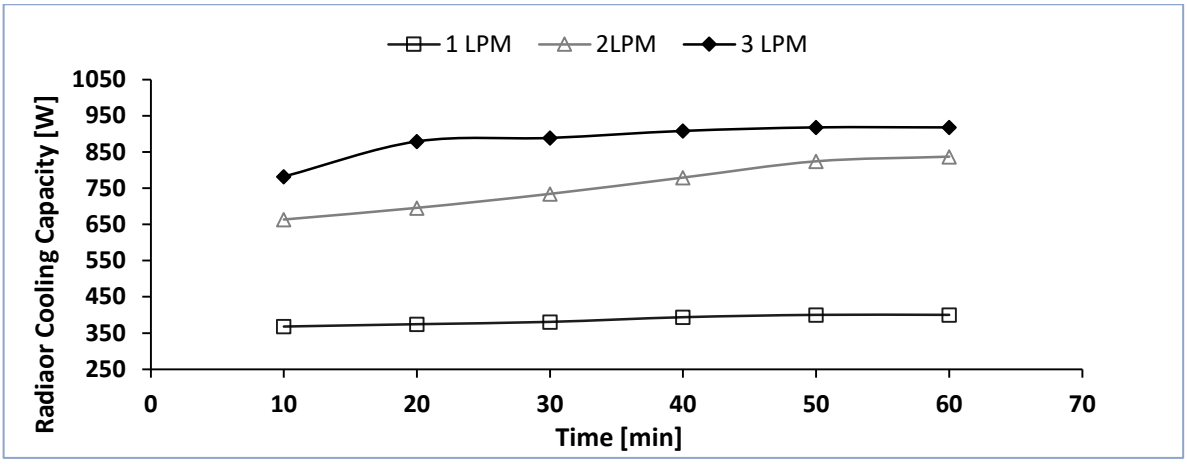

Fig. 4.28: Variation of cooling capacity with time for inlet oil temperature (50 °C).

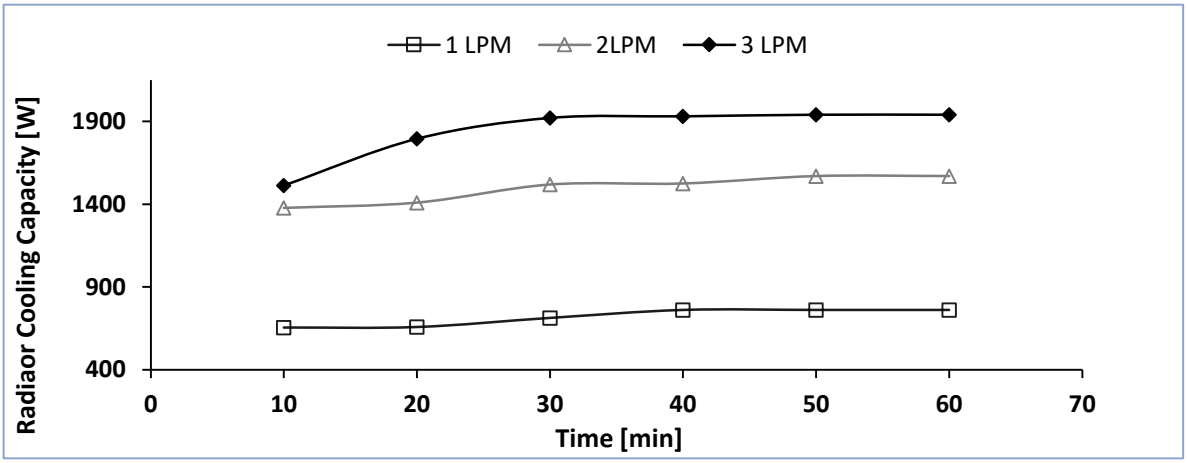

Fig. 4.29: Variation of cooling capacity with time for inlet oil temperature (60 °C).

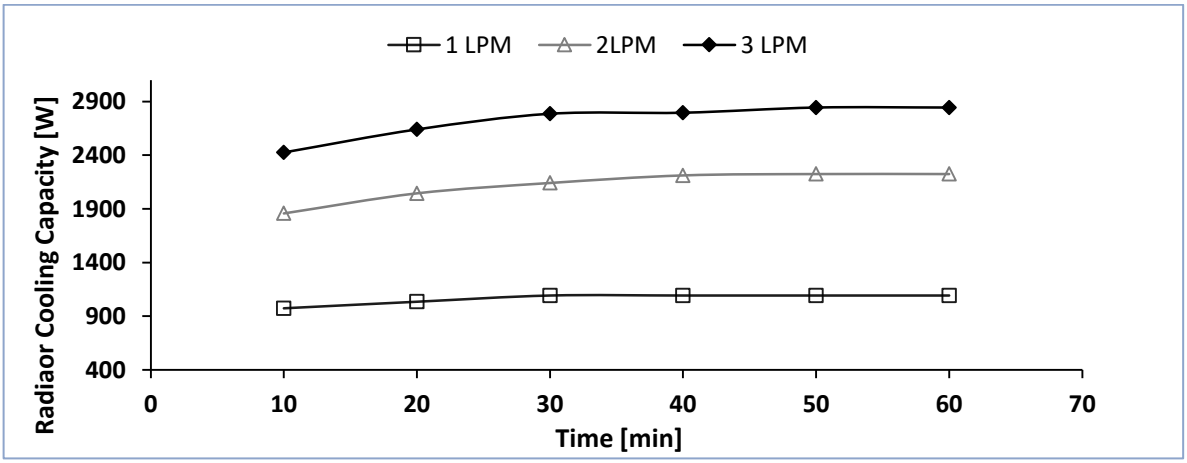

Fig. 4.30: Variation of cooling capacity with time for inlet oil temperature (70 °C).

4.5.1 (ODAF) Model with (35% MFHE)

This segment was created by increment a 35% metal foam into the radiator panel's voids. The average speed of the fans is 6.5 m/s. In contrast, the date and time are the same previous experiment. Figures 4.31, 4.32, and 4.33 show the temperature variation over time at all specified points along with the radiator for a flow rate of (3 ℓ/min) and inlet oil temperatures (50, 60, and 70 ºC). In general, the figures showed that the temperature decreased by a value of not more than three ºC at the middle of radiator panels and 1 ºC at the end panels of a radiator as time progressed. This is attributed to several reasons; the first is the transient comportment that begins at the start of the experiment and continues until the twenty-fifth minute. Next, the system reaches a steady-state, with almost no temperature variation over time. The same trends have occurred for the two other flow rates, 1 and 2 ℓ/min. The second reason can be attributed to significant conduction occurring at interconnected pores when the porosity of metal increasing to reach 35%. This, in turn, improves the transfer of fluid heat from the wall to the surrounding surface compared with Dixit et al. [70]. This was positively affected by the radiator panels.

Figures 4.34, 4.35, and 4.36 demonstrate stability and uniformity of heat transfer Shang et al. l compared with **[79],** of radiator cooling capacity and the operation with inlet oil temperatures all oil flow rates. Furthermore, it's intelligible from the figures that the cooling capacity increases with the flow rate increases to reach its maximum value (1149.8, 2017.6, 3000W) at a flow rate of 3 ℓ/min**.**

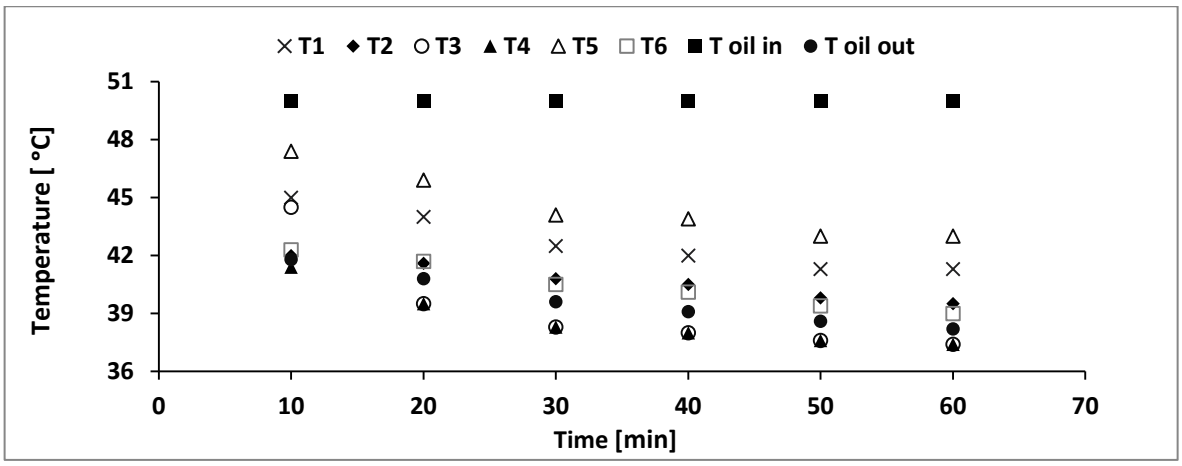

Fig. 4.31: Variation of radiator temperatures with time for oil flow rate (3 ℓ/min) and inlet oil temperature (50 °C) and ($\Delta T = 11.8$ °C).

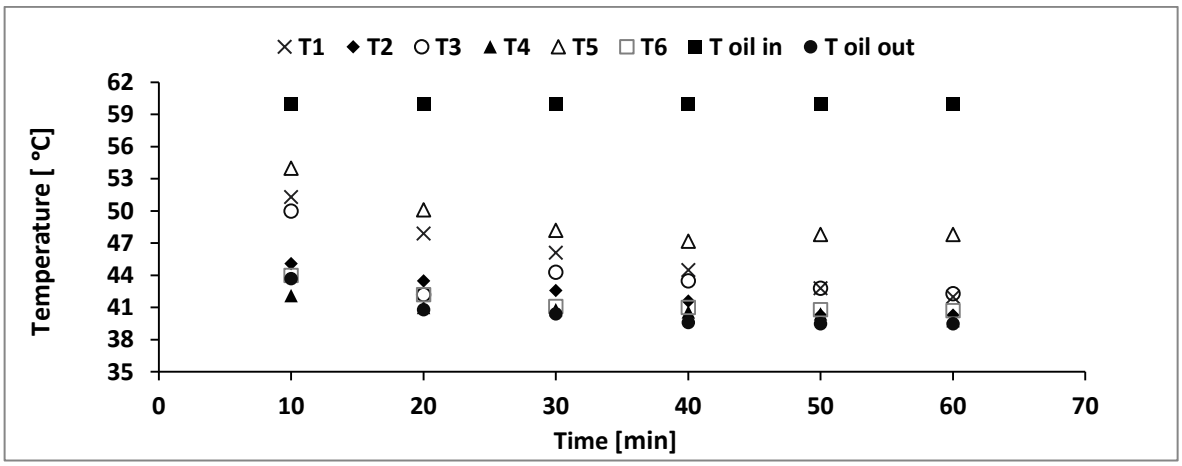

Fig. 4.32: Variation of radiator temperatures with time for oil flow rate (3 ℓ/min), inlet oil temperature (60 °C) and ($\Delta T = 20.5$ °C).

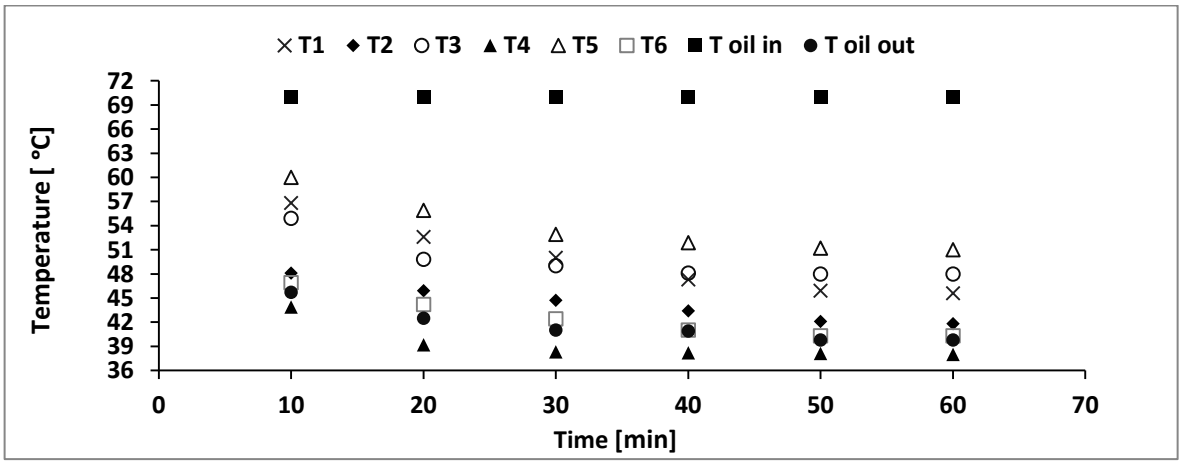

Fig. 4.33: Variation of radiator temperatures with time for oil flow rate (3 ℓ/min), inlet oil temperature (70 °C) and ($\Delta T = 30.2$ °C).

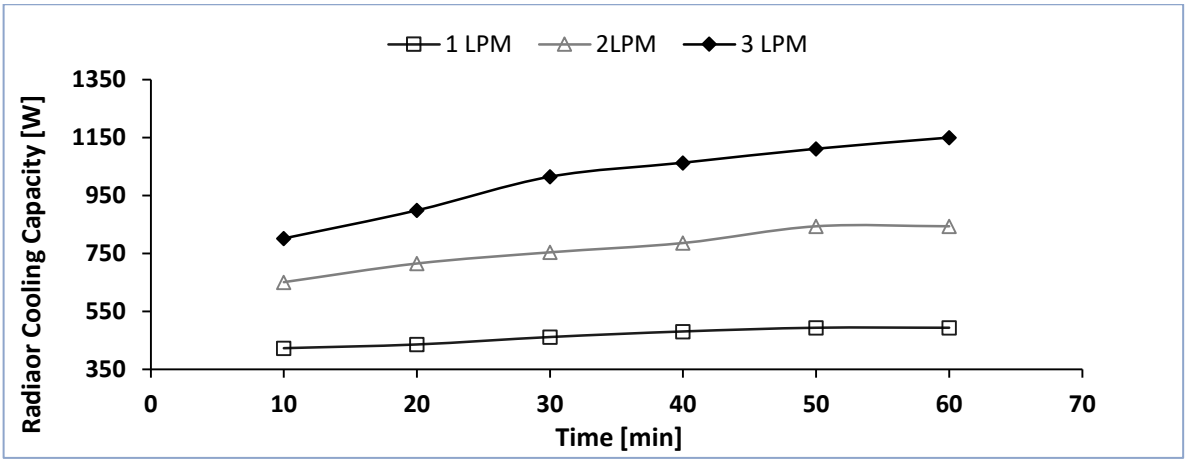

Fig. 4.34: Variation of cooling capacity with time for inlet oil temperature (50 °C).

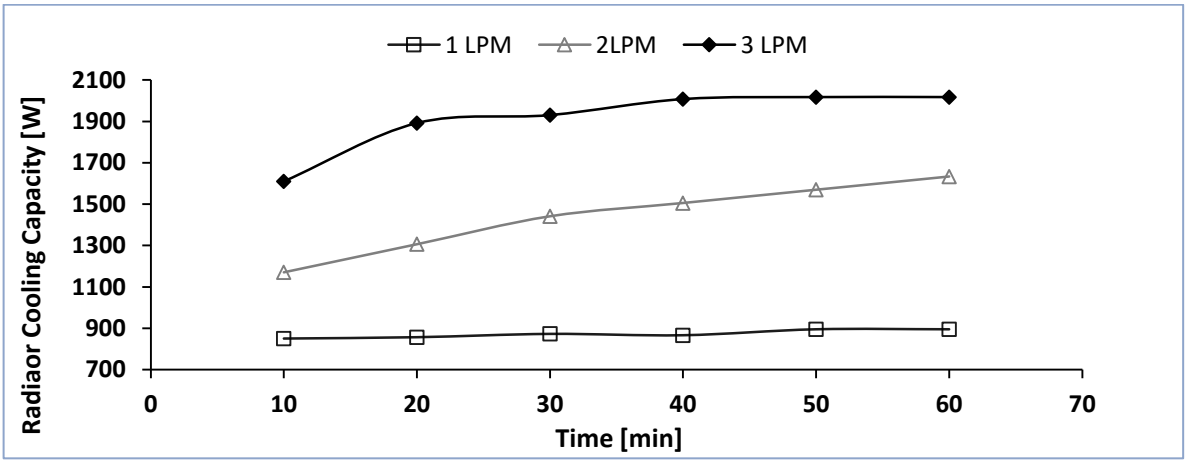

Fig. 4.35: Variation of cooling capacity with time for inlet oil temperature (60 °C).

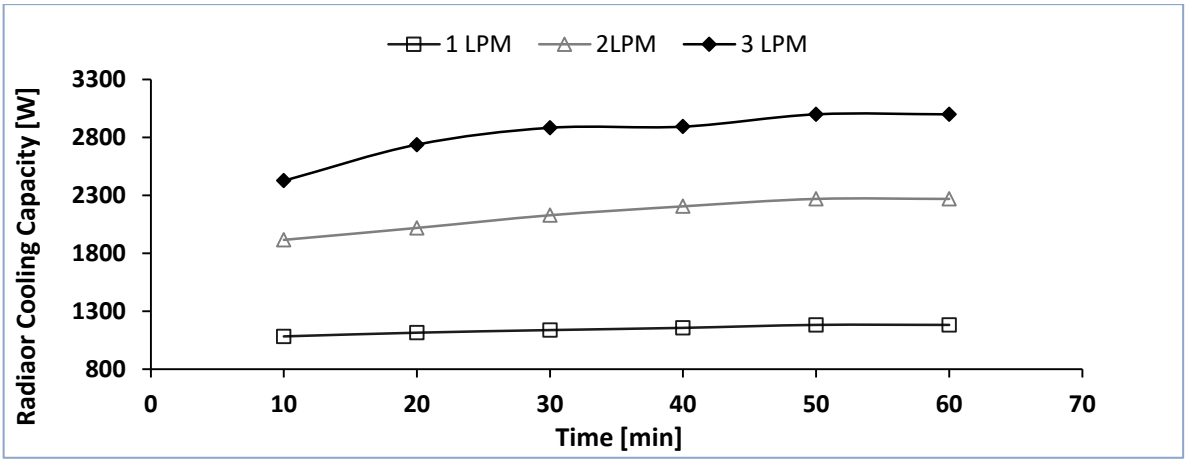

Fig. 4.36: Variation of cooling capacity with time for inlet oil temperature (70°C).

4.6 Effect of Metal Foam Porosity on Cooling Capacity

This discussion described maximum cooling capacity for all flow rates on two models and compared it with and without metal foam sponge. The results are as follows.

4.6.1 ODAN Model

This part presents the effects of cramming the radiator panels in transformers with metallic foam whose porosity ranges from (17% to 35%). This study was carried out through the results recorded from all previous experimental tests of the models. Thus, the study was carried out simultaneously with the previously mentioned weather conditions for the model tests. Experiments were performed for each oil flow rate (1, 2, 3 ℓ/min) at the inlet oil temperature (50, 60, and 70 ° C) to demonstrate the effect of foaming metallic sponges on the cooling capacity without fans worked. Subsequently, the maximum value of the cooling capacity is calculated by adding metallic foam and comparing it to the highest value of the cooling capacity without adding metallic foam.

It is clear from Figures (4.37) to (4.45) that cooling capacity increased with increased the porosity of metal foam sponge for the radiator panels' spaces along the time of operation with inlet oil temperature values at each flow rate. Simultaneously, it is evident from the figures that cooling capacity increased with increases the surface area of radiator vertical panels, also, the metallic foams indicated the relationship between the hot oil and the surrounding surface due to the high porosity of the metal foam that generated increases in turbulence flow of oil hot to reach maximum cooling capacity (422.6, 850.8, 1059.7W), (650.6, 1280.5, 1912.8), and (782, 1581, 2279W) at all inlet oil temperatures for each flow rate, at metal foam porosity reaches 35%. Figures (4.46, 4.47 and 4.48) illustrated the maximum cooling capacity for inlet oil temperatures (50, 60, and 70 ◦C), when volumetric oil flow rate (Q1= 1 ℓ/min), and these figures shows the maximum cooling capacity at metallic foam 35% for all cases of (Tin = 50, 60 and 70 ◦C).

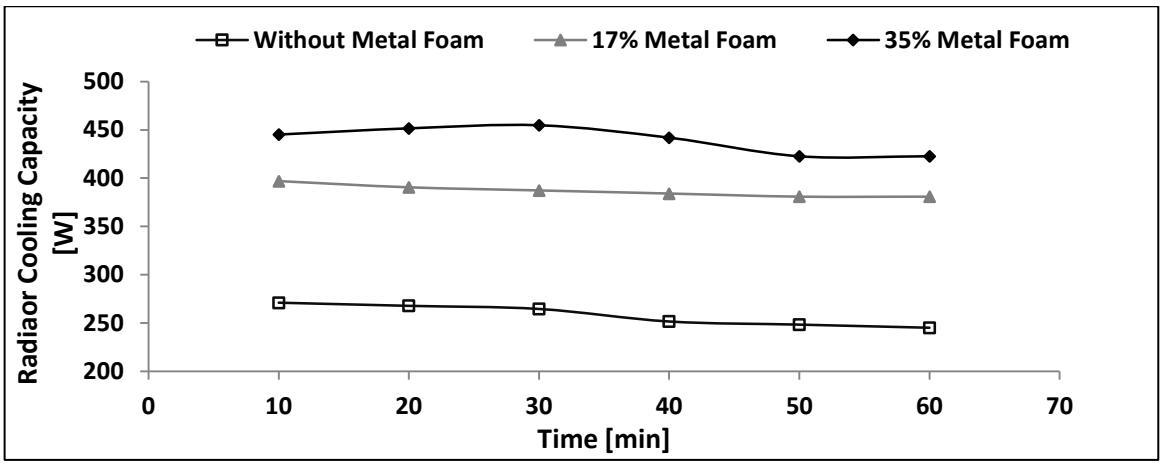

Fig. 4.37: Variation of cooling capacity with time for (Tin=50°C and Qin=1 ℓ/min)

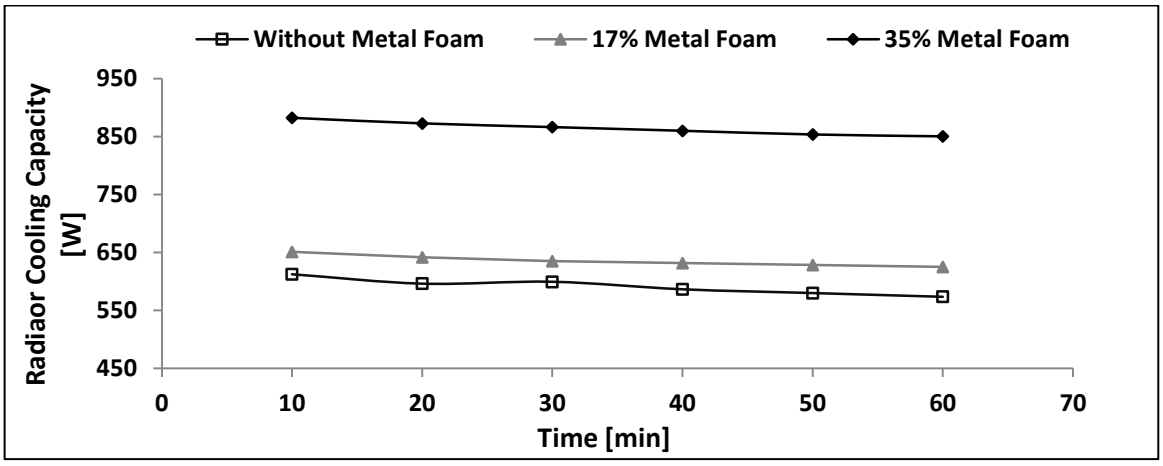

Fig. 4.38: Variation of cooling capacity with time for (Tin=60°C and Qin=1 ℓ/min)

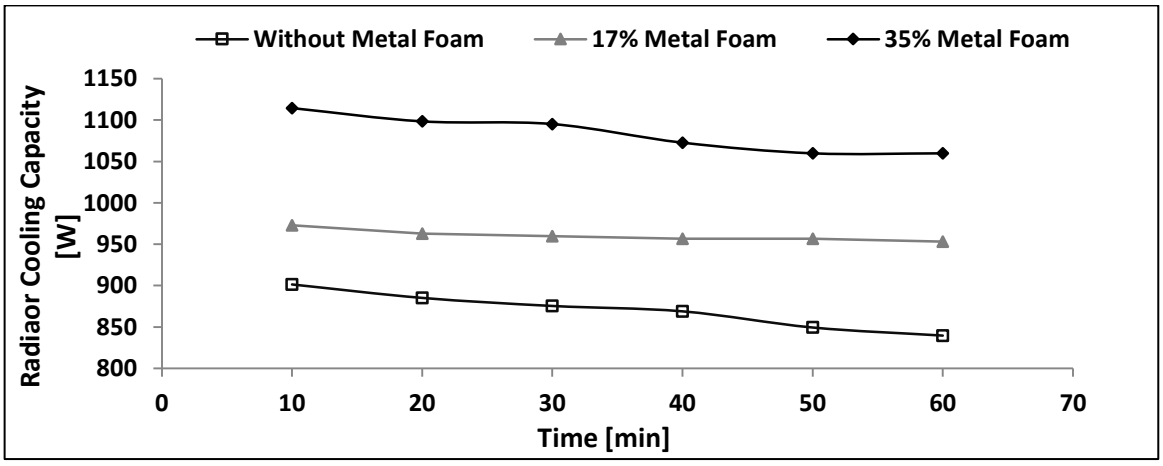

Fig. 4.39: Variation of cooling capacity with time for (Tin=70°C and Qin=1 ℓ/min)

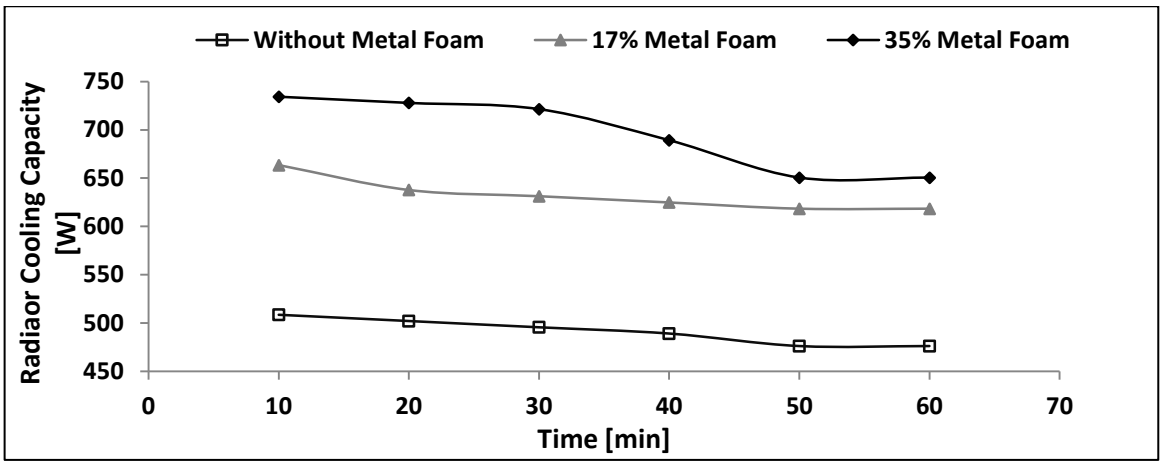

Fig. 4.40: Variation of cooling capacity with time for (Tin=50°C and Qin=2 ℓ/min)

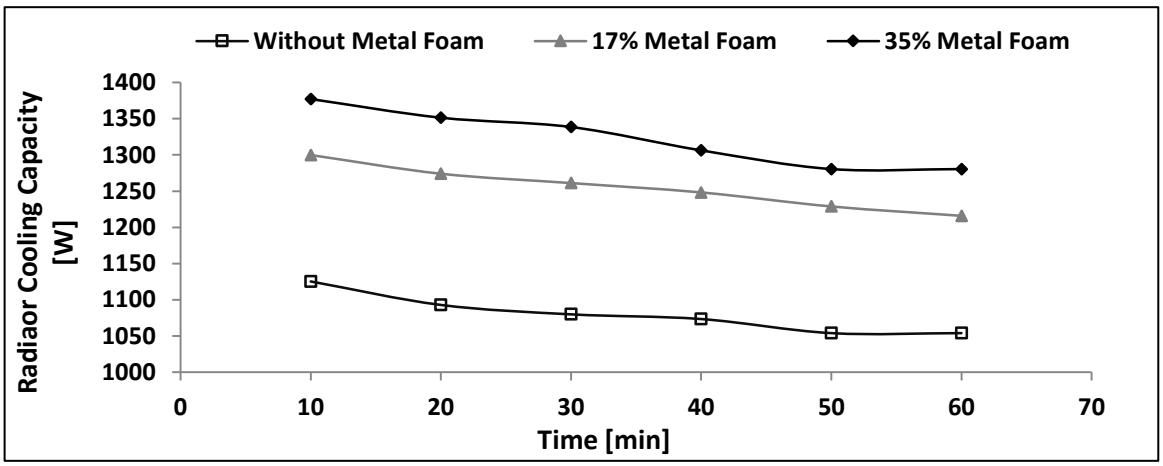

Fig. 4.41: Variation of cooling capacity with time for (Tin=60°C and Qin=2 ℓ/min)

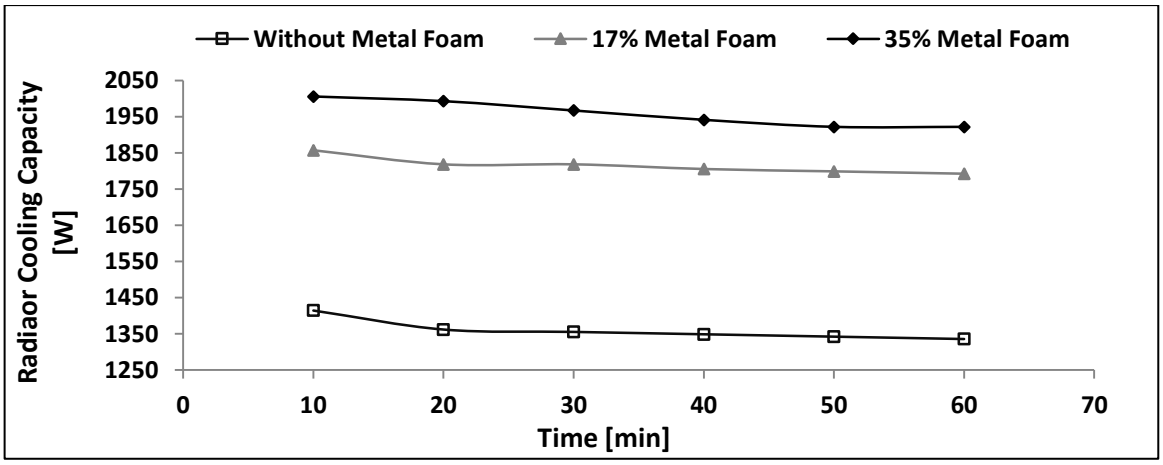

Fig. 4.42: Variation of cooling capacity with time for (Tin=70°C and Qin=2 ℓ/min)

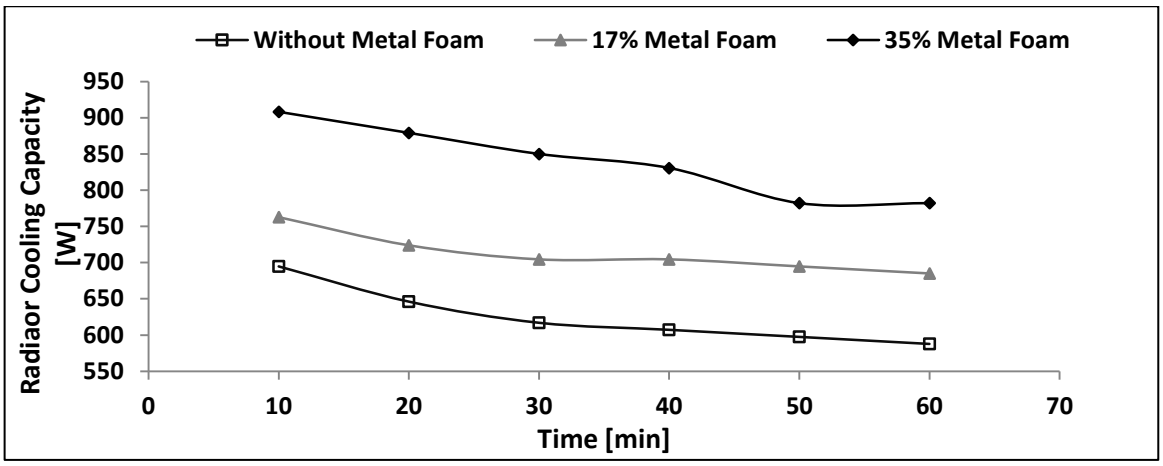

Fig. 4.43: Variation of cooling capacity with time for (Tin=50°C and Qin=3 ℓ/min)

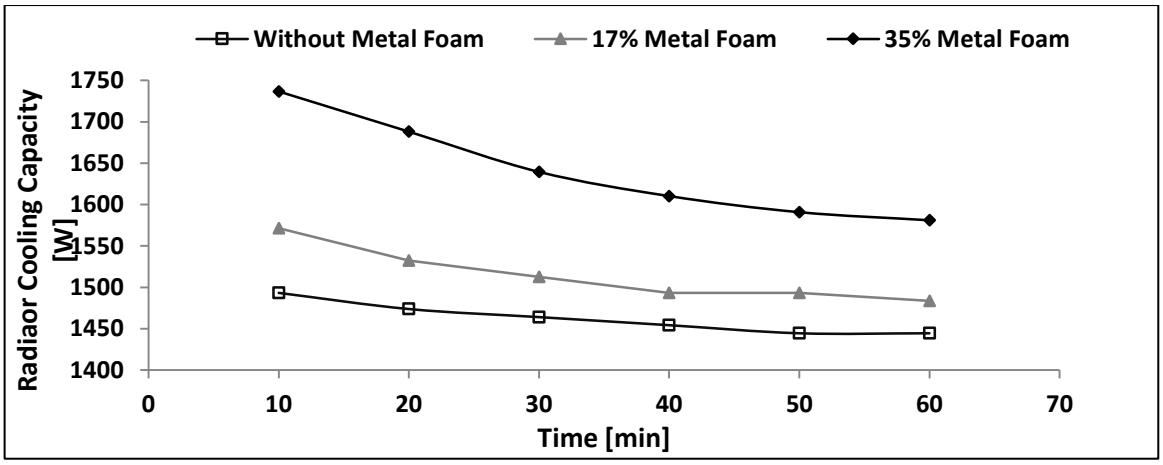

Fig. 4.44: Variation of cooling capacity with time for (Tin=60°C and Qin=3 ℓ/min)

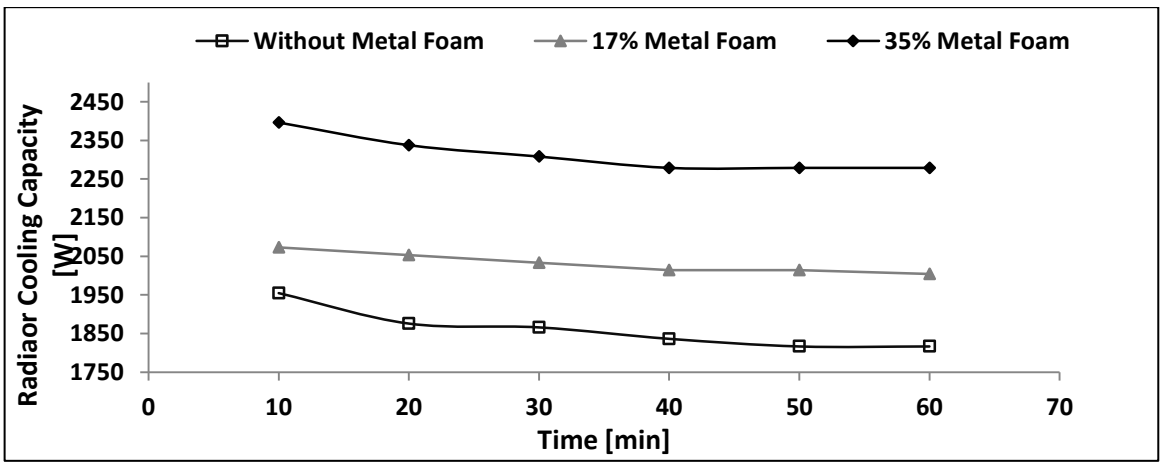

Fig. 4.45: Variation of cooling capacity with time for (Tin=70°C and Qin=3 ℓ/min)

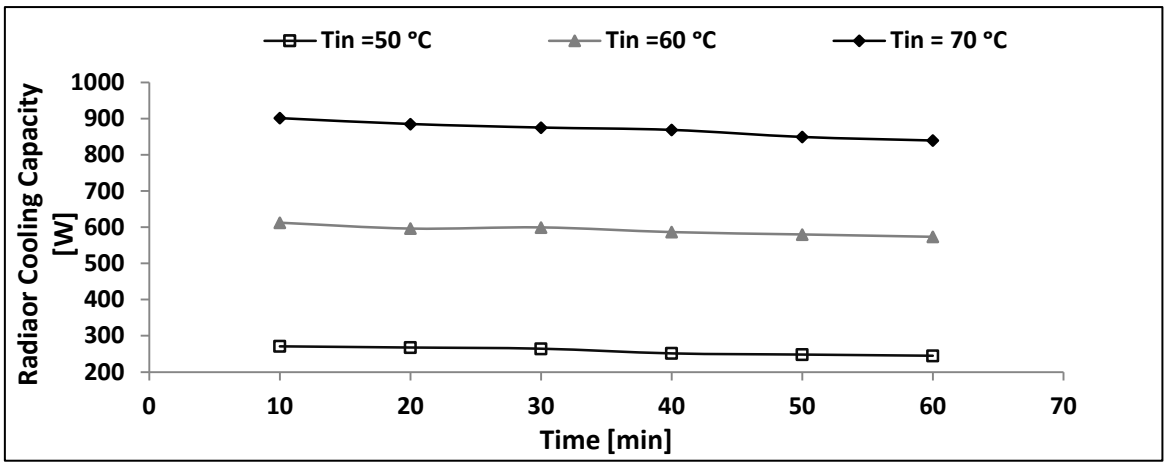

Fig. 4.46: Variation of cooling capacity with time for without metal foam and Qin=1 ℓ/min

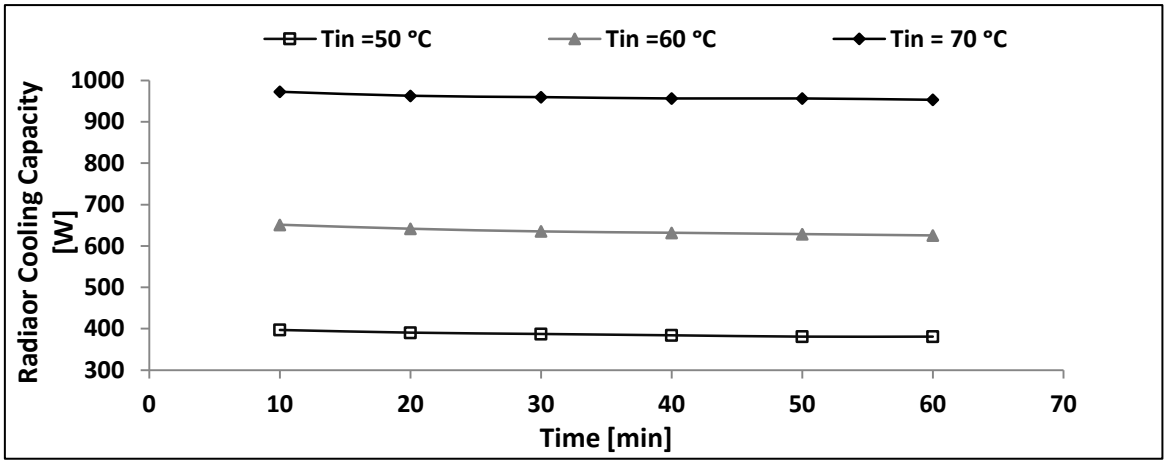

Fig. 4.47: Variation of cooling capacity with time for 17 % metal foam and Qin=1 ℓ/min

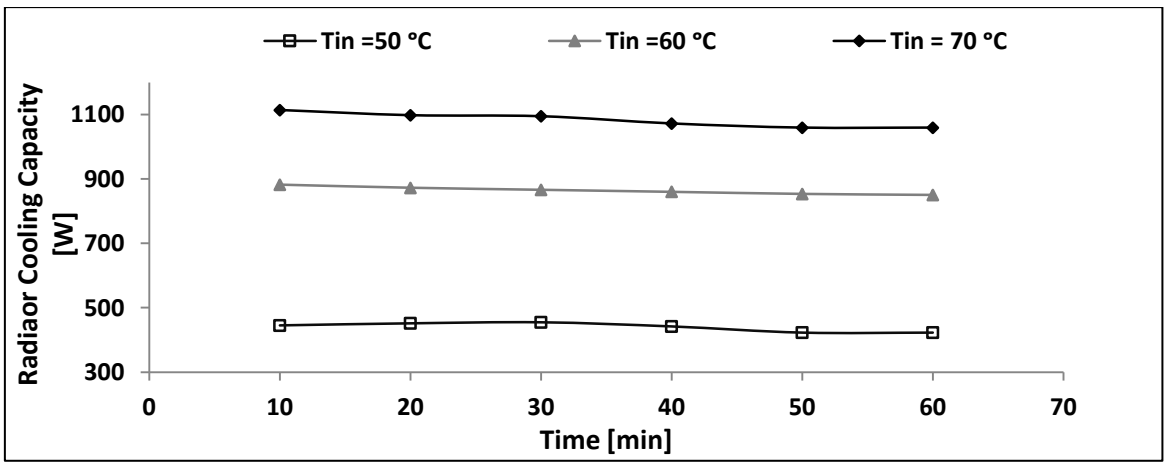

Fig. 4.48: Variation of cooling capacity with time for 35 % metal foam and Qin=1 ℓ/min

4.6.2 ODAF Model

This section explained the effect of adding metallic foam (17% and 35% porosity) to the radiator system. The average fans speed of 6.5 m / s is used for forced air. This research was carried out through the results recorded from all previous pilot tests of the models. Thus, the study was carried out simultaneously with the previously mentioned weather conditions for the model tests. Experiments were performed for each oil flow rate (1, 2, 3 ℓ/min) at the inlet oil temperature (50, 60, and 70 ° C) to demonstrate the effect of foaming metallic sponges on the cooling capacity.

Figures (4.49) to (4.57) demonstrated that cooling capacity increased with increasing the porosity of metal foam for crammed in panels' voids of transformer radiator, ranging from 17 to 35% along the time of operation with inlet oil temperature values at each flow. Also, it is visible from the figures that cooling capacity increased with increase the thermal conductivity of the panel walls due to the metallic foam physical properties have more thermal conductivity than panels, which it's enhancement heat transferred between the oil and panels wall to reach maximum cooling capacity (493, 895, 1181W), (843.5, 1633.7, 2269), and (1149.8, 2017.6, 3000W) at all inlet oil temperature for each flow rate, at metal foam magnitude of porosity 35%. On the other hand, when there is doubled influencing as (fans and metal foam), they may also be seen in Figures from 4.46 to 4.54, the increase in cooling capacity values due to increasing heat transfer forced convection and thermal conductivity of radiator panels compared with validate of Kaymaz (2015) [71].

Figures. (4.58, 4.59 and 4.60) show the effects of increased the radiator panel's surfaces through the increase in the porosity densities of metal foam sponges to reach 35 %. These figures are obtained at volumetric oil flow rate (Q1 =1 ℓ/min) and different inlet oil temperatures and metallic foam values. From the figures, it can be clearly seen that the maximum cooling capacity for each cases with raised when value of metal foam porosity is 35 %. The same trends are

occurred for the other flow rates, 2 and 3 ℓ/min.

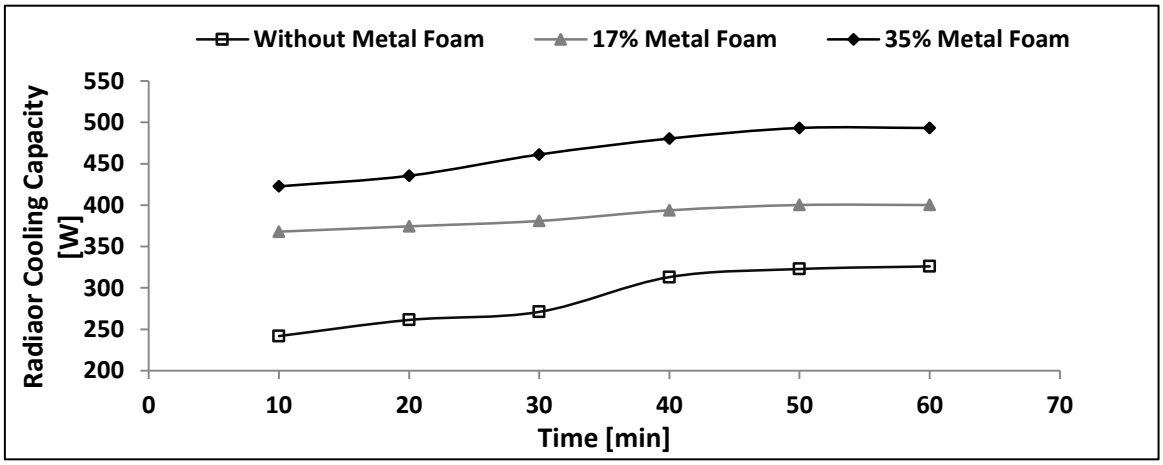

Fig: 4.49: Variation of cooling capacity with time for (Tin=50°C and Qin=1 ℓ/min)

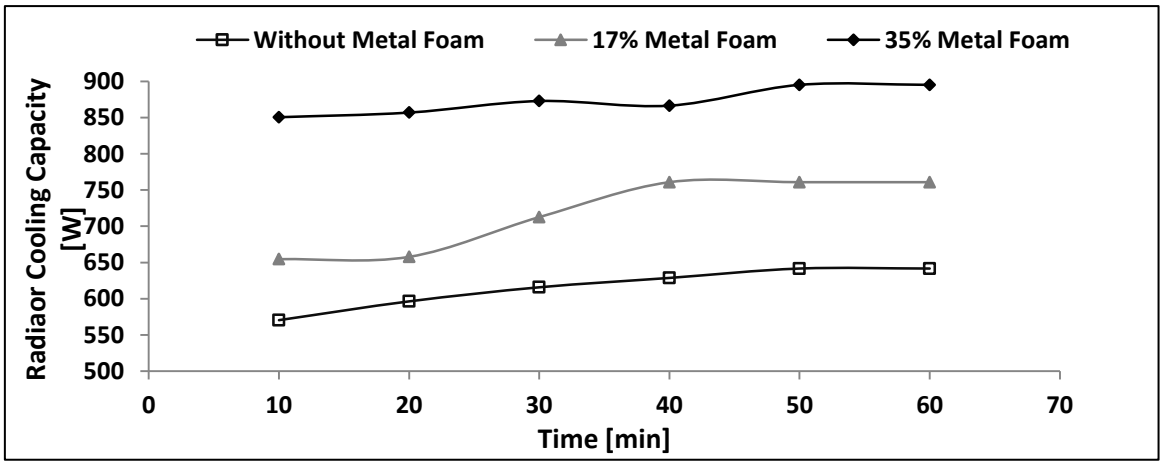

Fig. 4.50: Variation of cooling capacity with time for (Tin=60°C and Qin=1 ℓ/min)

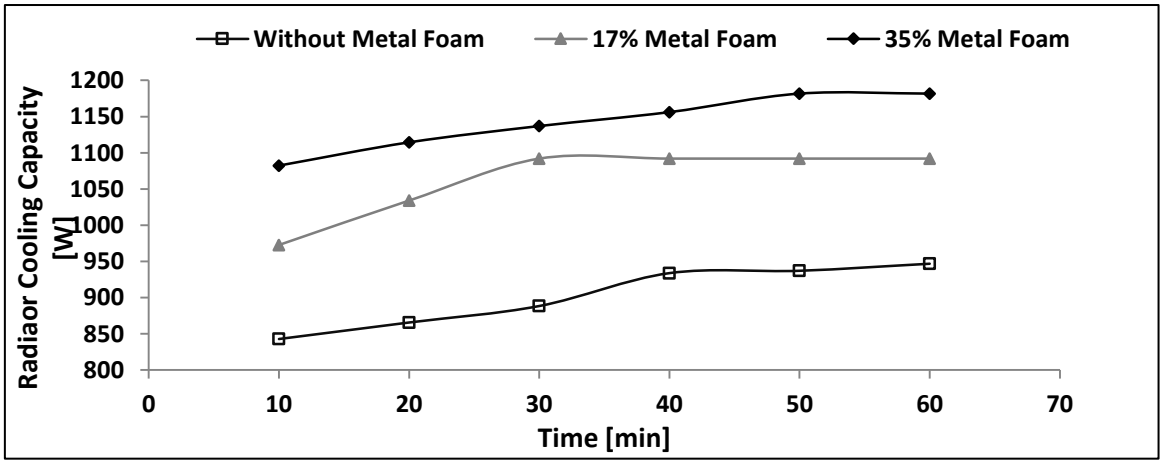

Fig. 4.51: Variation of cooling capacity with time for (Tin=70°C and Qin=1 ℓ/min)

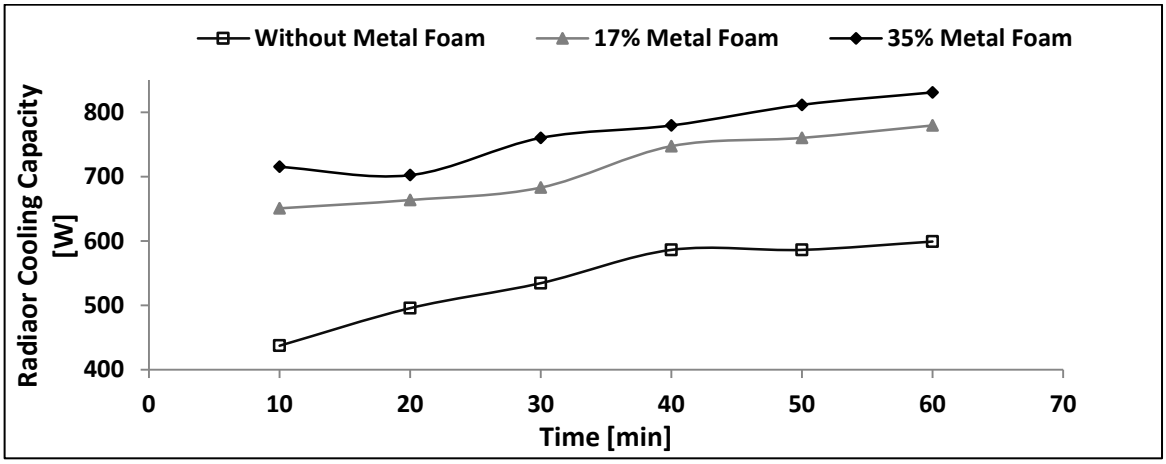

Fig. 4.52: Variation of cooling capacity with time for (Tin=50°C and Qin=2 ℓ/min)

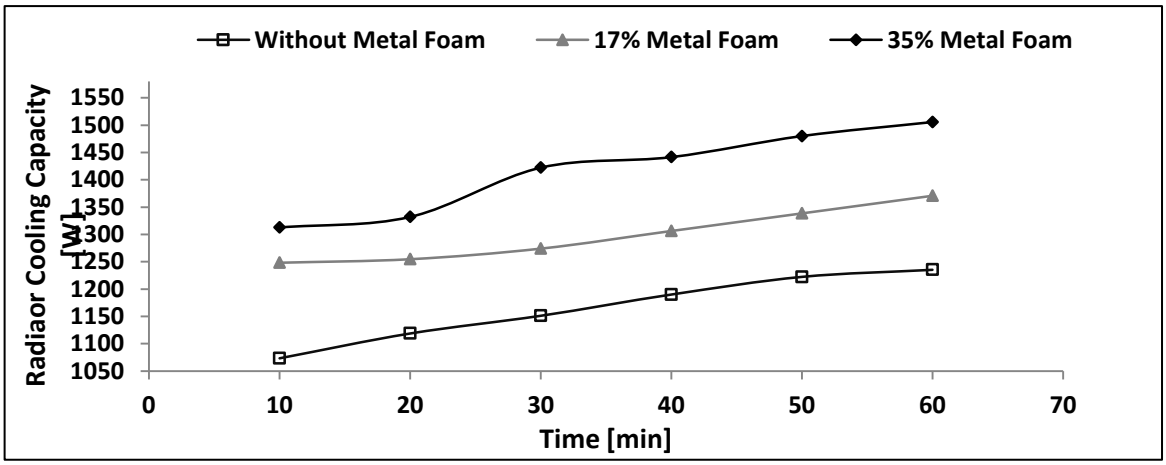

Fig. 4.53: Variation of cooling capacity with time for (Tin=60°C and Qin=2 ℓ/min)

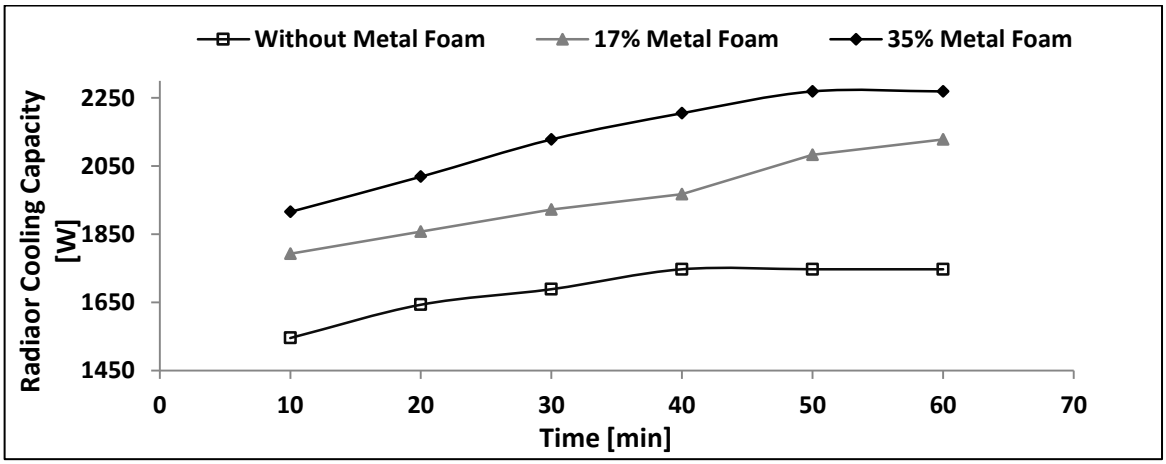

Fig. 4.54: Variation of cooling capacity with time for (Tin=70°C and Qin=2 ℓ/min)

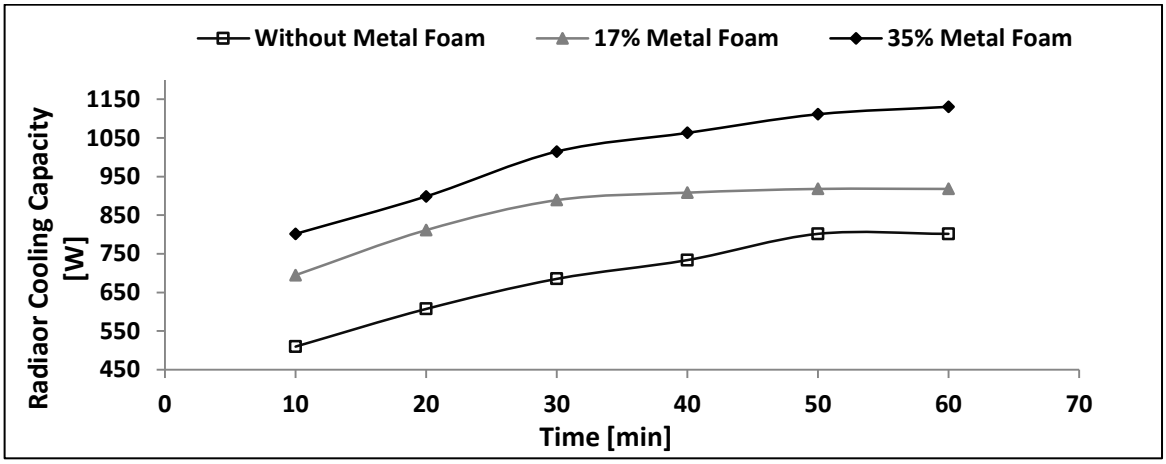

Fig: 4.55: Variation of cooling capacity with time for (Tin=50°C and Qin=3 ℓ/min)

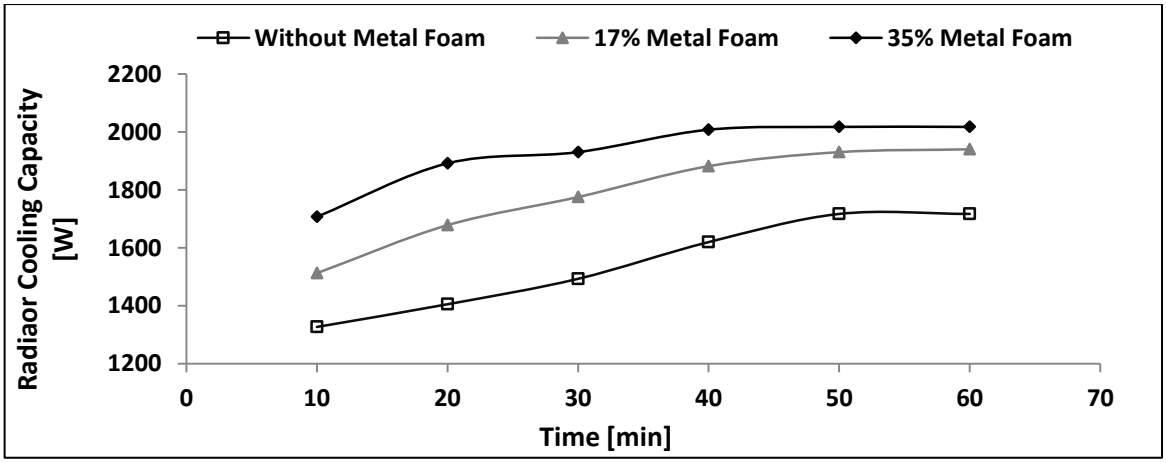

Fig. 4.56: Variation of cooling capacity with time for (Tin=60°C and Qin=3 ℓ/min)

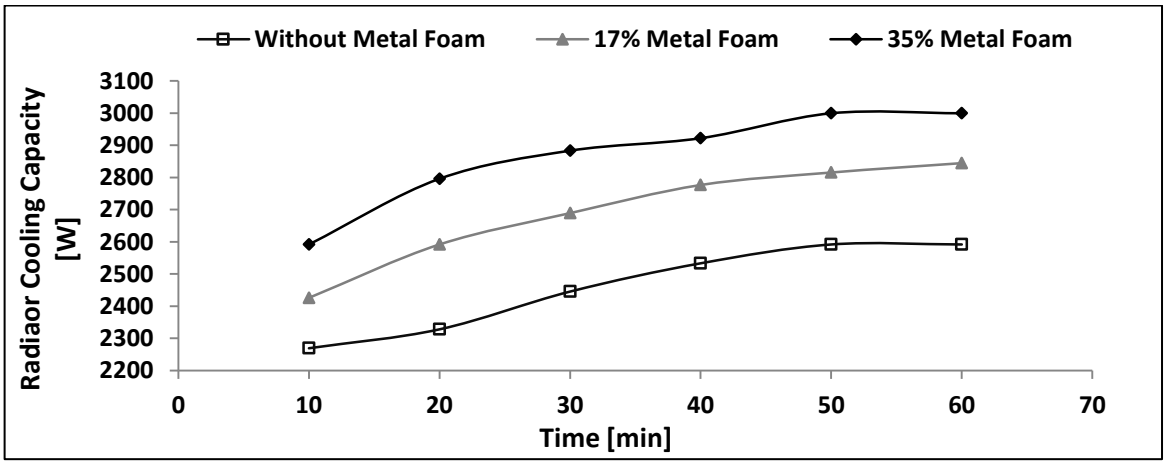

Fig. 4.57: Variation of cooling capacity with time for (Tin=70°C and Qin=3 ℓ/min)

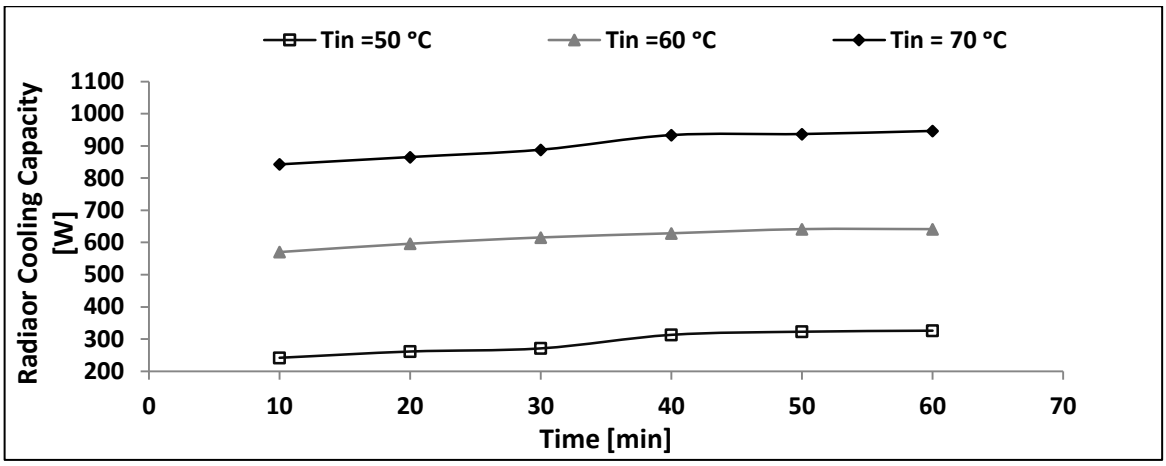

Fig. 4.58: Variation of cooling capacity with time for without metal foam and Qin=1 ℓ/min

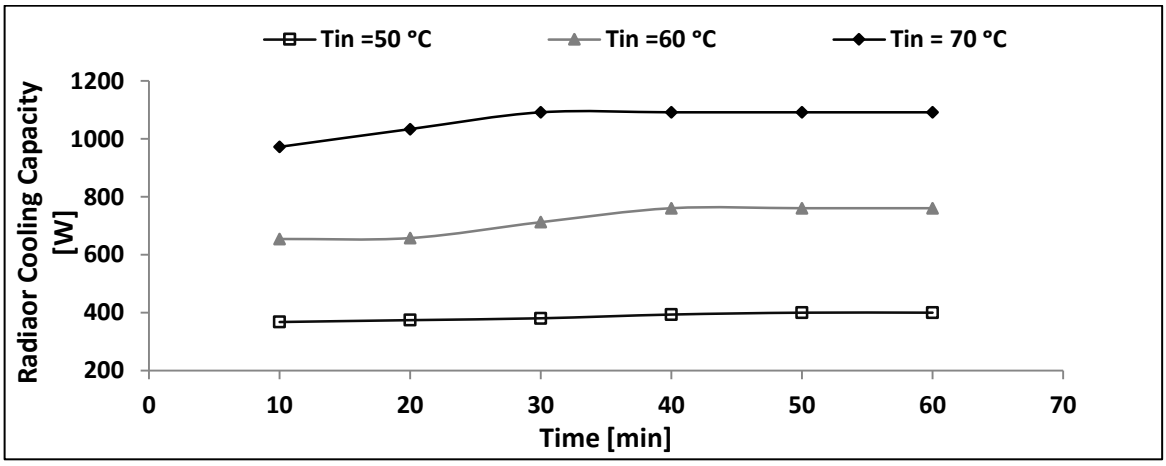

Fig. 4.59: Variation of cooling capacity with time for 17 % metal foam and Qin=1 ℓ/min

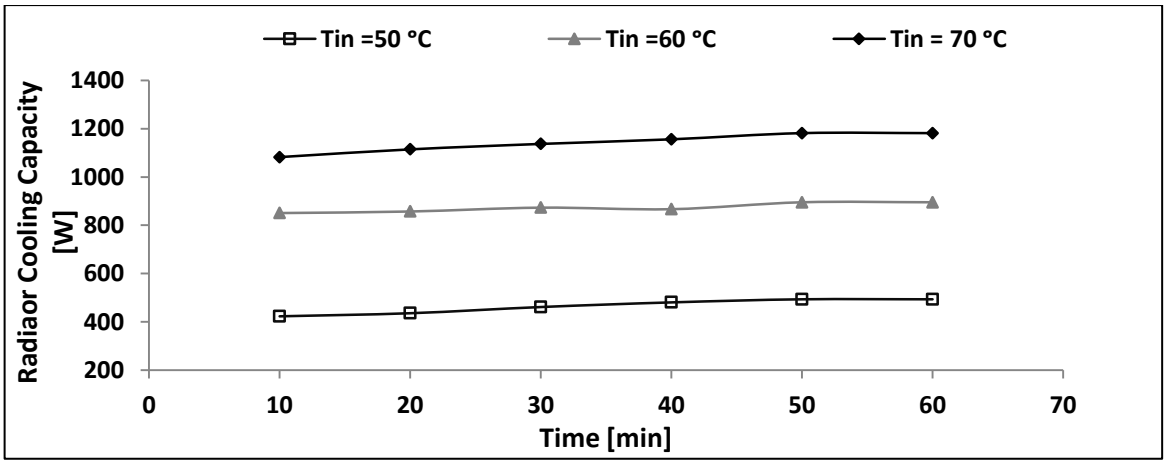

Fig. 4.60: Variation of cooling capacity with time for 35 % metal foam and Qin=1 ℓ/min

CHAPTER FIVE

CONCLUSION AND RECOMMENDATIONS

CHAPTER FIVE

CONCLUSION AND RECOMMENDATIONS

5.1 Conclusion

For large transformer radiator, the following concluded points determined the radiator cooling performance:

i. There are good responses between heat transfer and variation in operational parameters (oil flow rate, temperature, and airflow) in experiment work.

ii. As the flow rate increased, the temperature difference between the top and bottom decreased because of the high volume flow rate.

iii. Cooling capacity value of radiator increases at the increase of flow rates.

iv. The maximum cooling capacity for oil temperature 70°C and flow rate is 3 l/min, with 17% porosity of metal foam and without using metal foam are (2003.9 and 1816.5) W, respectively. When model cooling is (ODAN).

v. Amount of cooling capacity with oil temperature 70°C and flow rate of 3 l/min with using effect of 17% porosity of metal foam and without using metal foam are (2844.3W and 2591.6W), respectively when typical of a model (ODAF).

vi. Value of maximum cooling capacity is (3000 W) when using metal foam heat exchanger (MFHE) system with porosity (35%), and ODAF model, oil flow rate and temperature are (3 l/min and 70 ◦C), respectively. While (2844 W) for (17%) porosity at the same cooling model.

vii. Variation of radiator temperatures for ODAN model increased with time not exceeding 10 ◦C to reach the steady-state after the minutes fifty from the experiment was started.

viii. Variation of radiator temperatures for the ODAF model increased with time not exceeding 7.5 ◦C to reach the steady-state after the minutes forty from the experiment was started.

ix. During the beginning of an experiment, variation of temperatures until steady-state (transient) are different from one model to another model.

x. Reaching the steady-state of variation of temperatures for ODAF model, and using metal foam with porosity of (35%), were faster than author models.

xi. The maximum cooling capacity increased with increases surface porosity density between the vertical panels of the radiator.

xii. Based on these tests' results, it may be observed that the radiator cooling performance could be applied to oil-filled large transformer radiators using the cooling mode forced or natural cooling.

5.2 Recommendations

Several studies can be carried out in the future to understand the behavior of radiators, including:

i. Studying the effect of changing radiator fins' shape that affects them by examining figures that differ from the traditional rectangular radiator panels, as in piercing or changing its geometric shapes.

ii. Using hybrid nanoparticles such as water-Cu nanoparticles with Al_2O_3, especially when applying forced convection to determine the best speed of the appropriate oil with the radiator's size and the amount of air circulating the radiator fins.

iii. Studying influence of nanoparticles on the metal foam sponges.

iv. Studying the forced convection transformer oil through oil-based microencapsulated phase change materials (MEPCM) suspension with multi-volume fractions %.

v. Using materials have thermal conductivity, light weight and suitable costs from other than aluminum, as nickel, coper and others in metal foam sponges.

REFERENCES

REFERENCES

[1] Del Vecchio, Robert M., et al. *Transformer design principles: with applications to core-form power transformers*. CRC press, 2010.

[2] Hosseini, R., M. Nourolahi, and Gevorg B. Gharehpetian. "Determination of OD cooling system parameters based on thermal modeling of power transformer winding." *Simulation Modelling Practice and Theory* 16.6 (2008): 585-596.

[3] Burgelman, Jean-Claude, Jarka Chloupková, and Werner Wobbe. "Foresight in support of European research and innovation policies: The European Commission is preparing the funding of grand societal challenges." *European Journal of Futures Research* 2.1 (2014): 55.

[4] Transmission Grid

[5] Kaymaz, Özben. Investigation of oil flow and heat transfer in transformer radiator. MS thesis. Izmir Institute of Technology, 2015.

[6] https://www.electricaleasy.com Transformers/ cooling methods of a transformers

[7] http://www.iran-transfo.com /earthlink oil-immersed transformer

[8] Paramane, Sachin B. "Significance of radiation heat transfer on cooling performance of transformer radiator." Transformers Magazine 6.3 (2019): 118-124.

[9] J. Harlow, "ELECTRIC POWER TRANSFORMER ENGINEERING", CRC Press LLC, U.S.A, (2004).

[10] Madhloom, Riyadh Noman, and Nariman Khalid Hashim. "Reduce no-load losses of Electrical Transformers by Increasing the Number Turns of Coils." DIYALA JOURNAL OF ENGINEERING SCIENCES 8.4 (2015).

[11] Franklin, Arthur Charles, and David Peter Franklin. The J & P transformer book: a practical technology of the power transformer. Elsevier, 2016.

[12] Sheldrake, Alan L. Handbook of electrical engineering for practitioners in the oil, gas and petrochemical industry. John Wiley & Sons Ltd, The Atrium, Southern Gate, Chi Chester, 2003

[13] IEC Pressboard and press paper for electrical purposes – Part 1 - 3, IEC6064:2004.https://new.abb.com/news/detail/9891/thermoplastic-insulation-in-power-transformers

[14] Wilson Power and Distribution Technologies Private Limited https://www.indiamart.com/wilson-power-distribution-tech.

[15] Transformers—Part, IEC Power. "2: Temperature Rise for Liquid-Immersed Transformers." IEC Standards; IEC (2011): 60076-2.

[16] Bo, C. H. E. N. "Magnetically controlled soft starter for high-voltage electric machines based on PLC regulatory system [J]." Engineering Journal of Wuhan University 2 (2012).

[17] Kefin Raily, Life of Transformer, Get Empowered with Doble, Febru-ary 20-24, 2017.

[18] Kaymaz, Özben. Investigation of oil flow and heat transfer in transformer radiator. MS thesis. Izmir Institute of Technology, 2015.

[19] Mohammed, "Enhancement and optiization of heat transfer for different elecrical transformer", Theses from the engineering Basrah university. September 2018.

[20] Kulkarni, Shrikrishna V., and S. A. Khaparde. Transformer engineering: design and practice. Vol. 25. CRC Press, 2004. [21] Kulkarni, Shrikrishna V., and S. A. Khaparde. Transformer engineering: design and practice. Vol. 25. CRC Press, 2004.

[21] Al-Ajmi, F., D. L. Loveday, and Victor Ian Hanby. "The cooling potential of earth–air heat exchangers for domestic buildings in a desert climate." Building and Environment 41.3 (2006): 235-244.

[22] Cheng, Lefeng, et al. "Hot spot temperature and grey target theory-based dynamic modelling for reliability assessment of transformer oil-paper insulation systems: A practical case study." *Energies* 11.1 (2018): 249.

[23] C. Rosas, N. Moraga, V. Bubnovich, and R. Fischer, "Improvement of the Cooling Process of Oil-Immersed Electrical Transformers Using Heat Pipes", IEEE Transactions on Power Delivery, Vol. 20, No. 2, pp (1955-1961), (2005).

[24] N. El Wakil, N. Chereches, and J. Padet, "Numerical study of heat transfer and fluid flow in a power transformer", International Journal of Thermal Sciences,Vol.45,No.6, pp (615–626), (2006).

[25] Zhou, L. J., et al. "Thermal overshoot analysis for hot-spot temperature rise of transformer." IEEE Transactions on Dielectrics and Electrical Insulation 14.5 (2007): 1316-1322.

[26] Torriano, F., M. Chaaban, and P. Picher. "Numerical study of parameters affecting the temperature distribution in a disc-type transformer winding." Applied Thermal Engineering 30.14-15 (2010): 2034-2044.

[27] Skillen, A., Revell, A., Iacovides, H.&Wu, W. (2011). Numerical prediction of local hot-spot phenomena in transformer windings. Applied Thermal Engineering, 36, 96-105.

[28] M. Djamali, and S. Tenbohlen, "A validated online algorithm for detection of fan failures in oil immersed power transformers", International Journal of Thermal Sciences,Vol.116 ,pp (224-233), (2017).

[29] Z. Radakovic, M. Jevtic, and B. Das, "Dynamic thermal model of kiosk oil immersed transformers based on the thermal buoyancy driven air flow", Electrical Power and Energy Systems,Vol. 92 ,pp (14–24), (2017).

[30] Münster, Tobias, et al. "Thermally Accelerated Aging of Insulation Paper for Transformers with Different Insulating Liquids." *Energies* 14.11 (2021): 3036.

[31] G. Swift, T. Molinski, and W. Lehn, "A Fundamental Approach to Transformer Thermal Modelling-Part I: Theory and Equivalent Circuit", IEEE Transactions on Power Delivery, Vol.16, No. 2, pp (171 – 175), (2001).

[32] S. Dejan, "Dynamic Thermal Modeling of Power Transformers", Ph.D. dissertation, Helsinki University of technology, (2005).

[33] R. Meshkatoddini, Sh. Abbaspour, "Aging study and lifetime estima-tion of transformer mineral oil", Am. J. Eng. Appl. Sci. Vol.1, No.4, pp (384–388), (2008).

[34] J. Gastelurrutia, J. Ramos, G. Larraona, A. Rivas, J. Izagirre, and L. Rيo," Numerical modelling of natural convection of oil inside distribution transformers", Applied Thermal Engineering, Vol.31, No.4, pp (493-505), (2011).

[35] M. Taghikhani, and A. Gholami, "Prediction of hottest spot temperature in power transformer windings with non-directed and directed oil-forced cooling", Electrical Power and Energy Systems, Vol. 31, No.7-8, pp (356–364),2009.

[36] B. Diaconu, S. Vaga, A. Oliveira, "Experimental study of natural convection heat transfer in a microencapsulated phase change material slurry", Journal of Applications Energy, Vol. 35, pp (2688–2693), 2010.

[37] Fonte, Carlos M., et al. "CFD analysis of core type power transformers." 21st International Conference on Electrical Distribution, Frankfurt, Germany. 2011.

[38] M. Srinivasan and A. Krishnan, "Prediction of Transformer Insulation Life with an Effect of Environmental Variables", International Journal of Computer Applications, Vol.55, No.5, pp (975–987),(2012).

[39] Wittmaack, Ralf. "CFD SIMULATION OF PRESSURE LOSS IN HVDC TRANSFORMER WINDING." Journal of Energy: Energija 63.1-4 (2014): 0-0.

[40] G. Shukla, H. Aiyer, "Thermal conductivity enhancement of transformer oil using functionalized nanodiamonds", IEEE Transactions on Dielectrics and Electrical Insulation, Vol. 22, pp (2185–2190), (2015).

[41] I. Fernndez, , F. Delgado, F. Ortiz, A. Ortiz, C. FernJndez, C. Renedo, A. Santisteban, "Thermal degradation assessment of Kraft paper in power transformers insulated with natural esters", Applied Thermal Engineering,Vol.104, pp (129–138), (2016).

[42] M. Hasan, "Improving the cooling performance of electrical distribution transformer using transformer oil – based MEPCM suspension", Engineering Science and Technology, an International Journal, Vol.20, No.2, pp (502-510), (2017).

[43] Paramane, Sachin B., et al. "CFD study on thermal performance of radiators in a power transformer: effect of blowing direction and offset of fans." *IEEE Transactions on Power Delivery* 29.6 (2014): 2596-2604.

[44] Fdhila, Rebei Bel, et al. "Thermal modeling of power transformer radiators using a porous medium based CFD approach." Second International Conference on Computational Methods for Thermal Problems, Dalian, China. 2011.

[45] Kim MG, Cho SM, Kim JK. Prediction and evaluation of the cooling performance of radiators used in oil-filled power transformer applications with non-direct and direct-oil-forced flow. Experimental Thermal and Fluid Science. 2013 Jan 1;44:392-7.

[46] Paramane, Sachin B., Wim Van der Veken, and Atul Sharma. "A coupled internal–external flow and conjugate heat transfer simulations and experiments on radiators of a transformer." Applied Thermal Engineering 103 (2016): 961-970.

[47] L. Garelli, G. Rodriguez, M. Storti, D. Granata, M. Amadei, M. Rossetti, "Reduced Model for the Thermo-Fluid Dynamic Analysis of a Power

Transformer Radiator working in ONAF mode", Applied Thermal Engineering, Vol.124, pp (855-864),(2017).

[48] N. Chereches, M. Chereches, L. Miron, and S. Hudisteanu, "Numerical study of cooling solutions inside a power transformer", Energy Procedia,Vol. 112 ,pp (314 – 321), (2017).

[49] Z. Radakovic, M. Jevtic, and B. Das, "Dynamic thermal model of kiosk oil immersed transformers based on the thermal buoyancy driven air flow", Electrical Power and Energy Systems,Vol. 92 ,pp (14–24), (2017).

[50] Azbar, Nawras Mohammed, Hayder Mohammad Jaffal, and Basim Freegah. "Enhancement of the Thermal Performance Characteristics of an Electrical Power Transformer." *Engineering Science & Technology* (2021): 1-21.

[51] Kim, S. Y., J. W. Paek, and B. H. Kang. "Flow and heat transfer correlations for porous fin in a plate-fin heat exchanger." J. Heat Transfer 122.3 (2000): 572-578.

[52] Pavel, Bogdan I., and Abdulmajeed A. Mohamad. "Experimental investigation of the potential of metallic porous inserts in enhancing forced convective heat transfer." J. Heat Transfer 126.4 (2004): 540-545.

[53] Salas, Ken I., and Anthony M. Waas. "Convective heat transfer in open cell metal foams." (2007): 1217-1229

[54] Dai Z, Nawaz K, Park Y, Chen Q, Jacobi AM. A comparison of metal-foam heat exchangers to compact multilouver designs for air-side heat transfer applications. Heat Transfer Engineering. 2012 Jan 1;33(1):21-30.

[55] Nawaz K, Bock J, Jacobi AM. Thermal-hydraulic performance of metal foam heat exchangers under dry operating conditions. Applied Thermal Engineering. 2017 Jun 5;119:222-32.

[56] Saeid, Nawaf H., Nurul Hasan, and Mohamed Hairol Bin Hj Mohd Ali. "Effect of the metallic foam heat sink shape on the mixed convection jet impingement cooling of a horizontal surface." Journal of Porous Media 21.4 (2018).

[57] Shenming, Xu, Yu Ran, Shen Limei, Wang Yupeng, and Xie Junlong. "The experimental study of a novel metal foam heat pipe radiator." Energy Procedia 158 (2019): 5439-5444.

[58] da Silva VA, de Neves Gomes LA. Analysis of natural convection in heat sink using OpenFOAM and experimental tests. Heat and Mass Transfer. 2019 Aug 1;55(8):2289-304.

[59] Oil-immersed transformer (ONAO) cooled system, (TOZIE IRAN TRANSFO ZANGAN/ CO. (P.J.S)), Type - TSUE6346, 53 N0. S0680543, Year 2008, Standard IEC-60289, 60076" http://www.iran-transfo.com/en/oil_immersed.php.

[60] Nynas Oil Company__https://www.naynas.com//en/product-areas/transformer-oils

[61] Baltazar, José Paulo Barbosa. "Modelling vertical plate radiators for electric transformers." (2014).

[62] Digital Oil Flowmeter- https://www.ebay.com/itm/171937109676

[63] Temperature data logger V2 specifications
https://www.ebay.com/itm/124505694771

[64] Thermometer device specification

https://www.ebay.com/itm/333481485744

[65] Hafeez, Pakeeza. A thesis, "Heat Transfer in Metal Foam Heat Exchanger at High" Temperature. Diss. 2016.

[66] Calmidi, Varaprasad Venkata. Transport phenomena in high porosity fibrous metal foams. University of Colorado at Boulder, 1998.

[67] Dixit, Tisha, and Indranil Ghosh. "An experimental study on open cell metal foam as extended heat transfer surface." *Experimental Thermal and Fluid Science* 77 (2016): 28-37.

[68] Viswanadham, B. V. S. "Advanced Geotechnical Engineering." Lecture No.2 (2016).

[69] Shang, Fumin, et al. "An experimental study on heat transfer performance of a pulsating heat pipe radiator for CPU heat dissipation." E3S Web of Conferences. Vol. 165. EDP Sciences, 2020.

[70] Dixit, Tisha, and Indranil Ghosh. "An experimental study on open cell metal foam as extended heat transfer surface." Experimental Thermal and Fluid Science 77 (2016): 28-37.

[71] Kaymaz, Özben. *Investigation of oil flow and heat transfer in transformer radiator*. MS thesis. Izmir Institute of Technology, 2015.

APPENDIX

APPENDIX A

CALIBRATION

A.1 Calibration

During the calibration of the measuring system, the relationship between the value of the measuring system's input and the system's stated output value is described. Volumetric flow rate, temperature panel, outdoor air, and oil temperature inlet, and outlet Radiator. The volumetric fluid flow rate is measured with a flow meter. The heat meter is used to measure the inlet and outlet's oils, and thermocouples and sensors use the data logger to measure the radiator's oil and plates' temperature and the outside air. Since these currencies are easy to handle and have the necessary measurement precision, accurate measurements may be checked either by calibrating or comparing the instruments with other suitable measuring devices in normal conditions.

A.2 Oil flowmeter calibration

Using cylindrical graduated glass vessels and a stopwatch, the volumetric rate device is set. The calibration measurements and test results are shown in the following section. With a stopwatch and graduated glass vessel, the calibrator time weight method is used to calibrate the volume flow meter. The calibration is achieved by flowing oil through a flow meter at various flow rates while simultaneously calculating the flow time needed by volume by the pail to fill the correct amount of working fluid. Calibration samples for volume flow meters as follows:

For each volumetric flow measurement, a volume of one liter of oil is used for one minute of testing.

Table. A.1: Oil flow meter calibration

Inspection Number	Monitor Time In (minute)	Oil discharge is a graduate vessel In (LPM)
1	1	0.98
2	1	0.97
3	1	0.966
4	1	0.97
5	1	0.98

The average volumetric flow rates.

V= $(v_1+v_2+v_3+v_4+v_5)/4$= (0.98+0.97+0.966+0.97+0.98)/5= 0.973 LPM the error of the volume flow meter = 1- 0.973 =0.027 LPM

% Error= (1-0.027)/1 ×100 = 2.7%

A.3 Sensors Temperature of V8 Data Logger Calibrations and 3K type thermocouples:

A mercury thermometer tests temperature sensors (S1 to S6) for Data Logger. A mercury thermometer also measures three thermocouples (T1 to T3), which are calibrated using the data in the Tables (A-2) and (A-3)

Table A.2: Calibration of V8- channels data logger with six sensors.

Mercury Thermometer °c	Sensor1 °c	Sensor2 °c	Sensor3 °c	Sensor4 °c	Sensor5 °c	Sensor6 °c
20	20.4	20.4	20.3	19.8	19.7	20.3
25	25.5	25.4	24.6	24.7	25.4	25.3
30	30.4	30.3	30.5	29.7	30.4	30.3
35	35.4	35.4	35.3	35.4	34.6	35.4
40	40.3	40.2	40.2	40.2	39.9	39.8
45	45.2	45.4	44.7	44.6	45.2	45.2
50	50.3	50.4	49.6	49.7	50.1	50
55	55.4	55.3	54.6	55.1	55.3	54.6
60	60.3	60.4	60.3	60.1	59.7	60.2
65	64.5	65.4	64.5	64.5	65.5	64.6

Table A.3: The calibration for 3 k- type thermocouple.

Mercury Thermometer °c	T1 °c	T2 °c	T3 °c
20	20.4	19.4	20.4
25	24.8	25.4	25.4
30	30.4	30.5	30.3
35	35.5	35.3	35
40	40.4	40.3	40
45	45.4	45	44.7
50	50.3	50	50.4
55	55.3	55.2	55
60	60.4	60.3	60
65	64.3	65	64.7

A.4 Wind Speed Sensor Calibration

The wind speed measurement system (anemometer) type (AM-4206M) used in all experiments testing has been calibrated with a standard Davis weather station located at 10 meters above ground level in Najaf Engineering Technical College in Iraq. This station calculates wind speed in millimeters per second (m/s), with a range of 0.1 to 89 m/s and a precision of 5%. The calibration results are shown in the graph below (A-4).

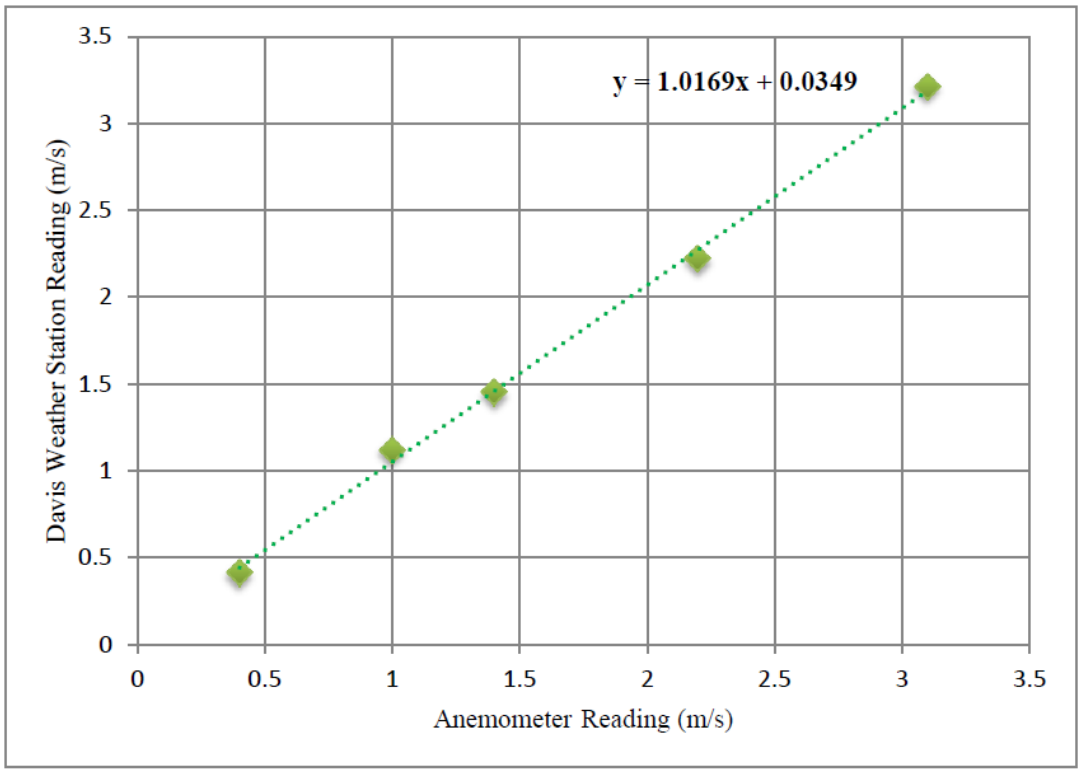

Fig. A-4: Anemometers Calibration

APPENDIX B

FOAM POROSITY CALCULATION

APPENDIX B

FOAM POROSITY CALCULATION

B-1 Porosity Calculation

For calculated the porosity of metal foam that used in an experimental test, we should find the volume of one piece of metal in in a graduated laboratory container with accurate measurements. Also must find the rigid volume (solid volume) for one piece of metal foam, after that calculate the void volume when used 20 pieces of metal foam and in second experimental test used 40 pieces. Now the porosity of the two cases can be calculated as the following steps.

a) Volume of metal in Laboratory is ($1.1 * 10^{-6}\ m^{3)}$

b) Solid volume of metal out the laboratory is ($1.57 * 10^{-4}\ m^3$)

c) $V_v = V_s - V$ *where, void volume = solid volume –metal volume in laboratory*

The void volume is ($1.56 * 10^{-4}\ m^3$)

d) V_t (*V total*) for the panel of radiator by multi the (length * width * high) is ($1.8 * 10^{-2}\ m^3$)

h) The void volume for 20 pieces is ($3.18 * 10^{-3}\ m^3$)

i) The void volume for 40 pieces is ($6.24 * 10^{-3}\ m^3$)

Table. B-1: The porosity calculation results

Number of Metal Foam For Radiator Panel	Porosity Raito (ε)	Porosity %
20	0.17	17
40	0.35	35

APPENDIX C

EXPERIMENTAL WORK DATA

APPENDIX C

EXPERIMENTAL WORK DATA

Table. C-1: Data of experimental work for day (1/9/2020), Time from (05:00 PM to 12:00 AM), ($T_{ave;\ amb}$ = 40°C), and Flow rate (1 ℓ/min)

Cooling Model	**Temperature (°C)**										**Specific Heat**	**Mass Flow Rate**	**Cooling Capacity**
	$T_{oil,in}$	T1	T2	T3	T4	T5	T6	$T_{oil,out}$	ΔT	$T_{ave;oil}$	Cp (J/kg.k)	$\dot{m}_{oil}$ (W/m.k)	$P_{Radiator}$ (W)
ODAN	50	45.9	42.6	46.8	43.3	46.9	42.4	42.5	7.5	46.25	1956.37	0.0167	245
	60	49.4	42.9	52	43.5	52.6	42.7	42.6	17.4	51.3	1973.82	0.0167	573.6
	70	55.7	44.7	58.7	44.8	58.3	44.6	44.8	25.2	57.4	1996.63	0.0167	839.5
ODAF	50	43.9	41	43.4	41.7	44.8	41.3	40	10	45	1952.05	0.0167	326
	60	47	40.9	46	40.7	48	42.7	40.5	19.5	50.25	1970.19	0.0167	641.6
	70	50.9	40.9	49.5	40.9	52.9	42	41.5	28.5	55.75	1989.2	0.0167	946.7

Table. C-2: Data of experimental work for day (2/9/2020), Time from (05:00 PM to 12:00 AM), ($T_{ave;\ amb}$ = 40°C), and Flow rate (2 ℓ/min)

Cooling Model	**Temperature (°C)**										**Specific Heat**	**Mass Flow Rate**	**Cooling Capacity**
	$T_{oil,in}$	T1	T2	T3	T4	T5	T6	$T_{oil,out}$	ΔT	$T_{ave;oil}$	Cp (J/kg.k)	$\dot{m}_{oil}$ (W/m.k)	$P_{Radiator}$ (W)
ODAN	50	45.1	41	46.6	39.7	47	42.9	42.7	7.3	46.35	1956.71	0.0333	476
	60	52.5	43.3	53.5	42.6	52	43	44	16	52	1976.24	0.0333	1053.89
	70	60.6	51.1	61.8	51.4	62.7	48.4	50	20	60	2003.89	0.0333	1335.8
ODAF	50	41.9	37.6	40.3	36.9	43.5	37.9	40.8	9.2	45.4	1953.42	0.0333	599
	60	44.9	37.8	43	36.3	47.6	37.3	41.2	18.8	50.45	1971.40	0.0333	1235.29
	70	54.3	43.4	52.2	39.8	53.7	42	43.7	27.3	56.85	1993	0.0333	1747

Table. C-3: Data of experimental work for day (3/9/2020), Time from (05:00 PM to 12:00 AM), ($T_{ave;\ amb}$ = 40°C), and Flow rate (3 ℓ/min)

Cooling Model	**Temperature (°C)**										**Specific Heat**	**Mass Flow Rate**	**Cooling Capacity**
	$T_{oil,in}$	T1	T2	T3	T4	T5	T6	$T_{oil,out}$	ΔT	$T_{ave;oil}$	Cp (J/kg.k)	$\dot{m}_{oil}$ (W/m.k)	$P_{Radiator}$ (W)
ODAN	50	45	38.8	46.4	39.2	47	39	44	6	47	1958.96	0.05	587.6
	60	49.8	45.4	51	46.1	51.4	45.6	45.4	14.6	52.7	1978.66	0.05	1444.42
	70	60.8	50.7	62.5	50.2	63.8	50.6	51.9	18.1	60.95	2007.17	0.05	1816.5
ODAF	50	43.6	38.7	43.4	39.2	44.5	38.5	41.8	8.2	45.9	1955.15	0.05	801.6
	60	49	40	45	40.5	50	40	42.6	17.4	51.3	1973.8	0.05	1717.23
	70	56	44.7	50	45.9	56.3	44.8	44	26	57	1993.52	0.05	2591.58

Table. C-4: Data of experimental work for day (4/9/2020), Time from (05:00 PM to 12:00 AM), ($T_{ave;\ amb}$ = 40°C), and Flow rate (1 ℓ/min) With Metal Foam Porosity (MF 17%)

Cooling Model	**Temperature (°C)**										**Specific Heat**	**Mass Flow Rate**	**Cooling Capacity**
	T_{in}	T1	T2	T3	T4	T5	T6	T_{out}	ΔT	T_{ave}	Cp (J/kg.k)	$\dot{m}_{oil}$ (W/m.k)	$P_{Radiator}$ (W)
ODAN	50	43.8	39.2	46.4	39.5	46.4	38.7	38.3	11.7	44.15	1949.10	0.0167	380.8
	60	49.3	42.6	53.3	42.4	54.2	42.2	41	19	50.5	1971.05	0.0167	625.4
	70	54.5	43.6	58.9	43.3	60.5	43.3	41.3	28.7	55.65	1988.85	0.0167	953.2
ODAF	50	40.2	37.4	40.2	37.8	42.6	36.9	37.7	12.3	43.85	1948.07	0.0167	400.1
	60	42.2	38.3	41.9	36.8	46.8	37.2	36.8	23.2	48.4	1963.79	0.0167	760.8
	70	44.9	37.7	43.8	35.8	51.7	37.3	37	33	53.5	1981.42	0.0167	1091.97

Table. C-5: Data of experimental work for day (5/9/2020), Time from (05:00 PM to 12:00 AM), ($T_{ave;\ amb}$ = 40°C), and Flow rate (2 ℓ/min) With Metal Foam Porosity (MF 17%)

Cooling Model	**Temperature (°C)**										**Specific Heat**	**Mass Flow Rate**	**Cooling Capacity**
	T_{in}	T1	T2	T3	T4	T5	T6	T_{out}	ΔT	T_{ave}	Cp (J/kg.k)	$\dot{m}_{oil}$ (W/m.k)	$P_{Radiator}$ (W)
ODAN	50	45.1	40.8	45	41.8	48.1	40.3	40.5	9.5	45.25	1952.91	0.0333	618.36
	60	49	40	53.5	41	54.3	39.7	41.5	18.5	50.75	1971.92	0.0333	1215.9
	70	53.4	43,5	60	42.7	63.5	43.6	43	27	56.5	1991.79	0.0333	1792.4
ODAF	50	40.6	37.9	40.4	37	44.7	36	37.1	12.9	43.55	1947.04	0.0333	837
	60	41.6	37	41.2	35.3	46	36.1	36	24	48	1962.41	0.0333	1569.78
	70	46.2	39	45.2	35.3	52.6	38.6	36.3	33.7	53.15	1980.21	0.0333	2224.22

Table. C-6: Data of experimental work for day (6/9/2020), Time from (05:00 PM to 12:00 AM), ($T_{ave;\ amb}$ = 40°C), and Flow rate (3 ℓ/min) With Metal Foam Porosity (MF 17%)

Cooling Model	**Temperature (°C)**										**Specific Heat**	**Mass Flow Rate**	**Cooling Capacity**
	T_{in}	T1	T2	T3	T4	T5	T6	T_{out}	ΔT	$T_{ave;\ oil}$	Cp (J/kg.k)	$\dot{m}_{oil}$ (W/m.k)	$P_{Radiator}$ (W)
ODAN	50	46.8	42.6	49.6	42	47.8	42.6	43	7	46.5	1957.23	0.05	685
	60	52.5	44.8	56.8	56	55	44.9	45	15	52.5	1977.97	0.05	1483.4
	70	59	49.4	65.5	64.3	64	48.4	50	20	60	2003.89	0.05	2003.9
ODAF	50	42.2	40.2	38	37.9	43.2	40	40.6	9.4	45.3	1953.08	0.05	971.94
	60	43	41.3	43.2	35.4	48.8	38.8	40.3	19.7	50.1	1969.84	0.05	1940.3
	70	47	43.1	49	37.7	51.3	41.3	41.4	28.6	55.7	1989.03	0.05	2844.3

Table. C-7: Data of experimental work for day (7/9/2020), Time from (05:00 PM to 12:00 AM), ($T_{ave;\ amb}$ = 40°C), and Flow rate (1 ℓ/min) With Metal Foam Porosity (MF 35%)

Cooling Model	**Temperature (°C)**										**Specific Heat**	**Mass Flow Rate**	**Cooling Capacity**
	T_{in}	T1	T2	T3	T4	T5	T6	T_{out}	ΔT	$T_{ave;oil}$	Cp (J/kg.k)	$\dot{m}_{oil}$ (W/m.k)	$P_{Radiator}$ (W)
ODAN	50	44.1	37.8	47.2	37.4	46.5	37.6	37	13	43.5	1946.86	0.0167	422.6
	60	49	34.3	55.3	34.5	53.7	33.4	34	26	47	1958.96	0.0167	850.5
	70	52.3	39.5	58.3	40	58.1	38.4	38	32	54	1983.15	0.0167	1059.8
ODAF	50	37.5	35.3	37.4	34.5	40.4	33.9	34.8	15.2	42.4	1943.05	0.0167	493.2
	60	37.8	33.3	37.1	33	41.2	32.1	32.6	27.4	46.3	1956.54	0.0167	895.2
	70	37.8	35.6	38	33.6	40.5	34	34.2	35.8	52.1	1976.58	0.0167	1181.7

Table. C-8: Data of experimental work for day (8/9/2020), Time from (05:00 PM to 12:00 AM), ($T_{ave;\ amb}$ = 40°C), and Flow rate (2 ℓ/min) With Metal Foam Porosity (MF 35%)

Cooling Model	**Temperature (°C)**										**Specific Heat**	**Mass Flow Rate**	**Cooling Capacity**
	T_{in}	T1	T2	T3	T4	T5	T6	T_{out}	ΔT	$T_{ave;\ oil}$	Cp (J/kg.k)	$\dot{m}_{oil}$ (W/m.k)	$P_{Radiator}$ (W)
ODAN	50	45.6	40.7	48.8	41	48	40.7	40	10	45	1952.07	0.0333	650.6
	60	51.8	44.6	56.1	43	55.6	43.8	40.5	19.5	50.25	1970.19	0.0333	1280.5
	70	54.7	44.4	61.8	42.3	60.7	42.4	41	29	55.5	1988.34	0.0333	1921.8
ODAF	50	40.5	38.1	40.3	37.2	43.1	37.2	37	13	43.5	1946.86	0.0333	843.55
	60	44	39.1	43.9	37.4	48.9	38	35	25	47.5	1960.68	0.0333	1633.74
	70	43.3	38.5	44.4	35.4	50.4	36.3	35.6	34.4	52	1979	0.0333	2269.04

Table. B-9: Data of experimental work for day (9/9/2020), Time from (05:00 PM to 12:00 AM), ($T_{ave;\ amb}$ = 40°C), and Flow rate (3 ℓ/min) With Metal Foam Porosity (MF 35%)

Cooling Model	**Temperature (°C)**										**Specific Heat**	**Mass Flow Rate**	**Cooling Capacity**
	Tin	T1	T2	T3	T4	T5	T6	Tout	ΔT	$T_{ave;oil}$	Cp (J/kg.k)	$\dot{m}_{oil}$ (W/m.k)	$P_{Radiator}$ (W)
ODAN	50	46.1	42.1	48.3	42	47.6	42.2	42	8	46	1955.50	0.05	782.20
	60	52	44,7	56.7	55.2	54.9	44.3	44	16	52	1976.24	0.05	1581
	70	58.6	49.6	63.4	63.6	63.6	47.4	47.2	22.8	58.6	1999.05	0.05	2279
ODAF	50	41.3	39.5	37.4	37.4	43	39	38.2	11.8	44	1948.39	0.05	1149.87
	60	42	40.3	42.3	39.8	47.8	40.7	39.5	20.5	49.75	1968.45	0.05	2017.68
	70	45.6	40.9	48	38	51	39.5	39.8	30.2	54.9	1986.26	0.05	3000

APPENDIX – D

LIST OF PUBLICATIONS

APPENDIX – D

LIST OF PUBLICATIONS

Al-Furat Journal of Innovations in Mechanical and Sustainable Energy Engineering (FJIMSE) Published by Al-Furat Al-Awsat Technical University (ATU) / Iraq
ISSN: 2710-3374

Effect of Additives on Enhancing the Heat Transfer of Large Oil-Transformer Radiator in Transmission Grid

Aymen Abdul Kareem [1, a, *], Zaid M. Al-Dulaimi [2, b], HassanainGh. Hameed [1, c]

[1]Department of Power Mechanics Engineering, Engineering Technical Collage / Al-Najaf, Al-Furat Al-Awsat Technical University (ATU), Najaf, Iraq
[2]Technical Institute of Diwaniyah/ Al-Furat Al-Awsat Technical University (ATU) / Al-Diwaniyah, Iraq
[a]aymen.abdulkareem@student.atu.edu.iq
[b]Dulaimizm@atu.edu.iq
[c]hassanain.hameed@atu.edu.iq
[*]Corresponding Contact: aymen.abdilkaareem@atudent.atu.edu.iq

https://dx.doi.org/10.52262/150821-02

Abstract. The current paper aims to experimentally investigate the cooling capacities of the transformer radiator following two different cooling methodologies. The first method used oil direct air natural (ODAN), based on a free convection heat transfer. The second method follows the forced convection principle in an oil blunt air force (ODAF) that requires an air-blower fan to cool the oil. Hence two fans of the same properties were used with an average speed of 6.5 m/s. Both experiments were performed with an inlet oil temperature of (70°C) when the oil flows of (1, 2, 3 l/m). Maximum cooling capacity showed an acceptable improvement when using an oil flow rate of 3 l/m. It was 2620 Watts for the transformer utilizing the ODAF method of cooling. On the other hand, the transformer with ODAN cooling method reached only 1908 Watts.

Keywords: Large Transformer Radiator, Fan, Mineral oil, Oil Pump

Design Engineering

ISSN: 0011-9342 | Year 2021
Issue: 8 | Pages: 13756 - 13772

Review of Oil Cooling Methods for Large Transformer Coils in the Transmission Grid

Aymen Abdul Kareem[1, a], HassanainGh. Hameed[2,b] and Zaid M. Al-Dulaimi[3,c]

[1] Student, Technical College Najaf, AL-Furat Al-Awsat Technical University, Iraq

[2] Asst. Prof, Technical College Najaf, AL-Furat Al-Awsat Technical University, Iraq

[3] Asst. Prof, Technical Institute of Diwaniyah, AL-Furat Al-Awsat Technical, Iraq

[a]aymen.abdulkareem@student.atu.edu.iq,[b]hassanain.hameed@atu.edu.iq,[c]Dulaimizm@atu.edu.iq

* aymen.abdulkareem@student.atu.edu.iq

Abstract. Large oil-cooled transformers in power transmission networks have become a need for the whole world because they have two functions: the first is to raise the electric power voltage, and the second is commonly used to reduce the voltage. This is the rise and down of voltage for the transformers and the loads on them, especially in the hot climate season. Their temperature rises, so it needs coolers to reduce high temperatures to keep the input coil (windings) isolated from breakdown or explosion. The global challenge was finding a way to cool these transformers, so the experiments were experimental and numerical. Among these experiments, the best non-conductive oils were used. They can reduce the temperature of the internal parts of the transformers. Among the methods of oil cooling is either heat transfer by natural convection(AN) or forced convection(AF), so in this study, its will try to look at the modern method of reducing the temperature of the oil, taking into account several aspects, including economic, environmental, local and other important aspects.
Keywords: The large transformer,radiator cooling types

Introduction

Electrical power transformers connected to the transmission and distribution networks are a device to reduce electrical voltage to deliver appropriate power to consumers. Transformers have a great job in our lives. The first electrical transformer was discovered in 1882, a transformer consisting of a primary coil and several secondary windings to obtain secondary electrical voltages.

The great global challenge is to deliver electrical power from very long distances to the cities and villages with the lowest costs and the lowest losses because the electric power is equal to

الخلاصة

يتم فقد بعض الطاقه وتتحول الى حرارة اثناء عمل المحول الكهربائي. هذا الفقدان للطاقة يؤدي الى ارتفاع في درجة حرارة المحول لذلك يجب التحكم بهذه الحرارة من خلال حلول التبريد المتاحه. ان عمل المحول بدرجات حرارة عالية يؤدي الى تدهور المكونات ويقلل من عمر المحول الكهرابئي. ولاجل ديمومة عمل المحول يتم غمر ملفات المحول بشكل عام في خزان مموج مملوء بالزيت، يبرد الزيت الحار من خلال المبادلات الخارجية للمحول الكهربائي وهذه المبادلات هية مشعات قياسية من الواح عمودية رفيعة. التي تنقل حرارة الزيت الى الهواء المحيط بعملية الحمل القسري او الطبيعي.

الهدف من هذا العمل هو إيجاد قدرة التبريد القصوى والتغيرات في درجات الحرارة لألواح الراديياتير الرأسية بشكل تجريبي. تم استخدام ثلاث قيم لمعدلات تدفق الزيت (١ ، ٢ ، ٣ لتر / دقيقة) وثلاث قيم متغيرة لدرجة الحرارة (٥٠ ، ٦٠ ، ٧٠ درجة مئوية). تم استخدام نقل الحرارة لتبريد الزيت في كلا التكوينين ، الهواء الطبيعي للزيت المباشر (ODAN) ، والهواء القسري الزيت المباشر (ODAF). أيضًا تم استخدام طريقة جديدة في المبادل الحراري الخارجي للمحول، لتطوير نقل الحرارة للزيت المبرد عن طريق إضافة إسفنجات رغوية معدنية للمبادل الحراري (MFHE). أظهرت النتائج عند استخدام نموذج (ODAN) بدرجات حرارة مدخل الزيت (٥٠ ، ٦٠ ، ٧٠ درجة مئوية) على التوالي. فأن قدرات التبريد القصوى هي (٥٨٧,٦ ، ١٤٤٤,٤ ، ١٨١٦,٥ واط) عندما يكون معدل تدفق الزيت ٣ لتر / دقيقة. كما أظهرت النتائج عند استخدام نموذج (ODAF) بدرجات حرارة مدخل الزيت (٥٠ ، ٦٠ ، ٧٠ درجة مئوية) على التوالي. تبلغ سعات التبريد القصوى (٨٠١,٦ ، ١٧١٧,٢ ، ٢٥٩١,٦ واط) بمعدل تدفق الزيت ٣ لتر / دقيقة.

يستخدم العمل حاليًا طريقة التبريد الجديدة من خلال استخدام مبادل حراري للرغوة المعدنية (MFHE) من خلال استغلال الوسط المسامي والتحكم في قيمة مساميته والتي بلغت (١٧٪ و ٣٥٪) على التوالي. أظهرت النتائج قدرة التبريد القصوى لكلا النموذجين (ODAN) و (ODAF) ، مقارنة عند استخدام طريقة التبريد الجديدة (MFHA) بقيمتين مختلفتين للمسامية (١٧٪ و ٣٥٪) حيث أظهرت النتائج المسامية بـ (٣٥٪). المعتمدة نشطة لتطوير المبادل الحراري للمحول الكهربائي. النتائج التي تم الحصول عليها بشكل أساسي عند استخدامها (MFHE) المبردة بـ (٣٥٪) من المسامية في حالة (Fans Off) ؛ فأن قدرات التبريد القصوى هي (٧٨٢ ، ١٥٨٠,٩ ، ٢٢٧٨,٩ واط) بمعدل تدفق زيت ٣ لتر / دقيقة. أظهرت النتائج الثانوية عند استخدامها (MFHE) المبردة بنسبة (٣٥٪) مسامية ، في حالة (Fans ON) ، فأن قدرات التبريد القصوى (١١٤٩,٨ ، ٢٠١٧,٦ ، ٣٠٠٠ وات) بمعدل تدفق الزيت ٣ لتر / دقيقة.

جمهورية العراق

وزارة التعليم العالي والبحث العلمي

جامعة الفرات الاوسط التقنية الكلية التقنية الهندسية ـ نجف

دراسة تجريبية لتحسين اداء التبريد لمحولات القدرة الكهربائية

رسالة مقدمة الى

قسم تقنيات ميكانيك القوى

كجزء من متطلبات نيل درجة الماجستير تقني في الهندسة الميكانيكية (حراريات)

تقدم بها الطالب

أيمن عبد الكريم عباس

(بكالوريوس هندسة تقنيات السيارات ٢٠١٠)

اشراف

الاستاذ المساعد الدكتور زيد معن

الاستاذ المساعد الدكتور حسنين غني

محرم ١٤٤٣ هـ